# The outer transmembrane domain of the Kesv channel determines its intracellular localization

**A molecular and microscopic analysis of protein sorting**

TECHNISCHE UNIVERSITÄT DARMSTADT

Vom Fachbereich Biologie der Technischen Universität Darmstadt

zur Erlangung des akademischen Grades

eines Doctor rerum naturalium

genehmigte Dissertation von

Dipl.-Biol. Thomas Guthmann

aus Offenbach/Main

Berichterstatter: Prof. Dr. Gerhard Thiel

Mitberichterstatter: Prof. Dr. Adam Bertl

Tag der Einreichung: 10.04.2013

Tag der mündlichen Prüfung: 04.07.2013

Darmstadt 2013

D17

"Twenty years from now you will be more disappointed by the things you didn't do than by the ones you did do. So throw off the bowlines, sail away from the safe harbour. Catch the trade winds in your sails. Explore. Dream. Discover."

[Mark Twain]

# 1. Table of contents

# 2. Chapter 1 - General introduction

## 2.1. Ion channels

All cells and their organelles are surrounded by membranes. Among a pleitroph of membrane proteins, which are spanning these membranes, are ion channels. These proteins allow, as the name implies, ions to pass the membrane. Without these proteins membranes are, because of their hydrophobic and non-polar properties a very high thermodynamic barrier for the passive flux of ions (Hille, 2001). Ion channels can lower the energy barrier for ions to cross the membrane to 2 - 3 kcal/mol, which otherwise would be around 50 kcal/mol (Berneche & Roux, 2001; Parsegian, 1969). Hence ion channels are crucial for the fast exchange of ions across membranes; the speed with which ions can pass a channel is close to the free diffusion of ions in water e.g. $10^8$ ions/s (Hille, 2001; Lüttge & Kluge & Thiel, 2010).
Ion channels are generally highly selective for one type of ion. To achieve this fast and still selective transport they form in their middle a water filled pore, which provides a pathway for the movement of ions down of their electrochemical gradient (Hille, 2001). This mechanism is, in contrast to the active and energy consuming transport by ion pumps, passiv. This means that no energy has to be spend for the flux of ions via channels.

Ion channels are classified into different families according to their selectivity and gating mechanisms and gating properties. The main families are ligand-gated ion channels (Barry & Lynch, 2005), voltage-gated channels (Armstrong & Hille, 1998), light-gated channels (Nagel *et al.*, 2003), transient receptor potential channels (TRP) (Montell, 2005), mechanical-sensitive channels (Perozo, Kloda, Cortes, & Martinac, 2002), cycli-nucleotide-gated channels (Yau, 1994; Kaupp, 2002). Because of their selectivity for one type of ion the aforementioned voltage-gated channels can be subdivided into: voltage-gated potassium channels (Stühmer *et al.*, 1989), voltage-gated proton channels (DeCoursey, 2008), voltage-gated calcium channels (Dolphin, 2009) and voltage-gated sodium channels (Yu & Catterall, 2003).

The function of ion channels is essential for the life of cells no matter whether they are pro- or eukaryotic. Ion channels are for example responsible in prokaryotes for the extreme acid resistance of *Escherichia coli* (*E. coli*). In eukaryotes they play for example a key role in the communication between animal cells and the maintenance of cell tugor in plants (Iyer, Iverson, Accardi, & Miller, 2002; MacRobbie, 2006; Neher, 1992).

Because of their involvement in many physiological key functions, it became evident in the last two decades that a dysfunction of ion channels is at the root of many diseases. Diseases, which are caused by the malfunction of ion channels, are termed channelopathies. They include for example arrhythmias, diabetes, hyptertension, migrane and many more (Ashcroft, 2000).

### 2.1.1. Potassium channels

All potassium channels can be structurally classified into different families according to the number of transmembrane helices in each subunit. The number of helices can vary from 2 up to 8 (C. Miller, 2000). The following Figure 1 shows the most common blueprints of potassium channels:

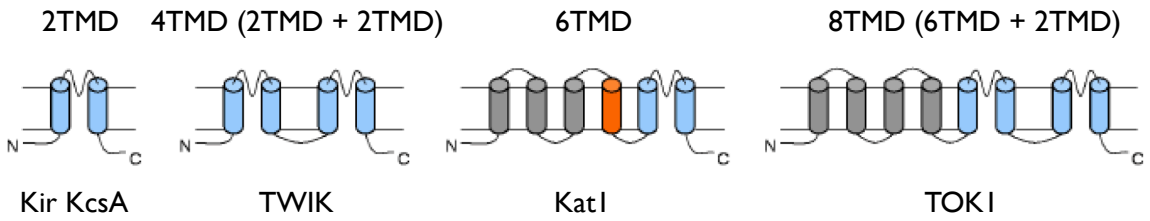


**Figure 1: Most common structures of potassium channels**. The transmembrane domains (TMD) building up the pore loop are shown in blue. Other membrane-spanning helices are shown in grey color. The orange helix indicates a voltage sensor to be found in channels with 6 helices (graphic modified (Balss, 2007)).

The most basic structure of potassium channels is that of a protein in which each subunit consists of a minimum of 2 transmembrane domains (2TMD). These two transmembrane domains are connected with an amino acid sequence, the so-called pore loop (p-loop). This loop is essential in the pore domain and will be described later in more detail. The eukaryotic Kir channel ($K^+$ inward-rectifier channel) and the prokaryotic KcsA channel of *Streptomyces lividans* (Doyle, 1998; Kubo 1992) are build in this way. The latter channel is very important in the field of $K^+$ channels because its structure was the first to be solved crystallographically at high resolution (Doyle, 1998).

Widely spreaded are also channels with 6 transmembrane domains (6TMD). This architecture is typical for voltage-gated channels (Kv channels). The potassium channel Kat1 ($K^+$ channel from *Arabidopsis thaliana*) is an example for this type of channels (Anderson, 1992; Schachtman, Schroeder, Lucas, Anderson, & Gaber, 1992). In this type of channels the pore loop is located between TMD5 and TMD6 of each subunit. Upstream of this pore domain are four transmembrane domains (TMD1-4). Important

in these channels is TMD4; it contains a series of positively charged amino acids, which function as voltage-sensor. Also these channels are functional as a tetramer.

Another architectural blue print of $K^+$ channels is that of the so-called tandem channels. They have 4 transmembrane domains (4TMD) in each subunit; each pair of them generates a pore loop. In this way only two subunits are required to build one functional channel. The TWIK channels are an example for the tandem type of $K^+$ channels (Lesage *et al.*, 1996). *Saccharomyces cerevisiae* has a potassium channel (TOK1 – two domain outward rectifier $K^+$ channel), which is also belonging to the tandem channels. This type of channels is consisting of 8 transmembrane domains (8TMD). A 6TMD motif is in this case followed by a 2TMD motif; as a dimer they create a functional channel (Ketchum, Joiner, Sellers, Kaczmarek, & Goldstein, 1995).

A common building motive of all potassium channels is the aforementioned pore module. This domain guarantees that potassium channels are generally very selective for potassium ions. That means that their selectivity for potassium is 10 up to 1000 times higher than that for sodium ions ($Na^+$) (Hille, 2001). This selectivity for potassium is based in the structure of the channel protein. After the resolution of the crystal structure of the $K^+$ channel pore it became evident that this selectivity for potassium is indeed based on the structure of the channel protein. The pore of a functional potassium channels is formed by four monomers of the 2TMD-type protein shown in Figure 1. These monomers are symmetrically grouped together around a water filled pore region. In this way the subunits build the characteristic tetrameric structure of potassium channels (see Figure 2) (Doyle, 1998; Jiang *et al.*, 2002; MacKinnon, 1991). The part of the pore loop, which lines the water filled pore, harbours the highly conserved signature sequence of eight amino acids TxxTxG(Y/F)G. This fold is characteristic for all members of the potassium channel families (Heginbotham, Lu, Abramson, & MacKinnon, 1994); it forms the conserved selectivity filter region in the pore that is responsible for the ion selectivity (Jan & Jan, 1992; C. Miller, 1992).

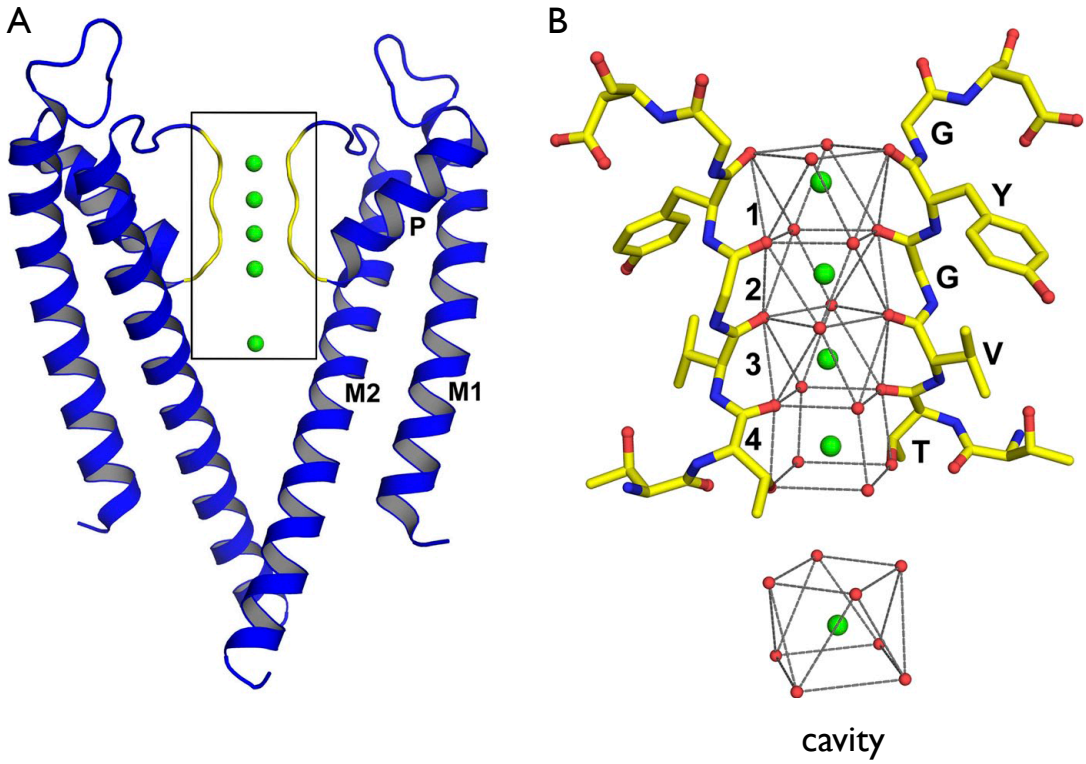


**Figure 2: Structure of the bacterial 2TMD potassium channel KcsA**. For clear view only two of the four subunits are shown. Left figure A: the two transmembrane domains are marked with M1 for the outer respectively M2 for the inner helix and the connecting p-loop with P. The filter region is highlighted in yellow and framed. Potassium ions are illustrated as green spheres. Right figure B: The selectivity filter with its characteristic amino acid sequence is presented. The four $K^+$ binding sites (oxygen atoms of the carbonyl groups) within the filter are named 1 – 4 from top to bottom. The potassium ion (green sphere) in the cavity is surrounded by eight water molecules (red spheres) (Graphic modified Alam & Jiang, 2011).

The selectivity filter promotes a fast and still selective passage of ions because the structure essentially mimics the hydration shell of ions. When passing the filter ions strip off their hydration shell when entering the filter region of a potassium channel. The oxygen atoms of the carbonyl groups of the amino acids of the filter region can now interact with the $K^+$ as a substitute for water Figure 2B) (Doyle, 1998). The selectivity of a potassium channel is based on the character and the orientation of these amino acids because they are responsible for the interaction with the passing ion (Jiang *et al.*, 2002). Also these amino acids are responsible for the size of the pore. If an ion does not have the correct size or if its electrochemical properties are not right the interaction between the ion and the oxygen atoms of the carbonyl groups is thermodynamically not favorable for passing the pore. For example: potassium and sodium are both monovalent cations. Even though sodium has with 95 pm the smallest ionic radius of the two ions it is only badly transported; it even blocks the potassium channel Kcv. Potassium on the other hand has an ionic radius of 133 pm (Plugge, 2000). This radius is equal to the distance of the ion to the carboxyl groups in the selectivity filter. Because of this “snuck fit” of the

ion into the cage of carboxyl residues the ion can slide easily through the filter. Because of its smaller size the sodium ion interacts in a much stronger manner with the oxygen of the carbonyl groups; as a result it is stuck in the filter and not transported.

### 2.1.2. The viral potassium channel Kcv and Kesv

The potassium channel Kcv ($K^+$ channel Chlorella Virus) from the green alga virus *Paramecium bursaria* Chlorella Virus 1 (PBCV-1) was the first viral protein with the structural and functional hallmarks of a potassium channel identified (Plugge, 2000).
Kcv is a structural protein of the PBCV-1 particle and is localized in the internal membrane of the capside. The viral channel can be heterologously expressed in various systems including *Xenopus* oocytes, various mammalian cells (human embryonic kidney 293 cells (HEK293)) and yeast. In these cellular systems the Kcv protein is synthesized into the secretory pathway from where it finally enters the plasma membrane. In the plasma membrane it can be measured with electrophysiological techniques (Balss *et al.*, 2008; Moroni *et al.*, 2002; Plugge, 2000). Kcv is probably synthesized on the rough ER and enters in this way the secretory pathway. From the endoplasmatic reticulum it reaches its final destination the plasma membrane.

The functional Kcv potassium channel is build in the same way as the pore module of larger $K^+$ channels. As detailed described in chapter 2.1.1 four monomers oligomerize as a tetramere in a functional channel. Each of the four monomers is build according to the characteristic 2TMD motif with the p-loop between the two helices (Figure 3A).
Kcv has a monomer-size of 94 amino acids (aa). Hence it is one of the smallest known potassium channels; despite of its small size it represents the the pore module of all complex potassium channels (Gazzarrini *et al.*, 2003; Plugge, 2000). In contrast to other potassium channels Kcv has no cytoplasmatic C-terminus (Figure 3A). On the N-terminus the channel has a short helix domain, which is presumably located at the interface between the membrane and the cytosol. The channel protein lacks any cytosolic domain on the C-terminus; such a C-terminal domain is essential for the gating mechanism of other potassium channels like KcsA (Cortes, Cuello, & Perozo, 2001).

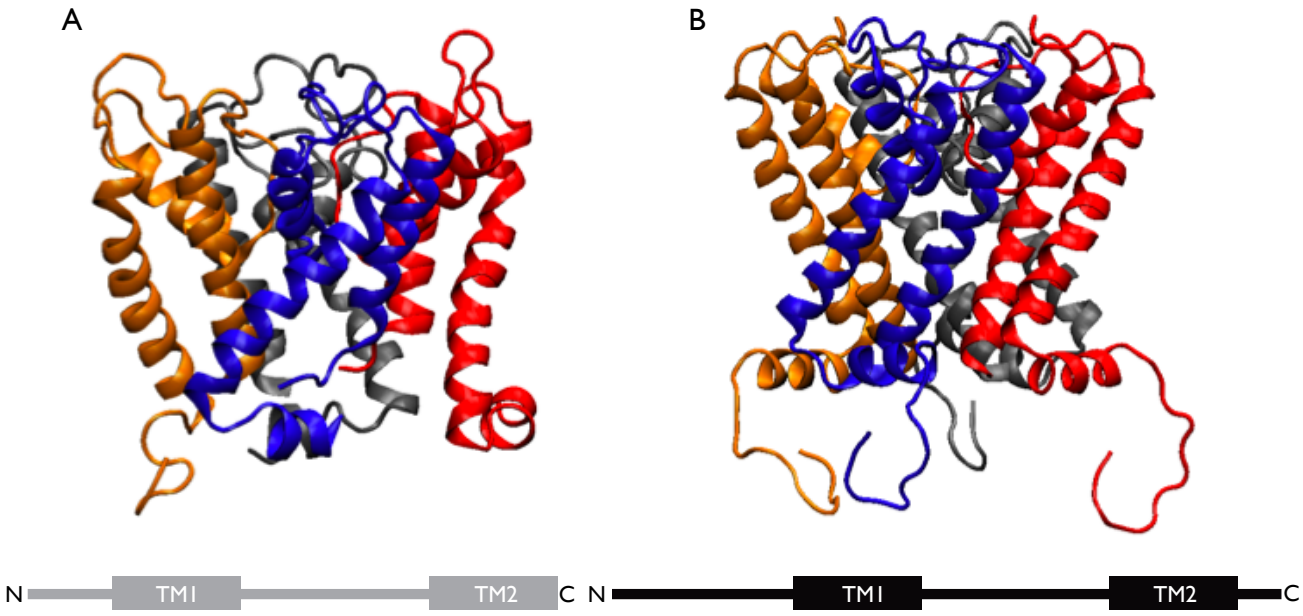


**Figure 3: Homology-model of the viral potassium channels Kcv and Kesv**. The four subunits of Kcv (**A**) and Kesv (**B**) are shown in the side view. Each subunit has its own color-code. The cartoon under each homology-model illustrates one monomer of each channel. The homology-model was kindly provided by Sascha Tayefeh (Kcv) respectively Sven Blumenschein and Stefan Kast (Kesv), Technische Universität Darmstadt 2008.

Another viral potassium channel Kesv ($K^+$ channel *Ectocarpus siliculosus* Virus) is from the brown alga virus *Ectocarpus siliculosus* Virus 1 (ESV-1). When this channel is expressed in mammalian cells it is sorted to the mitochondria (Balss *et al.*, 2008). Kesv is imported into the mitochondria in a voltage dependent manner by the TIM/TOM complex (Balss *et al.*, 2008). The requirement of a membrane voltage for the import implies that it is presumably sorted to the inner mitochondrial membrane; only proteins from the inner membrane need a membrane voltage for import (Neupert & Brunner, 2002; Neupert & Herrmann, 2007). In the mitochondria the channel is forming a tetramer (Balss *et al.*, 2008). It is not yet known whether the channel is active in the mitochondria. But experiments with isolated Kesv protein show that it generates channel activity when reconstituted into planar lipid bilayers (Braun, 2011).

The overall structure of Kesv is very similar to that of Kcv. Also Kesv is based on the tetrameric arrangement of four subunits with the characteristic 2TMD motif (Figure 3B).

Like Kcv it comprises the canonical pore module of more complex potassium channels. Kesv has a monomer-size of 124 aa. Compared to Kcv the N-terminus of Kesv, with a putative mitochondrial

targeting sequence, is longer. Kesv also has a little cytoplasmatic C-terminus (Etten, Graves, Boland, & Delaroque, 2002).

On the level of the primary structure, both channels have an overall protein identity of 29 %. A high degree of identity is present in the C-terminus with 41 %. An even higher identity is evident in the second transmembrane domain were the level of identity reaches 47 % (with a homology of 74 %) – see Figure 4.

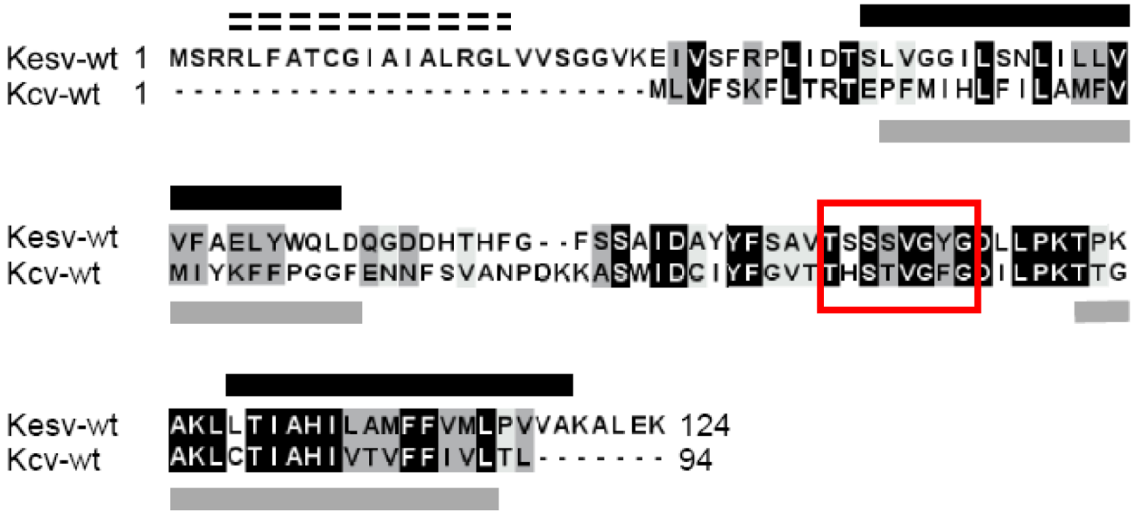


**Figure 4: Amino acid alignment of Kcv and Kesv.** The black bar indicates the transmembrane domains of Kesv. The grey bar indicates the transmembrane domains of Kcv. Identical amino acids have a black background. Homologous amino acids, depending on their level of homology, have a background of different grey values. The red box shows the highly conserved filter region (Balss *et al.*, 2008).

While both channels are very similar to each other the most outstanding difference is the aforementioned cellular localization: Kcv is located in the plasma membrane, Kesv on the other hand is found in the mitochondria.

The mechanisms underlying this difference in sorting of the two similar proteins is not fully understood yet and will be discussed in chapter 3. In this context the influence of the second transmembrane domain of Kesv on sorting will be discussed.

## 2.2. Protein transport and sorting in eukaryotic cells

The eukaryotic cell is divided in a multiplicity of different cellular compartments; they are all enclosed by membranes. This compartmentalization allows a simultaneously function of various biological reactions without that one disturbs the other. Each cellular compartment but also the membranes, which surround the compartments have their own configuration of characteristic proteins and specialized molecules. For example the mitochondria are the major organelles for ATP-synthesis and the nucleus is the most important organelle for the DNA replication respectively transcription (Alberts, 2011).

This compartmentalization of cells requires a distinct system for protein sorting. The compartment specific proteins are in this way distributed to the appropriate target compartment. The system is based on the fact that proteins have characteristic amino acid sequences, the so-called signal sequences, which guarantee a correct trafficking from the site of synthesis to the correct target. These signal sequences are recognized by a complementary receptor, which guides the protein along the correct way to its destination in an organelle. After reaching the final destination the signal sequence is often cut off (Alberts, 2011).

A minority of proteins is coded by organell specific genomes and synthesized directly in the organelles. Most of the proteins however are synthesized at ribosomes in the cytoplasm. With beginning of the translation the signal sequences, which are generally encoded at the N-terminus of a protein, are the first ones to emerge. Therefore these N-terminally encoded signal sequences have a high influence on the sorting of proteins; they determine whether a protein is sorted in co-translational or post-translational manner (Alberts, 2011).

The latter two modes of sorting, the co-translational or post-translational sorting, are the two major mechanisms for the distribution of proteins in cells: A general rule is that proteins, which travel via the secretory pathway to their final destination the plasma membrane, are sorted in a co-translational manner. Proteins, which end up for example in the mitochondria are sorted post-translational.

### 2.2.1. Co-translational protein sorting

Co-translationally sorted proteins enter the secretory pathway and many of them end up for example in the plasma membrane. Therefore a signal recognition particle (SRP) recognizes in an early phase of the translation on the ribosome an N-terminal signal sequence in the nascent protein. This signal typically consists of multiple hydrophobic amino acids like leucine or valine. The SRP binds in this process the hydrophobic part of the signal sequence at the starting-region of the protein and the translation of the protein is stopped. In the next step the complex of the ribosome with the nascent protein and the leftover of untranslated mRNA is targeted by the SRP to the SRP-receptor, an integral membrane protein complex of the endoplasmatic reticulum (ER). The receptor manages the interaction of the SRP-ribosome-complex with a protein-translocator. Because of that the SRP is separated away, the translation of the protein starts again and simultaneously the elongating protein is integrated in the membrane of the ER or translocated through the membrane in the ER lumen (Halic & Beckmann, 2005). Most of the proteins in the lumen of the ER making only a short stop over on their way in transport-vesicles to the golgi aparatus further on to the plasma membrane.

### 2.2.2. Post-translational protein sorting

Post-translational sorted proteins are transported after complete synthesis to their site of action. This can for example be the outer or inner membrane of mitochondria. For this transport specialized helper-proteins like the mitochondrial import stimulation factor (MSF) recognizes the N-terminal signal sequence of the nascent protein. The latter contains predominantly positive charged amino acids like lysine or arginine and is termed mitochondrial targeting sequence (MTS) or matrix targeting sequence (MTS) if the protein ends up in the mitochondrial matrix (Neupert & Herrmann, 2007). Because of the interaction of the MSF with the MTS the protein is completely synthesized at the free ribosomes; it remains unfolded as precursor protein and is transported in this form to the outer mitochondrial membrane (Neupert & Herrmann, 2007).

A second pathway for a post-translational protein sorting employs assisting proteins for folding and unfolding, the so-called chaperones. Especially one chaperon, the heat shock protein 70 (HSP70), binds to a hydrophobic sequence in the nascent protein, which is different from the MTS sequence. The complex of chaperon and precursor protein is then transferred to the outer mitochondrial membrane (Neupert & Herrmann, 2007).

An important function of the MSF and the chaperone is that both prevent a premature folding or spontaneous folding of the precursor protein.

When the precursor protein arrives at the outer mitochondrial membrane, the import receptor of the TOM-complex (translocase of the outer mitochondrial membrane) recognizes the signal sequence. The interacting proteins (MSF or chaperone) are stripped off and the precursor protein enters the channel of the TOM-complex. From there it arrives in the space between the outer and inner membrane of the mitochondria, the so-called inter membrane space (Neupert & Herrmann, 2007). Depending on its final localization within the mitochondria the precursor protein is either (i) sorted by the SAM-complex (sorting and assembly machinery) into the outer mitochondrial membrane (ii) sorted by the TIM22-complex (translocase of the inner mitochondrial membrane 22) into the inner mitochondrial membrane or (iii) sorted by the TIM23-complex (translocase of the inner mitochondrial membrane 23) in the mitochondrial matrix (Neupert & Herrmann, 2007). The final folding of the protein occurs in all cases at the site in which the protein is active.

### 2.2.3. Dual targeting of proteins

The eukaryotic cell is divided in a multiplicity of different cellular compartments. This allows a simultaneous operation of different biochemical reactions within one cell. For this purpose each cellular compartment has a distinct set of specific proteins. Because of this specificity a protein, which is for example active in the plasma membrane, is not found in the mitochondria or vice versa. In rare cases however it has been reported that the same kind of protein can also be located in two different cellular compartments. This non-canonical sorting, which has been termed "dual targeting" can be located in two or more cellular compartments and can adopt different functions.

The mechanism underlying dual targeting of proteins is not yet fully understood. There are only a few cases for which it is known how the same or very similar proteins end up in two different cellular compartments. One mechanism for dual targeting is the existence of two genes, which encode for slightly different proteins. These proteins can differ in the presence or absence of a specific signal sequence. In this way two different translation products are created, which are sorted to different cellular compartments (Martelli *et al.*, 2007).

Another possibility is that multiple mRNAs of which only one encodes for example a mitochondrial targeting sequence are generated from one gene. This may occur by multiple transcription initiation sites on a gene or by mRNA splicing. For the tRNA synthetase in yeast for example two transcripts are encoded: a long one with an MTS for a sorting to the mitochondria and a short one, which lacks this signal sequence, and is hence resident in the cytoplasm (Wang *et al.*, 2003). Splicing is involved in the case of rat renin: the full-length transcript encodes an ER N-terminal signal sequence and the short version lacks this signal because of alternative splicing (Clausmeyer *et al.*, 1999).
Also alternative translation initiation sites can influence the cellular localization of the same protein: the full-length protein of the *Arabidopsis thaliana* holocarboxylase synthetase 1 for example is harbouring a chloroplast/mitochondria signal sequence; the short cytosolic version in contrast lacks this (Puyaubert, Denis, & Alban, 2008).

Of course also a single translation product can be recognized and targeted into different cellular compartments. The amino acid composition of mitochondrial and chloroplast signal sequences are similar: they contain many positively charged and hydrophobic amino acids. Due to this ambiguous character of the signal sequence the translation product can be recognized by the receptor for mitochondrial or chloroplast targeting. The competitive affinity of the receptors for a signal sequence is in this case determining the cellular localization. Such a mechanism is described for example in the case of the amino acyl-tRNA synthetases of *Arabidopsis thaliana* (Berglund *et al.*, 2009).
Also a protein can harbour two signal sequences, each for a different cellular compartment. Here again the affinity of the receptors to the signal sequence respectively to the accessibility of the signal sequence determining the cellular localization (Carrie *et al.*, 2008; Frechin *et al.*, 2009).

In other cases the targeting of proteins can be influenced by the cellular environment or changes within the cell. Recent studies show, that the catalytic subunit of telomerase (TERT) is excluded from the nucleus during oxidative stress. In this case it is imported into mitochondria where it protects the mitochondrial DNA from reactive oxygen species (Ahmed *et al.*, 2008).

The few mechanisms for dual targeting of proteins outlined above show, that dual targeting is a dynamic process. It allows the cell to react to varying conditions and it provides a high degree of flexibility.

Dual targeting is also known for some membrane proteins. One example are potassium channels, which can be found in the plasma membrane and in mitochondria. The best-documented example is

the voltage-gated potassium channel Kv1.3; this outward rectifier is the main potassium channel in T-lymphocytes where it is located in the plasma membrane. Under specific circumstances the same Kv1.3 channel can also be found in the inner membrane of mitochondria (Leanza *et al.*, 2012; Szabò *et al.*, 2005). Yet the principal of function for this dual localization of Kv1.3 is not understood.

In the context of understanding the mechanism of dual targeting of membrane proteins in general and for potassium channels particular, the minimal potassium channels Kcv and Kesv are very interesting. Both proteins, which were presented in chapter 2.1.2, are very similar. But still both proteins exhibit a very different cellular localization: Kcv is in the plasma membrane, Kesv on the other hand is found in the mitochondria, and there probably in the inner membrane (Balss *et al.*, 2008).
Recent studies have shown that an elongation of the second transmembrane domain of Kesv redirects the channel from the mitochondria into the secretory pathway. It finally reaches its destination in the plasma membrane where the activity of this Kesv mutant can be measured (Balss *et al.*, 2008). While the experimental data show that a position sensitive elongation of TMD2 can fully reverse the trafficking of the Kesv channel, the mechanisms by which this alteration in sorting occurs is not fully understood yet. It is possible that the second transmembrane domain requires a physical extension for the change in sorting or that the physicochemical flavor of the respective TMD2 needs to be changed. To address this question respectively for a better understanding of the sorting of proteins into different compartments the influence of the second transmembrane domain of Kesv in sorting is the subject of this thesis. An understanding of the sorting of the minimal potassium channel Kesv could contribute for a better understanding of the sorting of more complex potassium channels or in a more general way: which signals are important for the sorting of channels.

## 2.3. References


Ahmed, S., Passos, J. F., Birket, M. J., Beckmann, T., Brings, S., Peters, H., Birch-Machin, M. A., et al. (2008). Telomerase does not counteract telomere shortening but protects mitochondrial function under oxidative stress. *Journal of Cell Science*, *121*(Pt 7), 1046–1053.

Alam, A., & Jiang, Y. (2011). Structural studies of ion selectivity in tetrameric cation channels. *The Journal of general physiology*, *137*(5), 397–403.

Alberts, B., Johnson, A., Lewis, J., Raff, M., Roberts, K., & And Walter, P. (2011). *Molekularbiologie der Zelle*. (Bruce Alberts, A. Johnson, J. Lewis, M. Raff, K. Roberts, & P. Walter, Eds.)*Amino Acids* (Vol. 54, p. 1725).

Anderson, J. (1992). Functional expression of a probable Arabidopsis thaliana potassium channel in Saccharomyces cerevisiae. *Proceedings of the …*, *89*(May), 3736–3740.

Armstrong, C. M., & Hille, B. (1998). Voltage-gated ion channels and electrical excitability. *Neuron*, *20*(3), 371–80.

Ashcroft, FM (2000) Ion Channels and Disease: Channelopathies. Academic Press

Balss, J (2007) Unterschiedliche zelluläre Sortierung zweier viraler K+-Kanäle: Die Bedeutung der zweiten Transmembrandomäne als Sortierungssignal. *Technischen Universität Darmstadt*

Balss, J., Papatheodorou, P., Mehmel, M., Baumeister, D., Hertel, B., Delaroque, N., Chatelain, F. C., et al. (2008). Transmembrane domain length of viral K+ channels is a signal for mitochondria targeting. Proceedings of the National Academy of Sciences of the United States of America, 105(34), 12313–8.

Barry, P. H., & Lynch, J. W. (2005). Ligand-gated channels. *IEEE Transactions on NanoBioscience*, *4*(1), 70–80.

Berglund, A.-K., Pujol, C., Duchene, A.-M., & Glaser, E. (2009). Defining the determinants for dual targeting of amino acyl-tRNA synthetases to mitochondria and chloroplasts. *Journal of Molecular Biology*, *393*(4), 803–814.

Berneche, S., & Roux, B. (2001). Energetics of ion conduction through the K+ channel. *Nature*, *414*(November), 73–77.

Blumenschein & Kast (2008) Homologiemodellierung von Kcv und Kesv und Molekulardynamische Simulation. Technische Universität Darmstadt

Braun, C. (2011) Rekonstitution von Kanalproteinen in planaren Lipid Bilayern. Technische Universität Darmstadt

Carrie, C., Murcha, M. W., Kuehn, K., Duncan, O., Barthet, M., Smith, P. M., Eubel, H., et al. (2008). Type II NAD(P)H dehydrogenases are targeted to mitochondria and chloroplasts or peroxisomes in Arabidopsis thaliana. *FEBS Letters*, *582*(20), 3073–3079.

Clausmeyer, S., Stürzebecher, R., & Peters, J. (1999). An alternative transcript of the rat renin gene can result in a truncated prorenin that is transported into adrenal mitochondria. *Circulation Research*, *84*(3), 337–344.

Cortes, D. M., Cuello, L. G., & Perozo, E. (2001). Molecular architecture of full-length KcsA: role of cytoplasmic domains in ion permeation and activation gating. *The Journal of general physiology*, *117*(2), 165–180.

DeCoursey, T. (2008). Voltage-gated proton channels. *Cellular and Molecular Life Sciences*, *65*(16), 2554–2573.

Dolphin, A. C. (2009). Calcium channel diversity: multiple roles of calcium channel subunits. *Current opinion in neurobiology*, *19*(3), 237–44.

Doyle, D. a. (1998). The Structure of the Potassium Channel: Molecular Basis of K+ Conduction and Selectivity. *Science*, *280*(5360), 69–77.

Etten, J. L. Van, Graves, M. V, Boland, W., & Delaroque, N. (2002). Phycodnaviridae – large DNA algal viruses Brief Review. *Archives of Virology*, 1479–1516.

Frechin, M., Senger, B., Brayé, M., Kern, D., Martin, R. P., & Becker, H. D. (2009). Yeast mitochondrial Gln-tRNA(Gln) is generated by a GatFAB-mediated transamidation pathway involving Arc1p-controlled subcellular sorting of cytosolic GluRS. *Genes & Development*, *23*(9), 1119–1130.

Gazzarrini, S., Severino, M., Lombardi, M., Morandi, M., DiFrancesco, D., Van Etten, J. L., Thiel, G., et al. (2003). The viral potassium channel Kcv: structural and functional features. *FEBS Letters*, *552*(1), 12–16.

Halic, M., & Beckmann, R. (2005). The signal recognition particle and its interactions during protein targeting. *Current opinion in structural biology*, *15*(1), 116–25.

Heginbotham, L., Lu, Z., Abramson, T., & MacKinnon, R. (1994). Mutations in the K+ channel signature sequence. *Biophysical journal*, *66*(4), 1061–7.

Hille, B. (2001). *Ionic channels of excitable membranes*. (B Hille, Ed.)*Sinauer Associates Inc Sunderland MA USA* (Vol. 3, p. 814).

Iyer, R., Iverson, T., Accardi, A., & Miller, C. (2002). A biological role for prokaryotic ClC chloride channels. *Nature*, *419*(October), 7–9.

Jan, L. Y., & Jan, Y. N. (1992). Structural elements involved in specific K+ channel functions. *Annual review of physiology*, *54*(36), 537–55.

Jiang, Y., Lee, A., Chen, J., Cadene, M., Chait, B. T., & MacKinnon, R. (2002). The open pore conformation of potassium channels. *Nature*, *417*(6888), 523–6.

Ketchum, K. A., Joiner, W. J., Sellers, A. J., Kaczmarek, L. K., & Goldstein, S. A. (1995). A new family of outwardly rectifying potassium channel proteins with two pore domains in tandem. *Nature*, *376*(6542), 690–695.

Leanza, L., Henry, B., Sassi, N., Zoratti, M., Chandy, K. G., Gulbins, E., & Szabò, I. (2012). Inhibitors of mitochondrial Kv1.3 channels induce Bax/Bak-independent death of cancer cells. *EMBO molecular medicine*, *4*(7), 577–93.

Lesage, F., Guillemare, E., Fink, M., Duprat, F., Lazdunski, M., Romey, G., & Barhanin, J. (1996). TWIK-1, a ubiquitous human weakly inward rectifying K+ channel with a novel structure. *the The European Molecular Biology Organization Journal*, *15*(5), 1004–1011.

Lüttge U., Kluge M., Thiel G. (2010) Botanik - Die umfassende Welt der Pflanzen. Wiley-VCH Verlag GmbH & Co. KGaA

MacKinnon, R. (1991). Determination of the subunit stoichiometry of a voltage-activated potassium channel. *Nature*, 232–235.

MacRobbie, E. a C. (2006). Control of volume and turgor in stomatal guard cells. *The Journal of membrane biology*, *210*(2), 131–42.

Martelli, A., Salin, B., Dycke, C., Louwagie, M., Andrieu, J.-P., Richaud, P., & Moulis, J.-M. (2007). Folding and turnover of human iron regulatory protein 1 depend on its subcellular localization. *The FEBS journal*, *274*(4), 1083–1092.

Miller, C. (1992). Ion Channel Structure and Function. *Science*, (October), 9–10.

Miller, C. (2000). An overview of the potassium channel family. *Genome Biology*, *1*(4), reviews0004.1–reviews0004.5.

Montell, C. (2005). The TRP superfamily of cation channels. *Sciences STKE signal transduction knowledge environment*, *2005*(272), re3.

Moroni, A., Viscomi, C., Sangiorgio, V., Pagliuca, C., Meckel, T., Horvath, F., Gazzarrini, S., et al. (2002). The short N-terminus is required for functional expression of the virus-encoded miniature K(+) channel Kcv. *FEBS Letters*, *530*(1-3), 65–69.

Nagel, G., Szellas, T., Huhn, W., Kateriya, S., Adeishvili, N., Berthold, P., Ollig, D., et al. (2003). Channelrhodopsin-2, a directly light-gated cation-selective membrane channel. *Proceedings of the National Academy of Sciences of the United States of America*, *100*(24), 13940–13945.

Neher, E. (1992). Channels for communication between and within cells Ion. *Bioscience reports*.

Neupert, W., & Brunner, M. (2002). The protein import motor of mitochondria. *Nature Reviews Molecular Cell Biology*, *3*(8), 555–565.

Neupert, W., & Herrmann, J. M. (2007). Translocation of proteins into mitochondria. *Annual review of biochemistry*, *76*, 723–49.

Parsegian, A. (1969). Energy of an ion crossing a low dielectric membrane: solutions to four relevant electrostatic problems. *Nature*, *221*(5183), 844–846.

Perozo, E., Kloda, A., Cortes, D. M., & Martinac, B. (2002). Physical principles underlying the transduction of bilayer deformation forces during mechanosensitive channel gating. *Nature Structural Biology*, *9*(9), 696–703.

Plugge, B. (2000). A Potassium Channel Protein Encoded by Chlorella Virus PBCV-1. *Science*, *287*(5458), 1641–1644.

Puyaubert, J., Denis, L., & Alban, C. (2008). Dual Targeting of Arabidopsis HOLOCARBOXYLASE SYNTHETASE1: A Small Upstream Open Reading Frame Regulates Translation Initiation and Protein Targeting1[W]. *Plant Physiology*, *146*(2), 478–491.

Schachtman, D. P., Schroeder, J., Lucas, W. J., Anderson, J. A., & Gaber, R. F. (1992). Expression of an Inward-Rectifying Potassium Channel by the Arabidopsis KATI cDNA. *Science*, *258*(December).

Stühmer, W., Ruppersberg, J. P., Schröter, K. H., Sakmann, B., Stocker, M., Giese, K. P., Perschke, a, et al. (1989). Molecular basis of functional diversity of voltage-gated potassium channels in mammalian brain. *The EMBO journal*, *8*(11), 3235–44.

Szabò, I., Bock, J., Jekle, A., Soddemann, M., Adams, C., Lang, F., Zoratti, M., et al. (2005). A novel potassium channel in lymphocyte mitochondria. *The Journal of biological chemistry*, *280*(13), 12790–8.

Wang, C.-C., Chang, K.-J., Tang, H.-L., Hsieh, C.-J., & Schimmel, P. (2003). Mitochondrial form of a tRNA synthetase can be made bifunctional by manipulating its leader peptide. *Biochemistry*, *42*(6), 1646–1651.

Yau, K. (1994). Commentary Cyclic nucleotide-gated channels : An expanding ion channels. *Proceedings of the National Academy of Sciences of the United States of America*, *91*(April), 3481–3483.

Yogev, O., & Pines, O. (2011). Dual targeting of mitochondrial proteins: mechanism, regulation and function. *Biochimica et biophysica acta*, *1808*(3), 1012–20.

Yu, F. H., & Catterall, W. a. (2003). Overview of the voltage-gated sodium channel family. *Genome biology*, *4*(3), 207.

# 3. Chapter 2 – The influence of the second transmembrane domain in the targeting of Kesv

## 3.1. Abstract

It's not easy to follow up the questions, which are the reasons for protein sorting and localization. Kcv and Kesv are two viral potassium channels, which are structurally very similar to each other but located in different cellular compartments (Etten *et al.*, 2002; Plugge, 2000). These channels were used in this study to test the influence of the second transmembrane domain of Kesv in its localization.
In this chapter a method is described to insert a randomized mutation in a distinct region of the viral potassium channel Kesv. A yeast screening system made it possible to search for functional Kesv mutants. Due to the combination of both methods at least two functional mutants of the potassium channel Kesv could be created that aren't any longer located in the mitochondria but in the plasma membrane.

## 3.2. Introduction

Viruses infect cells of various organisms. Because of their small size and limited genomic configuration they are not able to reproduce without a host. Viruses therefore conquer cells and use the cellular machinery of the host for their own purposes. Because viruses often hijack for this purpose host cell pathways they are good tools for understanding principle questions in the cell biology of the host (Barlowe, 2003; Ma *et al.*, 2001; Pelkmans & Helenius, 2003; Söllner, 2004).
In addition to their role in uncovering cellular pathways viruses also help to get more insights in structure function relations of proteins. This is mainly because viruses reduce the genetic information for protein coding sequences to as little as possible. In this way many viruses create proteins, which still reveal the function of large and complex homologous while the protein is reduced in size to a coremodul (Kang, Moroni, Gazzarrini, & Van Etten, 2003).
The literature shows that viral proteins are very good tools for understanding the sorting of cellular proteins (Karniely & Pines, 2005; Miyazaki & Kida, 2005). In previous studies the sorting of two miniature viral potassium channels was examined (Balss *et al.*, 2008). One channel, Kcv, is from the green alga virus *Paramecium bursaria* Chlorella Virus 1 (PBCV-1) and the other, Kesv, is from the brown alga virus *Ectocarpus siliculosus* Virus 1 (ESV-1). Despite their small size (monomer-size Kcv = 94 amino acids (aa); Kesv = 124 aa respectively) both channel proteins comprise the pore module of more complex potassium channels (Etten *et al.*, 2002; Kang *et al.*, 2003; Plugge, 2000).

On the level of the primary structure, both have an overall protein identity of 29 %. A high identity is present in the C-terminus with 41 %. An even higher identity is evident in the second transmembrane domain (TMD) were the level of identity reaches 47 % (with a homology of 74 % - see Figure 5) (Balss *et al.*, 2008).


**Figure 5: Alignment of Kesv and Kcv wildtype downstream of the selectivity filter.** The black bar indicates the second transmembrane domain of Kesv. The grey bar indicates the second transmembrane domain of Kcv. Identical amino acids have a black background. Homologous amino acids, depending on their level of homology, have a background of different grey values. The red square shows the region 111 - 115 of Kesv (graphic modified (Balss *et al.*, 2008)).

In contrast to their high degree of structural similarity the most outstanding difference is their cellular localization: Kcv is localized in the plasma membrane of heterologous expression systems (*Xenopus* oocytes, varius mammalian cells including human embryonic kidney 293 cells (HEK293) and yeast) (Balss *et al.*, 2008; Moroni *et al.*, 2002; Plugge, 2000). Kcv is probably synthesized on the rough ER and enters in this way the secretory pathway. From the endoplasmatic reticulum it reaches its final destination the plasma membrane. This is the typically pathway for plasma membrane proteins (Hegde & Keenan, 2011). Kesv on the other hand is found in the mitochondria and there presumably in the inner membrane. It is imported into the mitochondria in a voltage dependent manner by the TIM/TOM complex (Balss *et al.*, 2008).

A comparison of the primary structure of both channels uncovered a domain in the N-terminus of Kesv with a characteristic mitochondrial import sequence. When this sequence is fused to the green fluorescent protein (GFP) it is able to guide GFP into the mitochondria. In further experiments however it turned out that a deletion or mutation of this domain has no effect on the localization of Kesv (Balss *et al.,* 2008). From the results of these experiments it was concluded that this C-terminal signaling domain is neither sufficient nor essential for the sorting of Kesv into mitochondria.

Structural comparisons between Kcv and Kesv and mutagenesis experiments showed that the sorting of Kesv depends in structural information in the second transmembrane domain of the channel. Structural prediction algorithms suggest that the second transmembrane domain of potassium channels with two transmembrane domains is generally 23 amino acids long. The second transmembrane domain of Kesv however appears shorter than that of complex channels and even

smaller than that of Kcv. The predicted length of TMD2 of Kesv is only 18 amino acids while that of Kcv seems to be 20 amino acids long (Balss *et al.*, 2008).

On the basis of this finding the TMD2 of Kesv was elongated by >2 hydrophic amino acids in position 113 (Balss *et al.*, 2008). Experiments on the sorting of the channel mutants show that Kesv can with this elongation of TMD2 be redirected from the mitochondria into the secretory pathway; it finally reaches its destination in the plasma membrane were its activity can be measured (Balss *et al.*, 2008). While the experimental data show that a position sensitive elongation of TMD2 can fully reverse the trafficking of the Kesv channel the mechanisms by which this alteration in sorting occurs is not fully understood yet. It is possible that the TMD2 indeed requires a physical extension for the change of sorting or that the physicochemical flavor of the respective TMD2 needs to be altered.

To address these questions in the context of structure function relations of proteins in an unbiased way randomly created libraries of mutants can be a powerful tool (Minor, 2009). There is no necessity to know the protein of interest in great detail or to have a clear hypothesis on the exact position for a mutation or on the amino acid, which is required. This combination of sequence randomization with a functional assay provides the possibility to look for structure function correlations in an unbiased manner. Randomization studies can be arranged in a short period of time and with a lower coast than traditional single point mutations. For example: to mutate the viral potassium channel Kesv into all possible amino acids $20^{124}$ point mutations would be necessary. This is an enormous and virtually impossible underpinning. The search for functional mutants in this amount of mutants would be another tough challenge. Hence the randomization approach, which guarantees the insertion of randomized mutations in the DNA sequence, only works with a robust screen system. The latter must be able to test a high amount of randomized mutants for function. Together randomization and functional screening provides the so-called system of directed evolution, which is a successful tool for high throughput analysis (Jäckel, Kast, & Hilvert, 2008; Minor, 2009).

This chapter combines the advantages of a randomization assay with the advantages of viruses as tools to understand complex processes of protein sorting within cells. Here parts of the second transmembrane domain of Kesv were subjected to randomization. In a yeast complementation assay only those mutants, which provide a functional $K^+$ channel that is sorted to the plasma membrane, are able to rescue the test yeast strain. The results of these experiments show that the sorting of the Kesv channel can be shifted from the mitochondria to the plasma membrane without extension of TMD2. A mutation of a few amino acids was sufficient to guarantee this shift in sorting.

## 3.3. Material and Methods

### 3.3.1. Heterologous Expression System

For the yeast complementation assay the yeast strain SGY1528 with the genotype Mat a ade 2–1 can 1–100 his 3–11,15 leu 2–3,112 trp 1–1 ura 3–1 trk 1::HIS3 trk 2::TRP1 (Tang *et al.*, 1995) was used (kindly provided by Dr. Minor UCSF, San Francisco).

### 3.3.2. Constructs and Mutagenesis

For the randomization studies the region in the second transmembrane domain of Kesv from position 111 - 115 (see Figure 5 respectively Figure 9) was chosen. Previous data had shown that an elongation of the second transmembrane domain downstream of position 113 was able to shift sorting of this protein (Balss *et al.*, 2008).
For the yeast complementation assay Kesv wildtype was cloned between the restriction sites EcoRI and XhoI (Balss *et al.*, 2008) in a modified pYES2 vector (Invitrogen 28 GmbH, Karlsruhe, Germany) as described by Daniel Minor who also provided kindly the modified pYES2 vector (Minor *et al.*, 1999).
The pYES2 vector was modified as follows:

- the PvuI restriction site at position 2516 was replaced by 5´ - GTAGGATCG - 3’
- the PvuI restriction site at position 4417 was replaced by 5´ - CAACGATTGGAG - 3’
- the Gal1-promtor was replaced by a Met25-promotor (the expression of the protein can be controlled by methionine in the media)

For the distinct randomization of the second transmembrane domain from position 111 - 115 a randomized site directed mutagenesis PCR (rSDM-PCR) with 5’ phosphorylated abutting primers (see Figure 6 and Figure 7) containing the randomization sequence, was performed using the Phusion™ Polymerase (Fermentas, St. Leon Roth, Germany) (Guthmann, 2009).

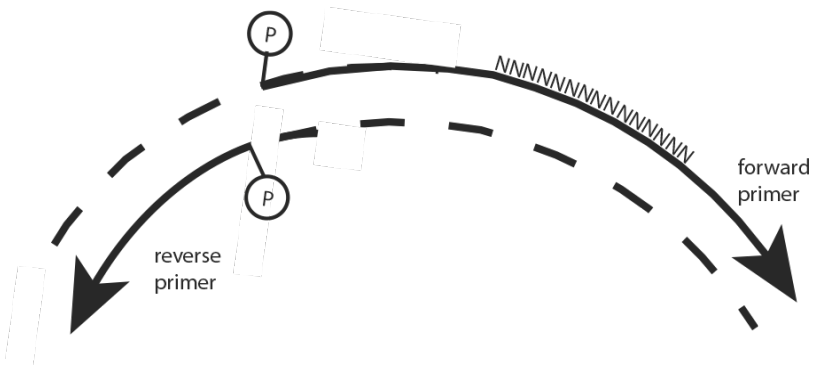


**Figure 6: Primer design for rSDM-PCR**. The forward primer carries the randomized region, shown by "N". The reverse primer is abutting to the forward primer. Both oligonucleotides carry a 5' phosphorylation "P".

The oligonucleotides were not complementary but abutting. This reduces the formation of hetero duplex DNA. The oligonucleotides were produced by Eurofins MWG Operon (Ebersberg, Germany).

```
forward primer: 5´- ACACATTTTGGCCATGNNNNNNNNNNNNNNNNCCCGTTGTCGCGAAG - 3´
reverse primer: 5´- GCGATGGTAAGCAATTTTGCCTT - 3´
```

**Figure 7: Primer sequences for the rSDM-PCR.** Only the forward primer carries the randomized region, shown by "N". The reverse primer is abutting to the forward primer. Both primers carry a 5' phosphorylation.

The PCR reagents were used as described in the Phusion™ protocol. The high amount of different oligonucleotides in the randomized primer mix implies ideally a number of $20^5$ (3.200.000) different forward primers. This predicts a high level of different optima in the annealing temperature. For this reason not a distinct annealing temperature was used but a temperature gradient for annealing (see Table 1). This procedure should favour an annealing of as many primers as possible.

**Table 1: Cycles of the rSDM-PCR**. The star indicates the temperature gradient of +/- 5 °C during the annealing.

| temperature | time | |
|---|---|---|
| 98 °C | 30 sec | |
| 98 °C | 8 sec | ⎫ |
| 65 °C* | 20 sec | ⎬ |
| 72 °C | 3:10 min | ⎭ |
| 72 °C | 10 min | |
| 4 °C | storage | |

Finally the PCR constructs were ligated (4 $\mu$l T4 buffer, 2 $\mu$l T4 DNA-Ligase, 22 °C for 45 minutes, inactivation: 65 °C for 20 minutes, Fermentas, St. Leon Roth, Germany) to get a "ready to use PCR solution" with circular plasmid DNA for the yeast transformation (Guthmann, 2009).

100 mM $K^+$

0.5 mM $K^+$

### 3.3.3. Yeast transformation and complementation assay

The eukaryotic organism *Saccharomyces cerevisiae* is relatively easy to manipulate genetically and is therefore frequently used as heterologous expression system.

Previous studies have shown that various potassium uptake systems (the potassium transporters Trk1p, Trk2p and the ion channels Nsc1p, Tok1p) are located in the plasma membrane of *Saccharomyces cerevisiae*. Among these the TRK-transporters are responsible in combination with an $H^+$-ATPase for a high affinity of potassium uptake. This allows yeast cells to grow on media with a micromolar potassium concentration. After deletion of the TRK-transporters yeast cells are no longer able to grow on media with a micromolar potassium concentration (A. Bertl, Bihler, Kettner, & Slayman, 1998; A. Bertl, Slayman, & Gradmann, 1993; Gaber, Styles, & Fink, 1988; Petrezsélyová, Ramos, & Sychrová, 2011).

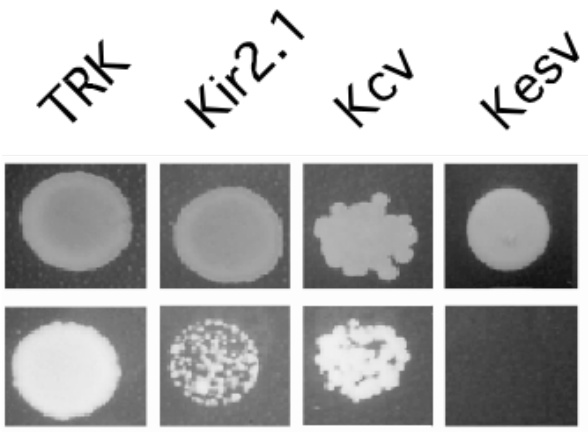


**Figure 8: Yeast complementation assay with different potassium channels.** The first row shows the growth on non-selective media with 100 mM potassium. The row below shows the growth on selective media with 0.5 mM potassium (modified graphic Balss *et al.*, 2008).

The lack of the endogenous potassium uptake system can be complemented by expression of different potassium channels respectively potassium transporters. Figure 8 shows that yeast mutants, which lack TRK1 and TRK2 are able to grow on media with a low potassium concentration when transformed with a functional potassium transporting protein (Balss *et al.*, 2008).

Without the complementation of the defective potassium uptake system in the plasma membrane by heterologous potassium channels the yeast mutant strain is not able to grow on media with a low potassium concentration (see Figure 8 Kesv). Thus the yeast complementation assay is suitable to examine whether a potassium channel is functional and also whether it is sorted to the plasma membrane.

The yeast complementation assays were done as described in Minor *et al.*, 1999. The yeast strain SGY1528 (trk1Δtrk2Δ) used in these experiments is deprived of its endogenous potassium uptake system. This strain fails to grow on media with a low potassium concentration (< 10 mM $K^+$) (Minor *et al.,* 1999).

The yeast cells were transformed with the Frozen-EZ Yeast Transformation II Kit™ (Zymo Research; Orange, USA) as described in the manufactures manual. After the transformation the yeast cells were plated on SD-URA+A+100$K^+$ plates (Baumeister, 2010). The plates were incubated for 2 - 3 days at 30 °C. Only the successful transformed yeast cells grew on the media.

For the yeast complementation assay agar plates with 100 mM $K^+$ (non-selective media), 1 mM $K^+$ and 0.5 mM $K^+$ (selective media) were used (Baumeister, 2010). For the experiments with liquid cultures, liquid selective media with the same potassium concentrations as above was used. This liquid media was inoculated with a yeast suspension in the dilutions 1:100 of an $OD_{600}$= 1 yeast solution (prepared and washed in the same manner as described in (Minor *et al.,* 1999). 250 µl of the diluted liquid culture were put in individual chambers of a 96 well plate (Biochrom AG, Berlin, Germany). The plate was incubated (30 °C and 230 rpm) and the $OD_{600}$ of the liquid cultures was measured after 0 h, 24 h and 48 h with a microplate reader (Tecan Infinite® 200).

### 3.3.4. Yeast plasmid preparation

After the growth of yeast cells on selective media a sequence analysis was made. Therefore the Zymoprep™ Yeast Plasmid Miniprep II (Zymo Research; Orange, USA) was used as described in the manufactures manual.

Additionally the following protocol was used:

- centrifugation of 2 - 3 ml of yeast over night culture for four minutes at 5.800 rpm (Biofuge pico, Heraeus, Hanau, Germany)
- discard the supernatant and resuspend the pellet in 200 µl of TE-buffer
- add 300 µl of $ddH_2O$ and 2.5 µl of mercaptoethanol

- incubation for 1 h at 30 °C and 230 rpm
- centrifugation at 5.800 rpm, discard the supernatant and resuspend the pellet in 200 $\mu$l of buffer S (1 M Sorbitol, 10 mM PIPES (pH 6,5))
- centrifugation at 5.800 rpm, discard the supernatant and resuspend the pellet in 200 $\mu$l of buffer S
- add 12 $\mu$l of zymolyase (1 mg/ml)
- incubation for 1 hour at 37 °C and 230 rpm
- centrifugation at 5.800 rpm and discard the supernatant

After the protocol described above the solution was ready for a plasmid preparation with the ZR Plasmid Miniprep™ - Classic Kit (Zymo Research; Orange, USA) as described in the manual.

### 3.3.5. Membrane protein analysis with Membrane Protein Explorer (MPEx)

The programm MPEx can be found on the following website: http://blanco.biomol.uci.edu/mpex/
The tool is based on a sliding-window analysis which represents a given amino acid sequence as a sequence of numbers representing physical or statistical properties. Hence it is possible to explore the local hydropathy of a peptide. The value provides a measure for the free energy, which is required for the partitioning of an amino acid in the context of a peptide between water and membrane (Snider, Jayasinghe, Hristova, & White, 2009).
The tool in its version 3.2 was used to examine physicochemical properties of various constructs of Kesv. For this purpose the $\Delta G$ values have been estimated within the region of Kesv, e.g. the amino acid positions 111 - 115, which were randomized. Therefore the amino acid sequence from the end of the filter region up to the end of Kesv (length 34 aa) was inserted as input file for analysis by the MPex algorithm. The Wimley and White Scale for partitioning of a peptide into octanol was used for these calculations. This scale is a measure for the free energy of transfer of individual residues in a peptide from water to the bilayer hydrocarbon core (Jayasinghe, Hristova, & White, 2001).

## 3.4. Results

The yeast strain SGY1528 is deprived of its endogenous potassium uptake systems TRK1/TRK2. Thus the strain can survive only on media with a high potassium concentration (Tang *et al.*, 1995). On media with a low potassium concentration yeast growth can be rescued if the cells are supplied with a functional potassium channel, which is located in the plasma membrane (see Figure 8).

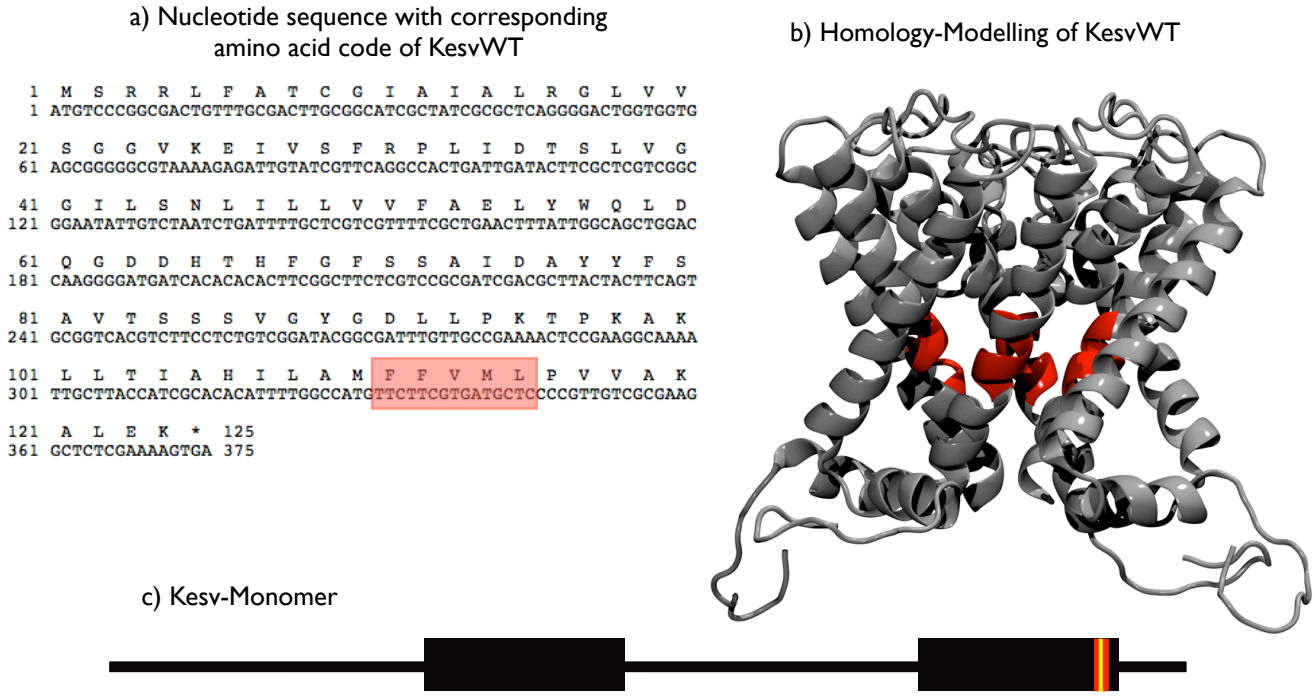


**Figure 9: Region of the rSDM-PCR in KesvWT.** The red square in the nucleotide/amino acid sequence of KesvWT (a) shows the region of the randomization from amino acid 111 - 115. (b) Homology-model of KesvWT presented as a tetramer. The red parts in the structure indicate the randomization region. In the cartoon of the Kesv monomer (c) the randomization region is highlighted in red; the yellow bar indicates the position in which an elongation was previously used to shift the sorting of the channel. Homology-model was kindly provided by Sven Blumenschein and Stefan Kast, Technische Universität Darmstadt 2008.

The wildtype form of the potassium channel Kesv (KesvWT), which is normally sorted to the mitochondria, was randomized in its second transmembrane domain from the amino acid in position 111 – 115 (see Figure 9). This was achieved by a special site directed mutagenesis PCR, which generated a library of randomized Kesv constructs (see 3.3.2). These constructs were used to transform the yeast strain SGY1528.

The Figure 10A shows a dense growth of transformed yeast cells on media with a non-selective high potassium concentration. On this plate all successfully transformed yeast cells can grow. The colonies found on the SD-URA+A+100$K^+$ plates were then transfered on selective plates with a low potassium concentration with the technique of replica plating (Figure 10B).

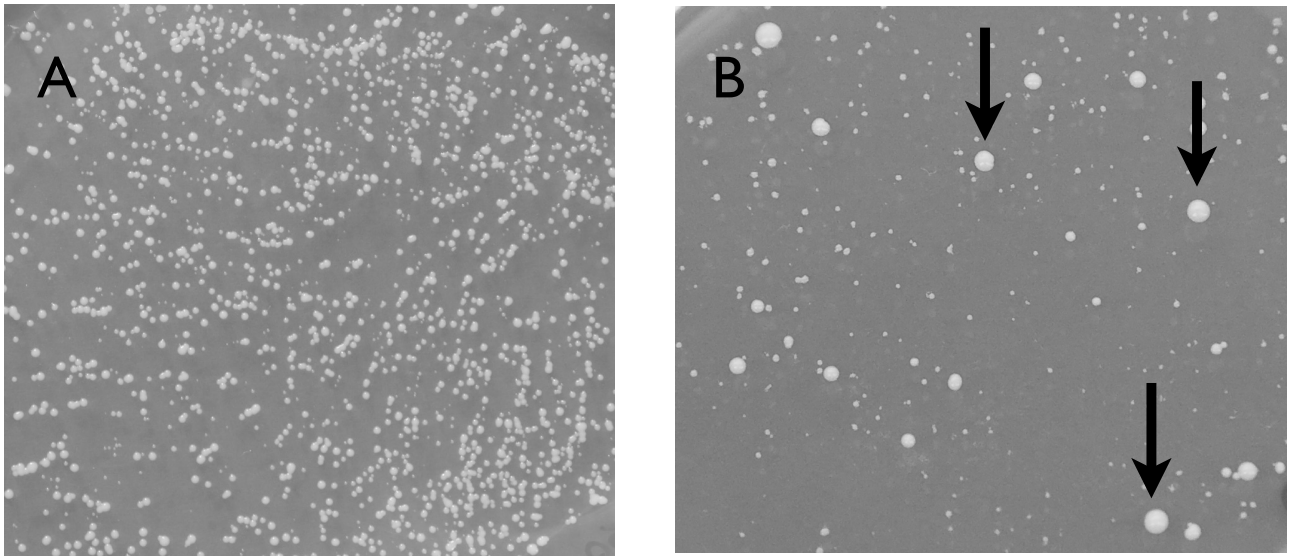


**Figure 10: Yeast growth on media with different potassium concentrations.** The data show the growth of a yeast strain deprived of its potassium uptake system. Only cells, which express a functional potassium uptake system can survive on selective media with a low potassium concentration. (**A**) After the yeast transformation there is a high density of yeast colonies on non-selective plates with SD-URA+A+100 $K^+$. After transferring the growing colonies on 1 mM $K^+$ selective media (**B**) only a few colonies (marked by arrows) survive on a background of dead yeast cells (graphic modified Guthmann, 2009).

In contrast to the growth on non-selective media, there is much less growth of colonies on the plate with 1 mM potassium. Theoretically on the selective plates with 1 mM potassium only transformed yeast cells with a functional randomized Kesv construct in the plasma membrane should survive. You can assume that these Kesv mutants are no longer sorted to the mitochondria but to the plasma membrane. There they are able to substitute the lack of endogenous potassium uptake systems (trk1Δtrk2Δ) in the yeast strain and they become therefore able to rescue growth under selective conditions. The big yeast colonies in Figure 10B highlighted by black arrows show successful growth of yeast mutants under selective conditions.

Yeast cells which express randomized constructs of Kesv, which are non-functional as channel or which are not sorted to the plasma membrane are not able to grow under these selective conditions. These dead yeast cells are still slightly visible as a background of tiny white dots; they must have been carried over during the replica plating procedure (Figure 10B).

It is expected that the randomization of the Kesv sequence by PCR will have an inherent technical bias for some amino acids over others. To obtain information on the variability of the randomization process independent on whether the resulting channel mutants are sorted to the plasma membrane or not sequences of yeast colonies grown on non-selective SD-URA+A+100K$^+$ plates have been analysed. Unfortunately nearly all of the samples could not be properly analyzed because of bad purity, i.e. after the yeast plasmid preparation the samples were contaminated with RNA or proteins; this interfered with the sequencing of the samples. To obtain the desired information from other sources randomized sequences from other experimental steps have been collected. The data in Figure 11 present a mix of sources for positive sequence analysis obtained from yeast colonies from SD-URA+A+100K$^+$ plates or 1 mM selective plates, that were made during the whole project.

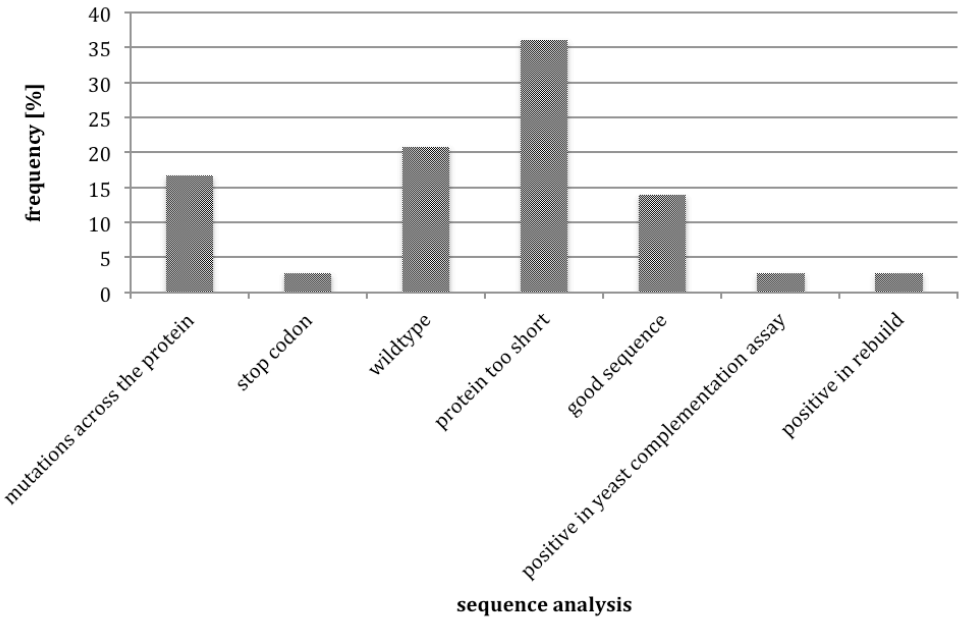


**Figure 11: Results of the sequence analysis**. The graphic shows that most of the sequences analyzed did not provide a sequence, which could be properly analyzed. Most of the data could not be used because it contained the wildtype sequence or mutations were occurring across the whole protein. Frequently the sequences were also shorter than the Kesv sequence.

From 115 sequences only 72 sequences showed a robust result. The others failed because of the aforementioned bad purity. Figure 11 provides an overview of the 72 sequences, which were successfully analyzed. The data contain many sequences (n=15) in which the randomized sequence is identical to the wildtype or where the whole protein is mutated in many different regions (n=12); the latter differ more from the wildtype than only in the randomized region. In other samples the sequences were too short and stopped before the randomized region. All the aforementioned sequences were discarded.

The data in Figure 11 show that only a few samples provided sequences, which could be used for further analysis. The variability of amino acids, which is generated by the randomization in these sequences (Figure 11 called “good sequences”), is illustrated in the following Figure 12. Also the sequences with a stop codon are included.

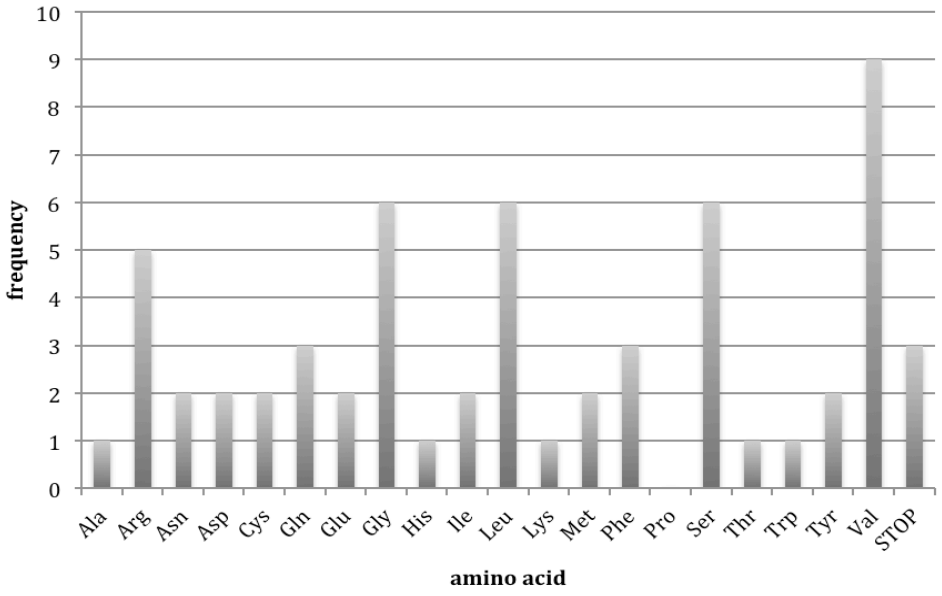


**Figure 12: Overview of the found amino acids.** Only the region from 111 - 115 of different sequences is presented. Amino acids like valine, glycine, leucine, serine occured most. Proline didn’t occure but a stop codon was found.

The data show that the randomization is indeed biased. Especially the amino acids valine, serine, leucine, glycine and arginine occurred most frequently. Only one amino acid - proline - is not found. Notably also three stop codons were generated. The low number of sequences, which were tested here, does not allow a complete statistical analysis for the probability of an amino acid in the randomized area. But the data show that all amino acids can in principle be generated by the randomization; only proline has a low probability to occure. The reason why some amino acids occurred more frequently than others might be due to the annealing temperature of the rSDM-PCR.

The following Table 2 presents the amino acid sequences in the randomized region from position 111 - 115, which were successfully analyzed:

**Table 2: Found sequences.** Only the region from 111 – 115 of Kesv is shown in its nucleotide sequence and the corresponding amino acid sequence.

| construct | nucleotide sequence | amino acid sequence |
|---|---|---|
| Kesv Random1 | TGGCTGAAGGTGAGT | Trp-Leu-Lys-Val-Ser |
| Kesv Random2 | TCTGGGACTGTGCTG | Ser-Gly-Thr-Val-Leu |
| Kesv Random3 | TATGGCAGTATGGCG | Tyr-Gly-Ser-Met-Ala |
| Kesv Random4 | GTGTTCGGGGTGAAT | Val-Phe-Gly-Val-Asn |
| Kesv Random5 | GTGCAACAAGTGGGG | Val-Gln-Gln-Val-Gly |
| Kesv Random6 | AATAGGCAGGGGCGT | Asn-Arg-Gln-Gly-Arg |
| Kesv Random7 | AGTATTATTGTGCTG | Ser-Ile-Ile-Val-Leu |
| Kesv Random8 | AGGAGGGATGATCGG | Arg-Arg-Asp-Asp-Arg |
| Kesv Random9 | TATGAGCATATGTCGC | Tyr-Glu-His-Met-Ser |
| Kesv Random10 | CTGGAACTGTGCTGCC | Leu-Glu-Leu-Cys-Cys |
| Kesv Random11 | GGCTGAGTGTGATTC | Gly-stop-Val-stop-Phe |
| Kesv Random12 | TTCGTGTGAAGTCTC | Phe-Val-stop-Ser-Leu |

In previous work by Guthmann, 2009 and Baumeister, 2010, in which the basic randomization protocol was established, the resulting sequences were analyzed directly after the replica plating; the sequences were not further tested in a yeast complementation assay. In the present study it occurred that many mutants, which were obtained after the replica plating were indeed false positives. These mutants were unable to rescue yeast growth in a subsequent complementation assay. The following Figure 13 illustrates such a yeast complementation assay in which some Kesv mutants did (KesvR1, KesvR2) and others did not (KesvR3, KesvR4) rescued growth.

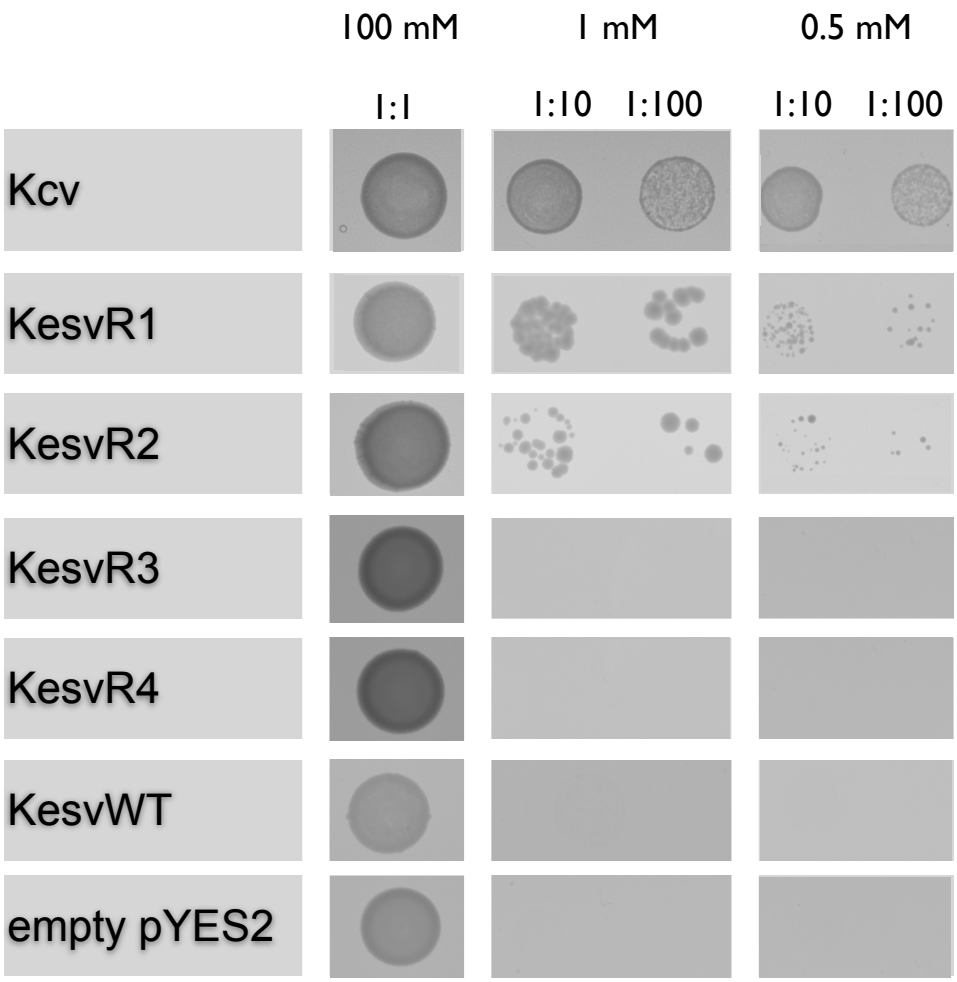


**Figure 13: Yeast complementation assay.** The assay was done with three different potassium concentrations in the media: 100 mM KCl (non-selective condition), 1 mM and 0.5 mM KCl (selective condition). Kcv, Kesv wildtype (KesvWT) and empty pYES2 vector (empty pYES2) serve as controls. The randomized constructs are KesvR1, KesvR2, KesvR3 and KesvR4. All constructs were spotted in different dilutions: 1:1 (undiluted), 1:10 and 1:100. Growth for 2 days.

The results of the yeast complementation assay in Figure 13 show that all 7 constructs can grow on non-selective media with a 100 mM potassium concentration. But in contrast on the selective media (with 1 mM respectively 0.5 mM potassium) only the yeast cells transformed with the Kcv construct and two of the randomized Kesv constructs (KesvR1 and KesvR2) are able to grow. Obviously the Kesv wildtype and the empty pYES2 vector fail to grow on a medium with a low potassium concentration. Important to note is that also the randomized Kesv constructs KesvR3 and KesvR4, which passed the first selection step of replica plating on selective media, are unable to rescue yeast growth. The results of these experiments suggested that the screening method is not rigid enough for eliminating false positives after the replica plating. The growth on 1 mM selective plates after replica plating can only be seen as a pre-selection.

For this reason all the sequences, which gave positive result in a yeast complementation assay, were rebuild and tested in a liquid yeast complementation assay to confirm the positive rescue in a robust way. As a result of this procedure probably not all the possible mutants, which rescue yeast growth, are collected. But the few sequences, which are obtained, are for sure real positives.

Liquid cultures with a low potassium concentration (0.5 mM) were therefore inoculated with a yeast suspension in the dilution 1:100. The respective yeasts were transformed with different channel constructs. Subsequently the optical density ($OD_{600}$) was measured immediately after inoculation (0 h) and again after 24 h and 48 h hours as described in chapter 3.3.3.

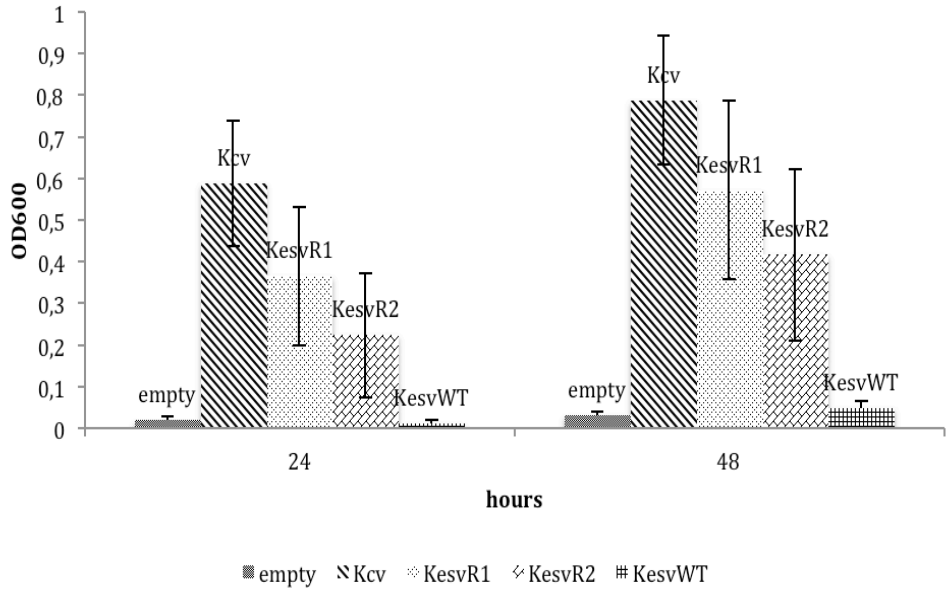


**Figure 14: Two randomized Kesv channels are able to rescue yeast growth.** Increase in optical densities at 600 nm ($OD_{600}$) of yeast cultures grown for 24 h and 48 h in liquid selective medium with 0.5 mM potassium. The cultures were inoculated with yeast transformed with the control constructs Kcv, KesvWT and empty pYES2 vector and with the randomized sequences KesvR1, KesvR2. Data are mean +/- standard deviation of n = 88 measurements for yeasts transformed with Kcv, KesvWT and empty pYES2 vector and n = 66 for yeast transformed with KesvR1, KesvR2.

The yeast growth in liquid culture confirms the results from the complementation assay on agar plates (see Figure 13). Again cells transformed with the negative controls KesvWT or the empty pYES2 vector fail to grow under selective conditions with a low potassium concentration of 0.5 mM. Cells expressing the positive control Kcv grow best. Cells transformed with KesvR1 or KesvR2 grow better than the negative controls but not as good as Kcv.

To test the significance between differences in the measured $OD_{600}$ values of the different constructs a Wilcoxon-Test was performed to compare the randomized constructs KesvR1 and KesvR2 with the

reference protein KesvWT and Kcv. The Wilcoxon-Test showed that all values are significantly different from the reference channels.

The data of the yeast complementation assays imply that the two randomized Kesv constructs (KesvR1 and KesvR2) can rescue yeast growth; by comparison they are not as efficient as Kcv but clearly better than KesvWT or the empty pYES2 vector respectively. The data suggest that the randomized Kesv constructs are now sorted to the plasma membrane where they can complement the potassium uptake system. Further support for this hypothesis by microscopic studies is presented in chapter 4.4.

On the basis of the aforementioned criteria to eliminate potential false positives the majority of sequences were discarded leaving only a few sequences for further analysis. With the combination of two rounds of selective growth tests on selective media two mutants that conferred growth to the yeast cells have been found. Finally the results show two Kesv mutants, which redirect Kesv from mitochondria to the plasma membrane and are able to rescue yeast growth. The nucleotide sequences and the corresponding amino acid sequences can be found in Table 3.

**Table 3: Two Kesv mutants positively redirect Kesv from mitochondria to the plasma membrane.** Rebuild sequences, which show a positive effect in the yeast complementation assay. Only the region from position 111 – 115 is presented. The amino acids valine, serine and leucine appear in both sequences. Amino acids, which are identical to the wildtype are highlighted in grey. Amino acids, which are identical but different in position are shown in bold.

| construct | nucleotide sequence | amino acid sequence |
|---|---|---|
| Kesv wildtype | TTCTTCGTGATGCTC | Phe-Phe-**Val**-Met-Leu |
| Kesv Random1 | TGGCTGAAGGTGAGT | Trp-**Leu**-Lys-**Val**-Ser |
| Kesv Random2 | TCTGGGACTGTGCTG | Ser-Gly-Thr-**Val**-Leu |

Table 3 and Figure 15 show that especially amino acids with a hydrophobic side chain like valine, leucine but also amino acids with a polar uncharged side chain like serine appear in both sequences. Also the aromatic amino acid tryptophan was found.
Notably also the amino acid lysine, with a positively charged side chain, appears.
A scrutiny of the data shows that valine is found in both randomized sequences at position 114.

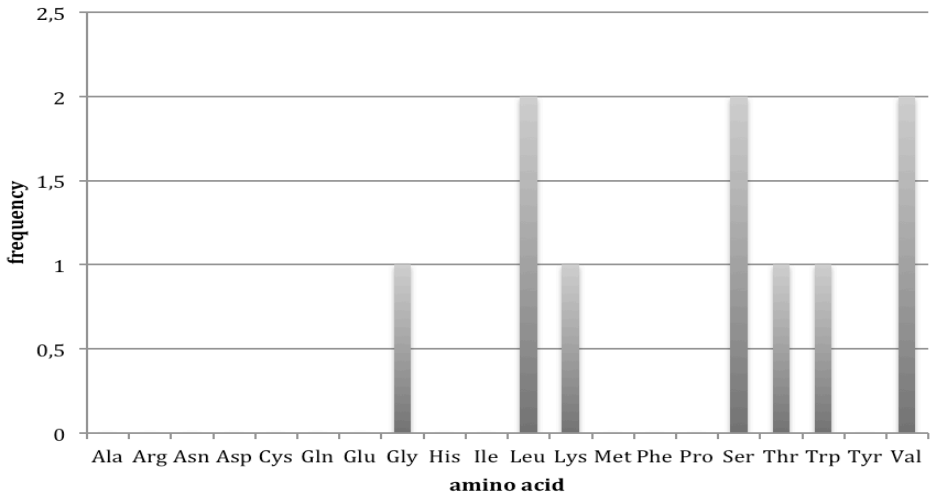


**Figure 15: Variability of found amino acids in the rebuild that redirect Kesv from mitochondria to the plasma membrane.** The amino acids valine, serine and leucine appear in both sequences.

In a previous study in which the sorting of Kesv was altered by an elongation of its second transmembrane domain (Balss *et al.*, 2008) a valine was inserted at position 114. To test whether a valine in this position is sufficient for an alteration in sorting a single point-mutation of Kesv wildtype in position 114 was created; a methione was here exchanged for a valine (KesvM114V).

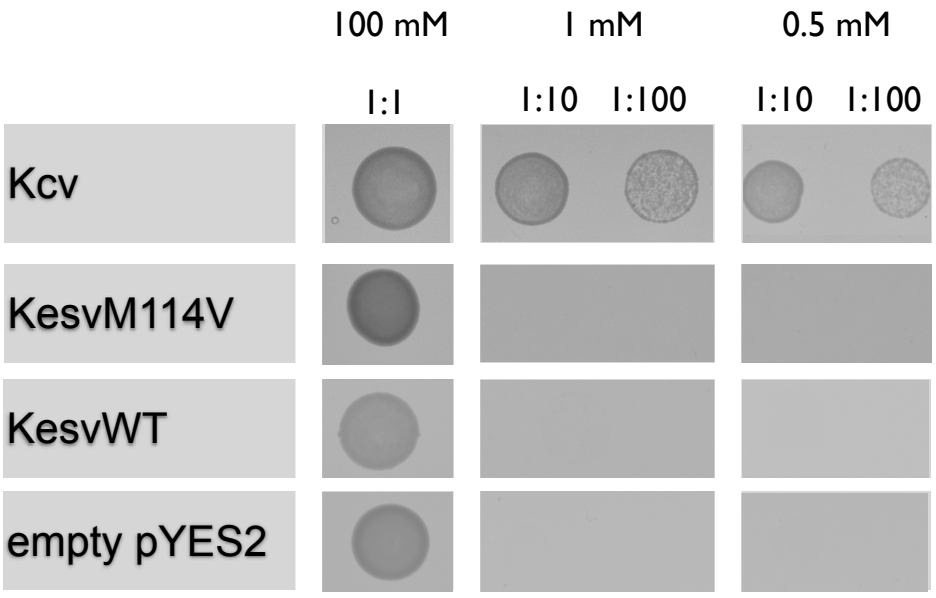


**Figure 16: Valine in position 114 is not sufficient for a shift in Kesv sorting**. The assay was done with three different potassium concentrations in the media: 100 mM KCl (non-selective condition), 1 mM and 0.5 mM KCl (selective condition). Yeast cells transformed with Kcv, Kesv wildtype (KesvWT) and empty pYES2 vector (empty pYES2) serve as controls. Yeast transformed with KesvM114V grow under non-selective conditions but not under selective conditions. All constructs were spotted in different dilutions: 1:1 (undiluted), 1:10 and 1:100. Yeast was grown for 2 days.

A test of this mutant in the yeast complementation assay (Figure 16) shows that it is not able to rescue yeast growth under selective conditions. This indicates that despite of its frequent appearance in position 114 in the randomized mutants, valine is not sufficient by itself to alter the targeting of Kesv.

## 3.5. Discussion

The primary structures of the two viral potassium channels Kcv and Kesv are very similar. In contrast to their high degree of structural similarity the most outstanding difference in heterologous expression systems is their cellular localization: Kcv is present in the plasma membrane while Kesv is in the mitochondria (Balss *et al.*, 2008). Previous experiments have shown that the two channels may exhibit subtile differences in the length of their outer transmembrane domain. The relevance of this difference in TMD2 for sorting was confirmed by experiments in which this domain of Kesv was elongated. This had the effect that the sorting of the mutant channel was redirected from the mitochondria to the plasma membrane (Balss *et al.*, 2008). In the context of these data the question immerged whether the change in sorting requires a physical extension of TMD2. Alternatively the extension could also modify the local physicochemical properties of the transmembrane domain and affect in this way the sorting. To tackle the question whether it is possible to alter the sorting of Kesv without an extension of TMD2 a combined method of sequence randomization and functional screening was employed. With this approach it is possible to search in an unbiased manner for mutations in TMD2, which affect trafficking of Kesv. Using a randomized site directed mutagenesis PCR a variety of different constructs could be created (Figure 12) and tested with a yeast complementation assay. The most important result of this study is that two Kesv mutants could be identified, which are able to rescue yeast growth under selective conditions (Figure 14 and Table 3). The results of these experiments clearly show that the outer transmembrane domain of Kesv contains sorting information for the channel. The trafficking route of the protein can be redirected from the mitochondria into the secretory pathway without a real extension of the second transmembrane domain. Hence it seems more likely that the physicochemical flavor of the domain is more important than the length of membrane spanning. This conclusion is consistent with the finding that in previous experiments the extension of TMD2 was only affecting sorting when it was done in the lower part of the transmembrane domain (Balss *et al.*, 2008). If the parameter length would have been the only determining factor such site specificity would have not been expected.

The detailed analysis of the mutants, which were generated in the randomization procedure, shows that the method generated many false positives. After eliminating obvious false positives such as mutants with stop codons or mutants, which were shorter than the Kesv protein, there were still several candidates, which were not able to complement yeast growth. The results of these experiments show that yeast cells may have been transfected with more than one mutant channel and that the one, which was sequenced was not the channel, which conferred yeast growth. On the background of these

data more false positive were eliminated by rebuilding the sequence, which emerged from the randomization/selection process, by distinct point mutations. With this long but careful procedure it was finally possible to extract two sequences, which are definitely able to rescue yeast growth on selective media. In this way it is not possible to take advantage of the randomization method, which generally provides a large library of mutants. But the few sequences, which were extracted, are at least reliable.

The functional tests with the two Kesv mutants with randomized sequences in TMD2 confirm that this channel can be sorted to the plasma membrane. The analysis of the respective sequences does however not provide a clear answer to the question on the amino acid flavor, which is responsible for this shift in sorting. Test experiments have shown that a valine, which is frequently found in position 114, is by itself not responsible for this shift. A scrutiny of the two positive sequences shows that both contain valine, leucine and serine. Maybe it is not important where these three amino acids in the second transmembrane domain appear, but that they appear in this constellation. Also in the sequence of Kcv wildtype valine and leucine can be found. Compared to the found randomized sequences of Kesv the valine has the corresponding position in Kcv respectively once leucine is at the corresponding position (see grey background markers in Table 4).

**Table 4: Comparison of the found positive sequences with Kesv respectively Kcv wildtyp.** The amino acids valine and leucine are highlighted with a grey background. Only region 111 – 115 of Kesv is shown.

| construct | nucleotide sequence | amino acid sequence |
|---|---|---|
| Kcv wildtype | TTCTTCATCGTTCTA | Phe-Phe-Ile-Val-Leu |
| Kesv wildtype | TTCTTCGTGATGCTC | Phe-Phe-Val-Met-Leu |
| Kesv Random1 | TGGCTGAAGGTGAGT | Trp-Leu-Lys-Val-Ser |
| Kesv Random2 | TCTGGGACTGTGCTG | Ser-Gly-Thr-Val-Leu |
| Kesv113VVV | TTCTTCGTGGTGGTG | Phe-Phe-Val-Val-Val |

In a recent study the propensity of an α-helical polypeptide to insert in a membrane was examined as a function of the individual amino acids which form the core of this helix (Hessa *et al.,* 2009). The result of this study was a ranking of the energy, which is required to insert any of the 20 amino acids into a membrane. The analysis of the present results shows that many of the mutated amino acids in the randomized area augment the propensity for the part of TMD2 to integrate into the membrane.

Compared to randomized sequences found in this study leucine and valine show a high propensity to be inserted into the membrane (see Figure 17).

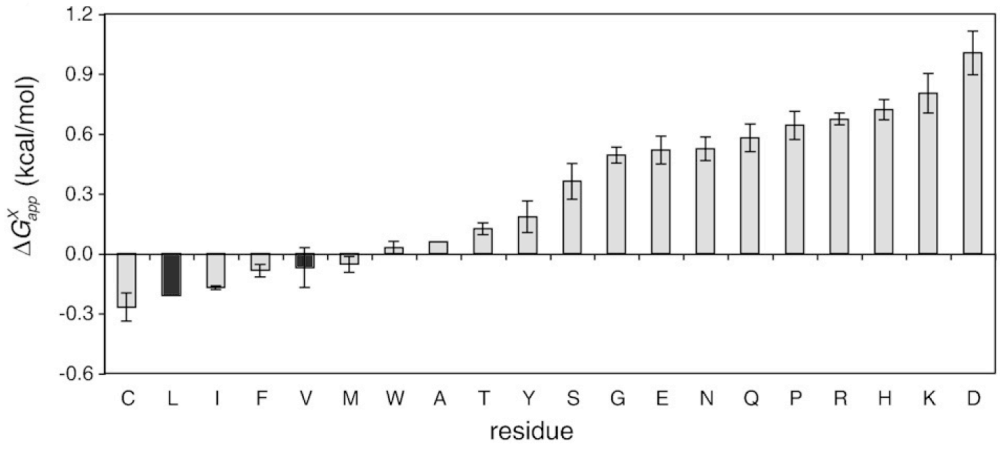


**Figure 17: Hydrophobicity scale for yeast.** Shown is the probability with that an amino acids is inserted into the membrane of yeast. Leucine and valine are marked with black bars and are well inserted into the membrane of yeast. (graphic modified Hessa *et al.*, 2009).

The present results however cannot fully interpreted in this manner. One of the randomized sequences contains a lysine, e.g. an amino acid, which requires a very high energy for insertion into the membrane. This finding argues against the hypothesis that a more hydrophobic flavor of the domain alone is sufficient for the alteration in sorting. Still it is possible that valine and leucine could compensate the properties of lysine, especially the positively charged side chain.

The amino acid lysine at position 113 may also contribute less to the energy for membrane insertion than apparent from Figure 17. The lysine is only five residues away from the end of the second transmembrane domain. Maybe the lysine with its positively charged side chain is in this position able to “snorkel”. In this case the core of the amino acid is inside the bilayer while the charged side chain is in the bilayer/water interface. This could support an orientation of the Kesv mutant in the plasma membrane (Gebhardt *et al.*, 2012).

There are computational tools available for analysing sequences in order to predicit the cellular localization of a protein. TargetP for example is such a tool. In order to examine whether the mutations in TMD2 of Kesv contain any information, which is recognized by these algorithms, the locations of Kcv, KesvWT and its mutants were analyzed by TargetP (Emanuelsson, Brunak, Von Heijne, & Nielsen, 2007). The results are shown in Table 5.

**Table 5: Prediction of the localization of the proteins based on TargetP**. The higher the score the more reliable. mTP stands for mitochondrial targeting peptide, SP for signal peptide. LOC stands for the final predicted localization of the protein and S for the secretory pathway.

| construct | mTP | SP | LOC |
|---|---|---|---|
| Kcv | 0.020 | 0.935 | S |
| KesvWT | 0.628 | 0.695 | S |
| KesvR1 | 0.653 | 0.729 | S |
| KesvR2 | 0.658 | 0.719 | S |

The algorithem correctly predicts the localization of Kcv; it is predicted to be in the plasma membrane. Already in the case of Kesv wildtype the predicted localization in the mitochondria occurs with a low probability. Important in the context of the present data is the finding, that the algorithm does not exhibit any apprechiable differences between KesvWT and the randomized mutants. The result of this analysis shows that the algorithm, which is based on established sorting information, does not consider the structural changes, which affected here the localization of Kesv. As expected from a search in the literature the sorting signal in TMD2 of Kesv is not a canonical signal.

In a previous study it was speculated that a particularly short second transmembrane domain of Kesv is crucial for its sorting to the mitochondria (Balss *et al.,* 2008). This short transmembrane domain of Kesv in comparison with other $K^+$ channels was predicted by the algorithm TMHMM 2.0 (*transmembrane prediction using Hidden Markov models*). The presumed relevance of this transmembrane domain for sorting was supported by experimental data, which revealed a shift in sorting of Kesv to the plasma membrane after extending the respective transmembrane domain (Balss *et al.,* 2008). In the context of these data it is interesting to analyze here with the TMHMM 2.0 algorithm, whether the mutations in the sorting mutants KesvR1 and KesvR2 also cause an extended transmembrane length. The respective analysis predicts that the mutant KesvR1 has the same length of the second transmembrane domain as the KesvWT channel. In the case of the KesvR2 mutant the algorithm even fails to recognize the second transmembrane domain. The result of this analysis implies that the length of the second transmembrane domain is not responsible for the shift in sorting of these mutants; it is more likely that the character of the amino acids in the respective region are important for the sorting.

The finding that the sorting of Kesv can be affected by mutations in the C-terminal part of the protein implies that the physicochemical flavor of this domain could be crucial. Since the respective domain is

part of a transmembrane domain a computational approach was employed, which focussed on the physicochemical character of this type of domains. The software Membrane Protein Explorer (MPEx), which is described in materials and methods, can predict on the basis of experimental data the ΔG value, which is required for the insertion of a peptide into a membrane (Snider *et al.*, 2009). Figure 18 shows the position dependent ΔG values predicted from the MPEx algorithm for the crucial domain between amino acid 111 - 115 within the second transmembrane domain of various Kesv constructs. The plot in Figure 18 shows that all values decrease gradually towards the C-terminus. This is consistent with the fact that the respective domain is at the downstream end of the transmembrane domain. Interesting to note is that the ΔG values for the two positive sorting mutants (KesvR1 and KesvR2) are in spite of their difference in the primary sequence quasi identical. Importantly the values for the two mutants are systematically lower than those of the KesvWT channel.

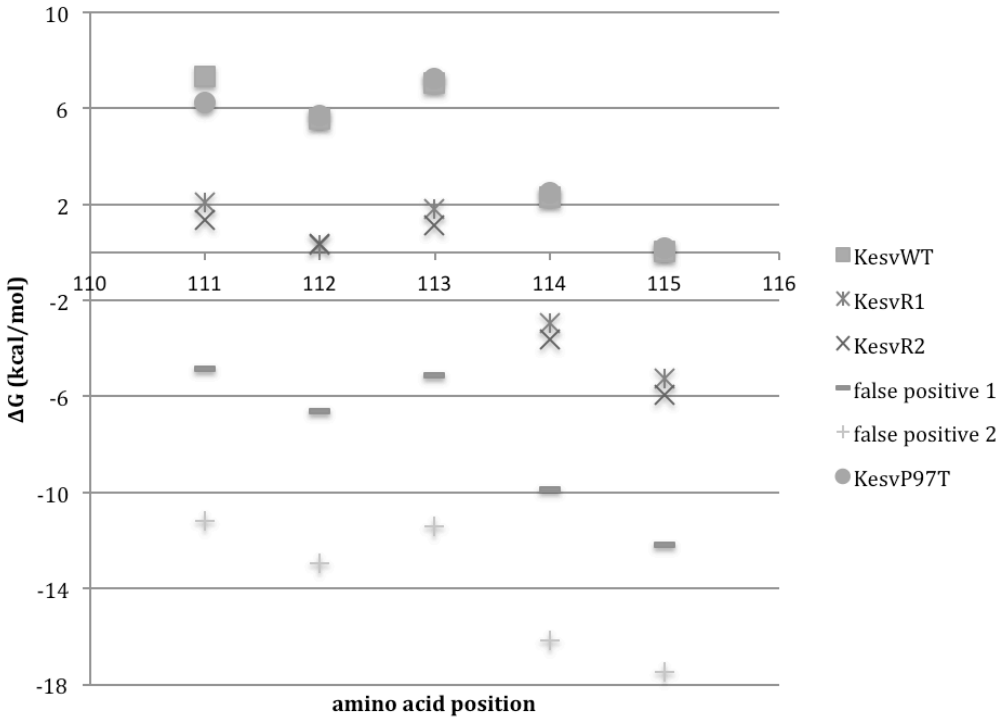


**Figure 18: Free energy (ΔG) values for the partitioning of amino acids in position 111 – 115 in different Kesv constructs from water into membranes.** The ΔG values were obtained for KesvWT, the two positive sorting mutants (KesvR1 & R2), two false positive mutants (false positive 1 & 2) and one Kesv mutant (P97T) from previous experiments (Balss *et al.*, 2008). The ΔG values estimates the energy, which is required for the partitioning of an amino acid in a peptide, from water into a membrane. These values were determined with the software Membrane Protein Explorer (MPEx). Note that the ΔG values of constructs, which are sorted to the mitochondria are high. Channels, which are sorted into the secretory pathway reveal a low ΔG value. This is the case for the mutants KesvR1 and R2, which were positively identified as sorting mutants and for the mutants, which were considered as false positives after multiple rounds of yeast complementation assays.

The second transmembrane domain of Kesv is important for the sorting of the channel (Balss *et al.*, 2008). In spite of the high identity in this region, KesvWT and Kcv differ in five amino acid positions in this domain. These are the positions P97, K98, L102, A109 and P116 in Kesv. To test the relevance of these positions for sorting, a Kesv mutant was generated in which these amino acids were converted into the corresponding amino acids of Kcv (named KesvP97T). The resulting mutant P97T+K98G+L102C+A109T+P116T was still sorted to the mitochondria (Balss *et al.*, 2008). Despite these changes this mutant (KesvP97T) remains in the mitochondria (Balss *et al.*, 2008). An analysis of the mutant with the algorithm MPEx shows that the ΔG values of this mutant are still similar to that of KesvWT (Figure 18). This is consistent with its mitochondrial sorting.

In contrast to the aforementioned constructs the false positive Kesv mutants, which were obtained from a randomization of position 111 - 115 after yeast complementation, show ΔG values, which are even lower than those of the positive sorting mutants KesvR1 and KesvR2.

Collectively the computational analysis of the different Kesv sequences shows a positive correlation between the ΔG values for the partitioning of an amino acid within a transmembrane domain into a membrane and the sorting of the Kesv channel. If the ΔG value is high in the critical region the channel is sorted to the mitochondria. A lowering of the value by mutagenesis apparently redirects sorting into the secretory pathway. It is worth noting that the lower ΔG value was found with channel constructs, which were positively identified as sorting mutants but also with those considered here as false positives. In the context of these data it is still possible that the false positives are indeed successful sorting mutants. The rigid selection procedure, which was applied in the identification of the mutants, may have eliminated these mutants from the list of positive sorting mutants.

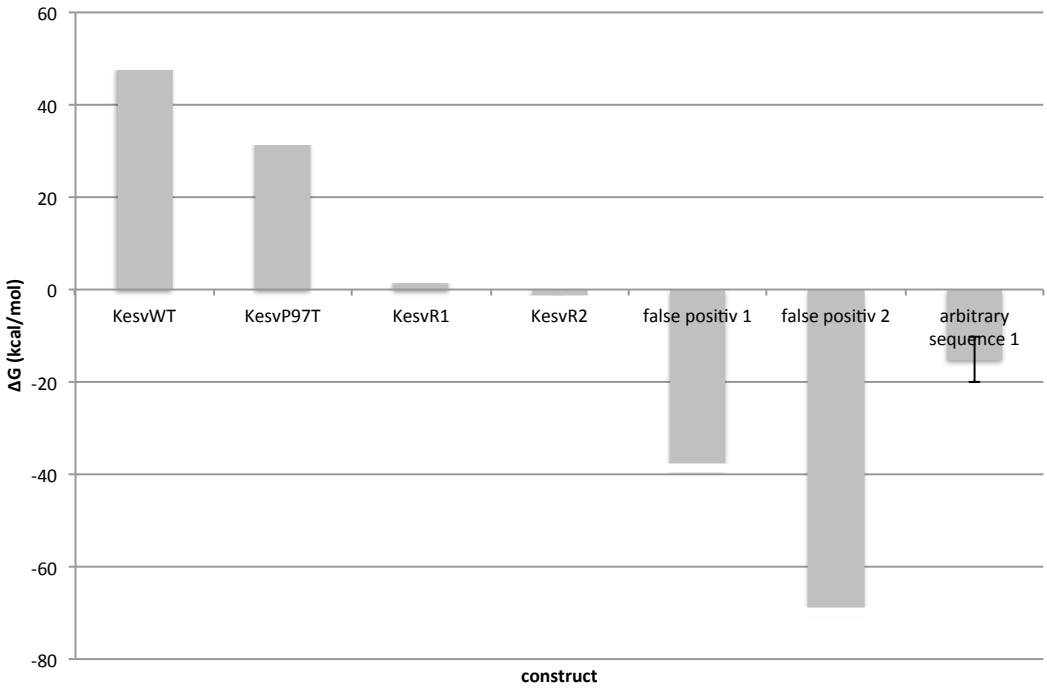


**Figure 19: Added up ΔG values from position 111 – 115 of different Kesv constructs.** The ΔG values were obtained for KesvWT, KesvP97T, the two positive sorting mutants (KesvR1 & R2), two false positive mutants (false positive 1 & 2) and 10 arbitrary sequences (arbitrary sequence). The arbitrary sequences are shown as mean +/- standard deviation. Note that the added up ΔG values from position 111 - 115 of the constructs, which are sorted to the mitochondria, are high. Channels, which are sorted into the secretory pathway reveal a ΔG value close to zero. Constructs which were considered as false positives after multiple rounds of yeast complementation assays and the arbitrary sequences show a high negative ΔG value. The values were determined with the software Membrane Protein Explorer (MPEx).

A summation of the ΔG values from the amino acid position 111 - 115 in Kesv again shows that a sorting of a channel to the mitochondria is correlated with a high ΔG value (Figure 19 KesvWT and KesvP97T). In contrast the two sorting mutants (KesvR1 & R2), which are directed to the secretory pathway show a value close to zero. In order to evaluate the significance of the high ΔG values in the channels, which are sorted to the mitochondria, in silico 20 Kesv mutants with random sequences between amino acids 111 – 115 have been generated. If a high ΔG value is significant for mitochondrial sorting the respective values of the random mutants should be lower. Indeed an analysis of the random mutants reveals ΔG values, which are distinctly lower than those of the KesvWT channel. The result of this analysis suggests an evolutionary pressure on the critical part of the transmembrane domain of Kesv for a successful sorting to the plasma membrane.

## 3.6. Conclusion

With the presented method it was possible to generate in a distinct region of the viral potassium channel Kesv mutants with randomized sequences. In combination with a robust functional screening system, which only allows yeast cells to grow under selective conditions when a functional Kesv channel is redirected from the mitochondria to the plasma membrane, it was possible to isolate sorting mutants. From a pool of potentially $20^5$ possible mutants two mutants could be found. These two mutants were able to rescue yeast growth in a yeast complementation assay indicating that the localization of Kesv has changed from mitochondria to the plasma membrane.

But within these mutations a general pattern couldn't be found explaining the reason for the change in sorting. This indicates once more the complexity of the targeting of the potassium channel Kesv.

But it also raises the question how large is the variability of the generated mutants in the rSDM-PCR because 35 % of the sequence material couldn't be analyzed respectively 37 % of the analyzed sequences showed a too short protein directly in the region of the randomization.

## 3.7. References


Balss, J., Papatheodorou, P., Mehmel, M., Baumeister, D., Hertel, B., Delaroque, N., Chatelain, F. C., et al. (2008). Transmembrane domain length of viral K+ channels is a signal for mitochondria targeting. *Proceedings of the National Academy of Sciences of the United States of America*, *105*(34), 12313–8

Barlowe, C. (2003). Signals for COPII-dependent export from the ER: what's the ticket out? *Trends in Cell Biology*, *13*(6), 295–300

Baumeister, D. (2010). *Einfluss der Transmembrandomänen auf die Funktion und Sortierung von Kaliumkanälen*. Technische Universität Darmstadt.

Bertl, a, Bihler, H., Kettner, C., & Slayman, C. L. (1998). Electrophysiology in the eukaryotic model cell Saccharomyces cerevisiae. *Pflügers Archiv : European journal of physiology*, *436*(6), 999–1013.

Bertl, A., Slayman, C. L., & Gradmann, D. (1993). Gating and Conductance in an Outward-Rectifying K+ Channel from the Plasma Membrane of Saccharomyces cerivisiae. *J Membr Biol*, *132*(3), 183–199.

Emanuelsson, O., Brunak, S., Von Heijne, G., & Nielsen, H. (2007). Locating proteins in the cell using TargetP, SignalP and related tools. *Nature Protocols*, *2*(4), 953–971.

Etten, J. L. Van, Graves, M. V, Boland, W., & Delaroque, N. (2002). Phycodnaviridae – large DNA algal viruses Brief Review. *Archives of Virology*, 1479–1516.

Gaber, R. F., Styles, C. a, & Fink, G. R. (1988). TRK1 encodes a plasma membrane protein required for high-affinity potassium transport in Saccharomyces cerevisiae. *Molecular and cellular biology*, *8*(7), 2848–59.

Gebhardt, M., Henkes, L. M., Tayefeh, S., Hertel, B., Greiner, T., Van Etten, J. L., Baumeister, D., et al. (2012). Relevance of lysine snorkeling in the outer transmembrane domain of small viral potassium ion channels. *Biochemistry*, *51*(28), 5571–9.

Guthmann, T. (2009). *Randomisierungsstudien am viralen Kaliumkanal Kcv*. Technische Universität Darmstadt.

Hegde, R. S., & Keenan, R. J. (2011). Tail-anchored membrane protein insertion into the endoplasmic reticulum. *Nature reviews. Molecular cell biology*, *12*(12), 787–98.

Hessa, T., Reithinger, J. H., Von Heijne, G., & Kim, H. (2009). Analysis of Transmembrane Helix Integration in the Endoplasmic Reticulum in S. cerevisiae. *Journal of Molecular Biology*, *386*(5), 1222–1228.

Jayasinghe, S., Hristova, K., & White, S. H. (2001). Energetics, stability, and prediction of transmembrane helices. *Journal of molecular biology*, *312*(5), 927–34.

Jäckel, C., Kast, P., & Hilvert, D. (2008). Protein design by directed evolution. *Annual review of biophysics*, *37*(1), 153–173.

Kang, M., Moroni, A., Gazzarrini, S., & Van Etten, J. L. (2003). Are chlorella viruses a rich source of ion channel genes? *FEBS Letters*, *552*(1), 2–6.

Karniely, S., & Pines, O. (2005). Single translation--dual destination: mechanisms of dual protein targeting in eukaryotes. *EMBO reports*, *6*(5), 420–5.

Ma, D., Zerangue, N., Lin, Y. F., Collins, a, Yu, M., Jan, Y. N., & Jan, L. Y. (2001). Role of ER export signals in controlling surface potassium channel numbers. *Science (New York, N.Y.)*, *291*(5502), 316–9.

Minor, D L, Masseling, S. J., Jan, Y. N., & Jan, L. Y. (1999). Transmembrane structure of an inwardly rectifying potassium channel. *Cell*, *96*(6), 879–91.

Minor, Daniel L. (2009). Searching for interesting channels: pairing selection and molecular evolution methods to study ion channel structure and function. *Molecular bioSystems*, *5*(8), 802–10.

Miyazaki, E., & Kida, Y. (2005). Switching the sorting mode of membrane proteins from cotranslational endoplasmic reticulum targeting to posttranslational mitochondrial import. *Molecular biology of the …*, *16*(April), 1788–1799.

Moroni, A., Viscomi, C., Sangiorgio, V., Pagliuca, C., Meckel, T., Horvath, F., Gazzarrini, S., et al. (2002). The short N-terminus is required for functional expression of the virus-encoded miniature K(+) channel Kcv. *FEBS Letters*, *530*(1-3), 65–69.

Pelkmans, L., & Helenius, A. (2003). Insider information: what viruses tell us about endocytosis. *Current Opinion in Cell Biology*, *15*(4), 414–422.

Petrezsélyová, S., Ramos, J., & Sychrová, H. (2011). Trk2 transporter is a relevant player in K+ supply and plasma-membrane potential control in Saccharomyces cerevisiae. *Folia microbiologica*, *56*(1),

Plugge, B. (2000). A Potassium Channel Protein Encoded by Chlorella Virus PBCV-1. *Science*, *287*(5458), 1641–1644.

Ramos, J., Alijo, R., Haro, R., & Rodriguez-Navarro, a. (1994). TRK2 is not a low-affinity potassium transporter in Saccharomyces cerevisiae. *Journal of bacteriology*, *176*(1), 249–52.

Snider, C., Jayasinghe, S., Hristova, K., & White, S. H. (2009). MPEx: a tool for exploring membrane proteins. *Protein science : a publication of the Protein Society*, *18*(12), 2624–8.

Söllner, T. H. (2004). Intracellular and viral membrane fusion: a uniting mechanism. *Current opinion in cell biology*, *16*(4), 429–35.

Tang, W., Ruknudin, a, Yang, W. P., Shaw, S. Y., Knickerbocker, a, & Kurtz, S. (1995). Functional expression of a vertebrate inwardly rectifying K+ channel in yeast. *Molecular biology of the cell*, *6*(9), 1231–40.

# 4. Chapter 3 – A method for sensitive and robust detection of plasma membrane proteins

## 4.1. Abstract

The observation of membrane proteins in their native environment is a challenging task that is based more than ever due to high-resolution analysis on the preparation of an authentic sample. In this chapter an optimized method for isolating the plasma membrane of living cells in a simple way is described. The method is compatible with a variety of cell-lines and even under conditions where the majority of the protein is located in intracellular compartments and only a small amount reaches the plasma membrane, the method is able to reliably report the plasma membrane location of proteins with high precision. Using reference proteins, which locate to various cellular compartments the purity of the isolated plasma membrane was verified and the localization of several membrane proteins was illustrated.

## 4.2. Introduction

Structure and function correlations of ion channel proteins are frequently examined in heterologous expression systems in combination with functional assays. After expression of channels in mammalian cells or in *Xenopus* oocytes their activity in the plasma membrane can be examined with electrophysiological methods (Moroni *et al.*, 2002). The yeast complementation assay, which has been shown in chapter 3.4 is an alternative assay to uncover functional potassium channels in the plasma membrane (Minor *et al.*, 1999). All these techniques rely on a positive signal, e.g. a measurable current or successful rescue of yeast growth. Therefore these approaches are not able to uncover the reason why some channels or mutants are not able to generate a current in mammalian cells and oocytes or why they are unable to rescue yeast growth. In principle the absence of a current or the failure to rescue yeast growth could be explained by a channel, which is still synthesized in a cell but non-functional. But it could also be the result of a lack of protein synthesis or a failed sorting of the channel into the plasma membrane (Balss *et al.*, 2008). Recent work on ion channel mutants, which are responsible for inherited diseases, has shown that an aberrant function of channels can be caused by mutants, which affect channel function and those which affect channel sorting (Niemeyer *et al.*, 2001). To address the question whether a mutation is affecting function, trafficking or sorting of a channel protein it is necessary to determine the intracellular localization of a channel protein. For this purpose channel proteins are frequently fused to GFP (green fluorescent protein). This method offers a convenient approach to label the protein of interest and study its location by microscopy. In

combination with fluorescent dyes, which are specific for cellular compartments it is even possible to specify the localization of a protein inside of cells.

Currently there are many different microscopic techniques available, which allow the imaging of living cells and which provide information on the distribution of fluorescent proteins in cells. The most widely used technique is confocal laser scanning microscopy (CLSM). This fluorescence microscopy technique offers the possibility to study the localization of cellular proteins and their intracellular sorting in a non-invasive manner. In contrast to biochemical assays the cells remain intact and no fixation like in electron microscopy is required. With this non-invasive approach it is possible to examine the intracellular transport of proteins with a high spatial and temporal resolution in real time. In principle, the intracellular sorting of potassium channels to the plasma membrane can in this way be examined independent of their functionality.

The aforementioned confocal laser scanning microscopy has many advantages over conventional epifluorescent microscopy and the main advantage is the good signal to noise ratio. On a CLSM a fluorescent protein can be excited with a distinct wavelength and within a distinct area. Photons emitted by fluorophors outside the focal plane are rejected by a pinhole in the detection beam path, so that only light of a distinct optical layer of the sample reaches the detector; scattered light outside the focal plane is eliminated as well (Semwogerere & Weeks, 2005). Under optimal conditions, a resolution of ~200 nm can be achieved. If we however consider the dimensions of proteins, the diameter of a membrane and the close packing of structures inside a cell it becomes clear that this resolution is not sufficient to unequivocally localize a channel protein inside the plasma membrane. The resolution of a confocal microscope does for example not allow to distinguish between a GFP labelled channel protein in the plasma membrane, in the cortical endoplasmatic reticulum (ER) or in vesciles close to the plasma membrane. Even the resolutions achieved by state of the art super-resolution microscopic techniques, such as stimulated emition depletion microscopy (STED) photoactivation localization microscopy (PALM), or stochastic optical reconstruction microscopy (STORM), which are below 50 nm, are not sufficient for this task (Hell, 2008; Heintzmann & Ficz, 2006; Willig, Rizzoli, Westphal, Jahn, & Hell, 2006)

Here, a modified method based on previous studies (Bezrukov, 2009; Heuser, 2000) is presented which provides a robust assay for the presence or absence of a protein in the plasma membrane of a mammalian cell. The method is based on confocal laser scanning microscopic imaging of isolated plasma membrane patches. Cells expressing a fluorescent protein of interest are adhered to a coverslip

via a poly-D-lysine coat. After adhesion on glass coverslips the cell body can be removed by an osmotic shock leaving only plasma membrane patches on the coverslip. In this way it is possible to detect proteins in the plasma membrane even if the great majority of the protein of interest is located in intracellular compartments. With conventional CLSM a low signal in the plasma membrane would be masked by strong signals from intracellular compartments.

With this robust tool for a detection of proteins in the plasma membrane of cells it was possible to analyse and verify the localization of two potential sorting mutants of Kesv mutants, which were introduced in chapter 3.4.

## 4.3. Material and Methods

### 4.3.1. Heterologous expression in mammallian cells

The following cell-lines were used:

- CHO (Chinese hamster ovary) cells (Tjio & Puck, 1958)
- COS7 (African Green Monkey *Cercopithecus aethiops* Fibroblast-like Kidney) cells (Gluzman, 1981)
- HEK293 (Human embryonic kidney 293) cells (Graham, Smiley, Russell, & Nairn, 1977)
- K562 (Human erythromyeloblastoid leukemia) cells (Lozzio & Lozzio, 1975)

All cell-lines mentioned above were cultured in the following manner:

The cells were grown in a 35 mm culture dish with DMEM/F12 (Biochrom AG, Berlin, Germany) media (10 % (v/v) FCS, 2.5 mM glutamine und 1 % (v/v) penicilline/streptomycine) at 37 °C with 5 % $CO_2$ until the cells reached a confluency of 60 – 70 %. The cells were then transiently transfected with the constructs shown in chapter 4.3.4 using 4 $\mu$g DNA and 12 $\mu$l Polyethylenimine (1 g/l) (PEI, Sigma Aldrich, Schnelldorf, Germany) as transfection agent (Boussif *et al.*, 1995). After incubating the transfected cells for 1 day, growth medium was removed first and the cells were detached by swilling with phosphate buffered saline (PBS, 8 g/l sodium chloride, 0.2 g/l potassium chloride, 1.42 g/l disodium hydrogen phosphate, 0.24 g/l potassium hydrogen phosphate; pH was adjusted with 1 M sodium hydroxide to 7.4). The detached cells were centrifuged for 4 minutes at 2.500 rpm (Biofuge pico, Heraeus, Hanau, Germany) and the pellet was resuspended in 1 ml of PBS. 300 $\mu$l of this cell suspension was transferred on a pretreated 25 mm round glass coverslip (see chapter 4.3.2); the latter was then placed in a 35 mm round culture dish. The culture dish was filled with 2 ml of PBS and the cells were incubated for a time of 15 minutes so that the cells could sediment and stick to the poly-D-lysine-surface of the pretreated coverslip. After 15 minutes of incubation the cells were ready for the preparation of the plasma membrane described in the later following chapter 4.3.3.

### 4.3.2. Cleaning and coating of coverslips

The surface of 25 mm round glass coverslips was functionalized to achieve a strong adhesion of cells to the surface. Only with this pretreatment it was possible to obtain clean isolates of the plasma membrane (as described in chapter 4.3.3).

All coverslips were therefore first incubated for 5 minutes in technical grade aceton (Applichem, Darmstadt, Germany) and dried under the hood at room temperature. Coverslips were then activated in a plasma cleaner (Zepto, Diener electronic GmbH + Co. KG, Ebhausen, Germany) for 2 minutes at power level 50 in water saturated ambient air.
This routine removes organic traces and creates a hydrophilic surface on the coverslips priming them for the coating process.

For the coating 40 $\mu$l of a 200 $\mu$g/ml poly-D-lysine-solution (poly-D-lysine hydrobromide, mol wt 30.000 - 70.000, Sigma Aldrich, Schnelldorf, Germany) was used. Poly-D-lysine (PDL) is a positively charged amino acid polymer and functions as non-specific attachment factor. It increases the number of available positively charged binding sites on a surface. Because it was reported that certain cells can digest poly-L-lysine here poly-D-lysine was used (Cohen, Kalish, Jacobson, & Branton, 1977; Das, Banerjee, Sil, & Sarkar, 1989).
The whole coating process was done in a spin coater (SPIN150 from SPS Europe Spincoating, Putten, Netherlands) to obtain a smooth coating layer of PDL. 40 $\mu$l of PDL on the coverslip were first spinned for 30 seconds at 500 rpm and then at 3.000 rpm for 30 seconds to finish the coating process.

### 4.3.3. Plasma membrane preparation

Several reports in the literature already provide protocols for the preparation of plasma membranes (Frankel *et al.*, 2006; Heuser, 2000; K. Miller, Shipman, Trowbridge, & Hopkins, 1991; Rutter, Bohn, Hohenberg, & Mannweiler, 1986; Bezrukov, 2009). The presented method is a further optimization of a successful protocol used in previous studies (Bezrukov, 2009). The specific treatment of the coverslips yields an improved adhesion of the cells to the surface, which allows for a thorough removal of the cell body by the osmotic treatment and subsequent washing steps. These improvements also liberate the method from the use of any special technical equipment such as an ultrasonic sample (Heuser, 2000). Also cells do not have to be monitored during the bursting process (Heuser, 2000).

Taken together the modifications of the method are able to considerably shorten the entire procedure to less than 1 hour; the original protocol required 1.5 days (Bezrukov, 2009). The pretreated glass coverslip and the cleanness of the isolated plasma membrane patch make high-resolution microscopy possible.

For the preparation of the isolated plasma membrane patches it is important that the coverslips are pretreated as described in chapter 4.3.2. Only then the part of the plasma membrane, which interacts with the coated coverslip will remain as an isolated plasma membrane patch. The procedure is as follows:

After cells had adhered to the coverslips the PBS solution was removed from the culture dish and replaced by 2 ml of ice-cold dd$H_2O$. The cells were incubated in the ice-cold dd$H_2O$ for 5 minutes causing them to swell and finally bursting. In the next step the water was removed and the coverslip was washed with fresh water by adding and removing 1 ml of dd$H_2O$ for 3 - 5 times. This step removes the first parts of cell debris. Afterwards it is still possible to recognize a grey glimmer on the coverslip, indicating many remaining cells. In the following step 2 ml of dd$H_2O$ were again added and by continuously pipetting the solution up and down for 1 minute at the edge of the culture dish a vortex was generated. The associated shear forces were removing the cell bodies. Again all cell debris were removed by changing the water for 3 - 5 times. In a further final step 2 ml of dd$H_2O$ were directly pipetted in a forceful manner on the coverslip. This pressurized water stream removed the last cell debris. This last step turned out to be critical; after this procedure no grey glimmer was left on the coverslip. In a final step the coverslip was cleaned from all remaining cell debris. For this purpose the water in the cell culture dish was changed for 5 times and the culture dish was tilted at a circa 45° angle so that the water could run over the coverslip to one edge of the culture dish. The cell debris, which collected in this corner were removed with a pipette.

The whole process of the plasma membrane preparation by bursting the cells due to an osmotic shock takes about 10 minutes and is illustrated in Figure 20.

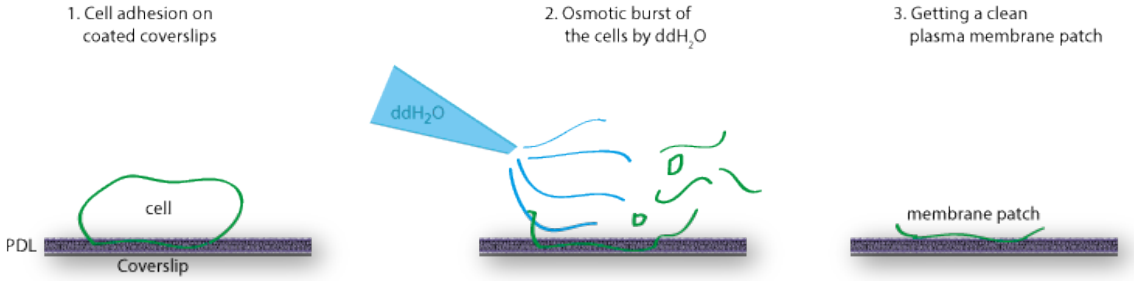


**Figure 20: Plasma membrane preparation by osmotic burst with $ddH_2O$.**

There are many alternative methods, which produce isolated plasma membrane patches. But none of them is as simple as the one described before. The following chapter will further show that the combination of osmotic shock with multiple harsh washing steps are able to obtain clean isolated plasma membrane patches. Neither ultrasonic (Heuser, 2000) nor the squashing of cells between two coverslips (K. Miller *et al.*, 1991; Rutter *et al.*, 1986) are as effective as the described method here.

### 4.3.4. Constructs and fusion proteins

To examine the purity of the plasma membrane, which remains attached to the coverlip after the preparation protocol, several fluorescent fusion protein markers, which localize to different cellular compartments were analyzed. To visualize the endoplasmatic reticulum pmKate2-ER (Evrogen, Moscow, Russia) was used. The vector encodes for the far-red fluorescent protein mKate2 and contains an N-terminal ER target signal and the C-teminal ER retention signal KDEL, both derived from calreticulin (Fliegel, Burns, MacLennan, Reithmeier, & Michalak, 1989; Munro & Pelham, 1987). For labelling mitochondria pmKate2-mito (Evrogen, Moscow, Russia) was used. It contains the mitochondrial targeting sequence (MTS) derived from the subunit VIII of human cytochrome C oxidase (COX) (Rizzuto *et al.*, 1989; Rizzuto, Brini, Pizzo, Murgia, & Pozzan, 1995).
For a labelling of the cytoskeleton pCMV-LifeAct™-TaqGFP2 (Ibidi GmbH, Planegg/Martinsried, Germany) was used; this protein stains the F-actin (Riedl *et al.*, 2008).

For the analysis of membrane proteins the two channels Kcv and Kat1 were used (Hertel *et al.*, 2005; Plugge, 2000); the channel Kesv was used as a sample for membrane proteins, which are sorted to the mitochondria (Balss *et al.*, 2008). The wildtype forms of the potassium channels Kcv, Kat1 and Kesv (without the stop codon) were cloned into the BglII and EcoRI site of the pEGFP-N2 vector (Clontech-

Takara Bio Europe, Saint-Germain-en-Laye, France) in frame with the downstream enhanced green fluorescent protein (EGFP). The potential Kesv sorting mutants described in Table 4 were also cloned in the pEGFP-N2 vector.
The Kesv chimera 3 and chimera 3.4 in the pEGFP-N2 vector were kindly provided by Charlotte v. Chappuis (Darmstadt, Germany, (Von Chappuis, 2013)).

Isolated plasma membrane patches are not visible without staining. Therefore the plasma membrane stain Cellmask™ Orange (Invitrogen GmbH, Karlsruhe, Germany) was used to visualize the patches on the coverslips. Cellmask™ Orange (CMO) is an amphipathic molecule, which provides a lipophilic part for membrane loading and a negatively charged hydrophilic dye for "anchoring" the sample in the plasma membrane (Rossignol, La Frazia, Chiappa, Ciucci, & Santoro, 2009). The membrane patches were incubated for 5 minutes with a final concentration of Cellmask™ Orange of 50 ng/ml in the CLSM chamber and were washed with PBS 3 times after the incubation.

### 4.3.5. Confocal Laser Scanning Microscopy (CLSM)

The microscopic analysis of cells and membrane patches was performed on a Leica TCS SP5 microscope (Leica Microsystems, Wetzlar, Germany) with the Software LAS AF Version 2.60 build 7266 (Leica Microsystems CMS GmbH, Heidelberg). Fluorescent proteins were excited with an argon laser at 488 nm or 514 nm, respectively, and a diode pumped solid-state laser (DPSS) at 633 nm with an overall power-level of 6 %. Images were acquired with the HCX PC APO lambda blue 63x/1.4 oil object lens. EGFP was excited with 488 nm and the emission was detected from 500 nm - 530 nm. MKate2 was excited with 633 nm and the emission was detected from 700 nm - 800 nm. Cellmask™ Orange was excited at 514 nm and the emission was detected from 570 - 670 nm. The overlay images shown in the results have been created with the open source software FIJI (http://fiji.sc), a distribution variant of the popular open source software ImageJ (http://rsb.info.nih.gov/ij).

## 4.4. Results

To examine membrane proteins in the plasma membrane of cells by fluorescence microscopy it would be desirable to have an isolated membrane as this would eliminate the contribution of fluorescent signals, which originate from intracellular compartments other than the plasma membrane. For a good microscopic resolution the membrane should be flat and clean without any unwanted cytoplasmatic structures, which could corrupt the imaging analysis. For the purpose of visualizing membrane proteins in the membrane of mammalian cells a method reported by Bezrukov (2009) was modified to obtain clean patches of plasma membrane in a robust and quick way. Even very small amounts of membrane proteins could be detected.

The following images show the results of the protocol detailed in materials and methods in which a small membrane patch is isolated from the plasma membrane of cells. All images presented here have been obtained according to the following routine:

1. cell growth and transfection
2. suspension of cells and subsequent adherence on PDL coated coverslips
3. cell burst and washing/cleaning of the isolated membrane patch
4. visualization of the plasma membrane patch and the proteins by CLSM

The first step was to determine the quality of the preparation. Figure 21 illustrates exemplary images of HEK293 cells before and after the plasma membrane preparation. The preburst images (Figure 21 a - c) clearly show the characteristic 3D-shape of HEK293 cells. Cells and their structure can also be seen using bright-field illumination.
After the osmotic burst the objects occur much thinner and less 3D-structural than the intact cells. They exhibit only a flat membrane patch, which is best seen in the side view (Figure 21f). The membrane patches, which remain after the osmotic cell burst are only visible when stained with CMO (compare Figure 21 d with f). In the bright-field the membrane patches are no longer detectable. The results of these experiments clearly show that only a flat membrane patch is left after the treatment.

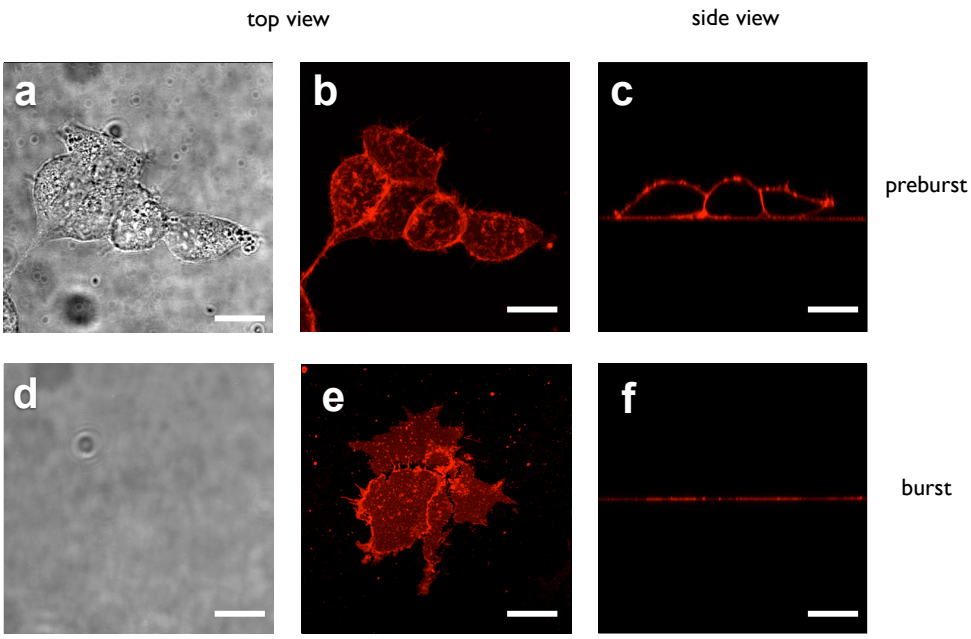


**Figure 21: Plasma membrane preparation of HEK293 cells.** The first row shows images of cells under control conditions prior to the bursting protocol (a - c). The second row shows images of cells after bursting of the cell body (d-f). Bright-field top view (a & d), fluorescence top view (b & e) and fluorescence side view (c & f). The images of the preburst cells in the first row show the characteristic 3D-shape of HEK293 cells. In contrast the second row with the bursted cells shows only a flat plasma membrane patch. The cells in the images b, c, e and f were stained with CMO (Scale bar = 10 µm).

To analyse the general applicability of the method several cell-lines were examined. The representative images in Figure 22 show that the method is compatible with HEK293, COS7, CHO and even the non-adherent suspension cells K562. In all cases only isolated membrane patches remained attached to the coverslip after removing the cell body by osmotic burst.

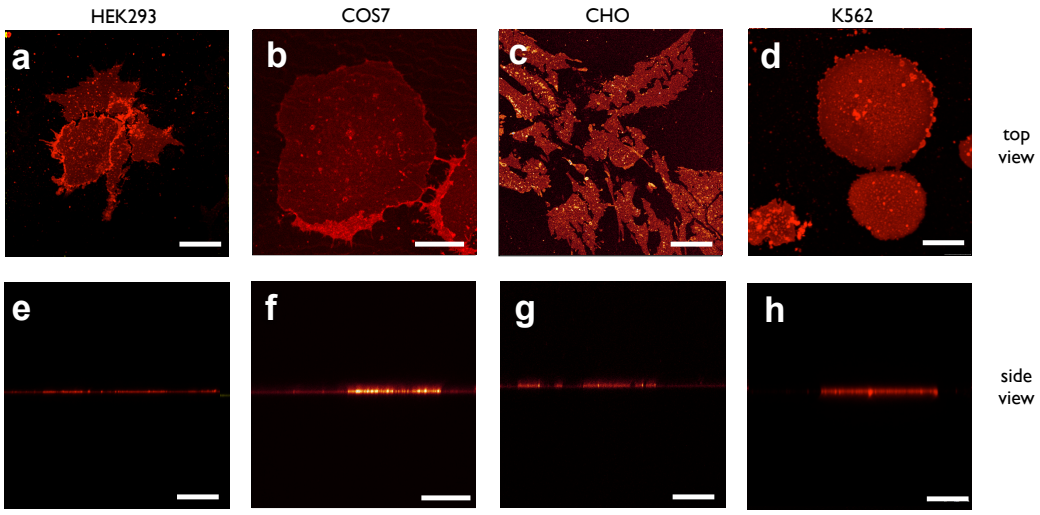


**Figure 22: Plasma membrane preparation of different cell-lines.** Isolated plasma membrane patches of HEK293 cells (a), COS7 cells (b), CHO cells (c) and K562 cells (d) were prepared as in Figure 21. The first row shows the successful preparation of plasma membrane patches from different cell-lines in top view. The second row illustrates the side view of these cells. In all cases only flat plasma membrane patches remain after the protocol. All cells stained with CMO (Scale bar = 10 µm).

After confirming that the protocol works with various different cell-lines the purity of the membrane preparation was examined. The main question was whether the membrane patches are still contaminated with any cellular compartment, which survive the bursting process and remain connected to or at the cytoplasmatic surface of the isolated plasma membrane patch. For this purpose the following fluorescent fusion protein markers for different cellular compartments (see chapter 4.3.4) were expressed in HEK293 cells:

- COX::mKate2 for mitochondria
- LifeAct™::TagGFP2 for cytoskeleton (F-Actin)
- KDEL::mKate2 for endoplasmatic reticulum
- Kat1::GFP for the plasma membrane

With Kat1, an inward rectifying potassium channel of *Arabidopsis thaliana*, which in mammalian cells is located in the plasma membrane, was used as a plasma membrane reference protein (Hertel *et al.*, 2005; Mikosch, Hurst, Hertel, & Homann, 2006).

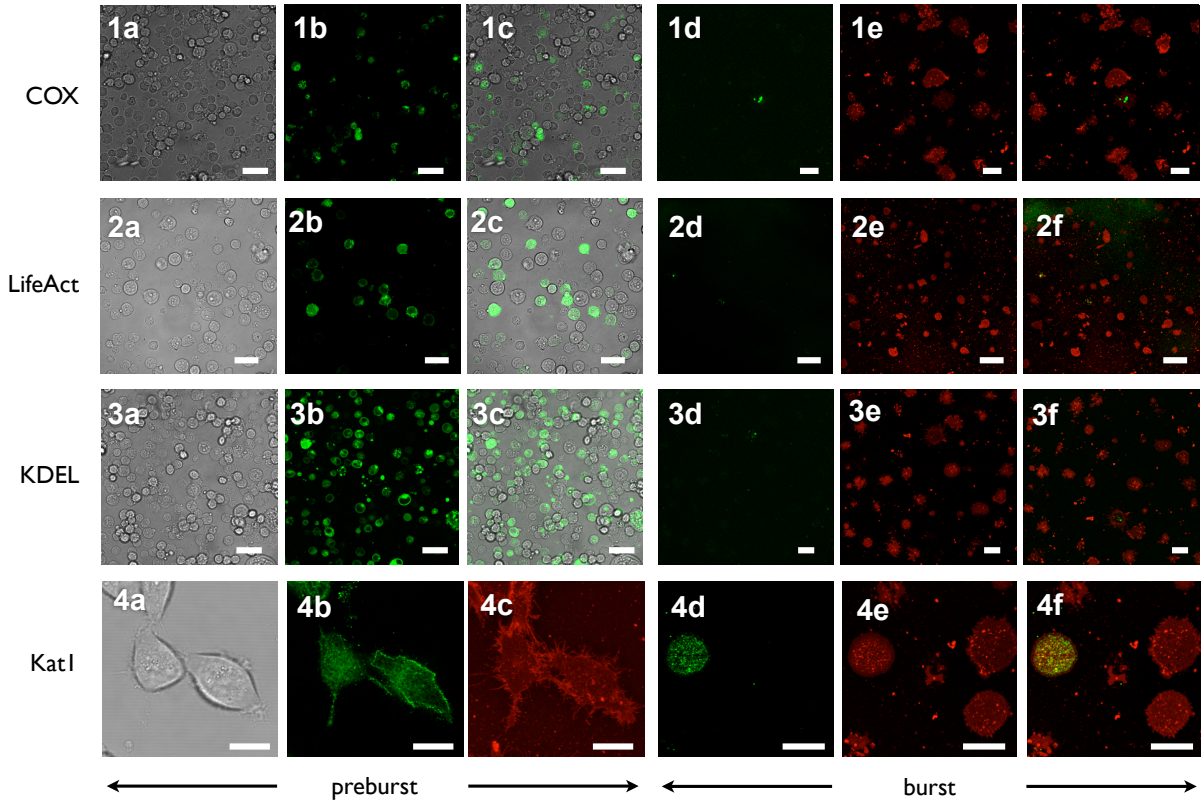


**Figure 23: Control for the purity of isolated plasma membrane patches**. All measurements have been done with HEK293 cells. Cells were imaged before (panel a - c) and after bursting (panel d - f). The images show cells in bright-field (column a) and the fluorescent images of cells expressing the fluorescent marker proteins (column b) indicated on the left. Column c is an overlay of a & b. After removal of the cell body by osmotic bursting the fluorescence of the marker proteins was recorded (coumn d) and membrane patches were stained with CMO (column e). Column f shows overlay of d & e. The images in row 1d – 3d show a tiny fluorescence of the markerprotein in contrast to a black background. This indicates that nearly 100 % of the cells are successfully bursted and the cellular compartments are removed. Cells were stained with CMO. Overlay images in the columns c & f have been created with Fiji (Scale bar = 10 µm).

Figure 23 shows HEK293 cells in bright-field (Figure 23 column a) and fluorescent images of the positively transfected cells. The latter show distinct fluorescence signals in line with the cellular sorting of the reference proteins (Figure 23 column b).

The overlay of the bright-field images with the fluorescence images of COX, LifeAct™ and KDEL transfected cells shows that a high number of cells are transfected (Figure 23 c column). After applying the protocol neither COX, LifeAct™ nor KDEL fusion proteins are detectable (Figure 23 column d). However, the isolated membrane patches are still visible when stained with CMO. Collectively the results of these experiments in Figure 23 show that the membrane patches are indeed clean and clear of cytosolic contaminations. Only a clean plasma membrane patch remains on the surface of the coated coverslip.

As a positive control the data also show that the fluorescence of the potassium channel Kat1, a channel which is known to be localized in the plasma membrane of HEK293 cells (Mikosch, Hurst, Hertel, & Homann, 2006), is visible before and after the burst protocol (see Figure 23). This result further shows that the flat structures on the coverslip, which are stained with CMO, are indeed isolated plasma membrane patches. The data further confirm that membrane proteins can be uncovered in these isolated plasma membrane patches without any contribution of fluorescence from intracellular compartments.

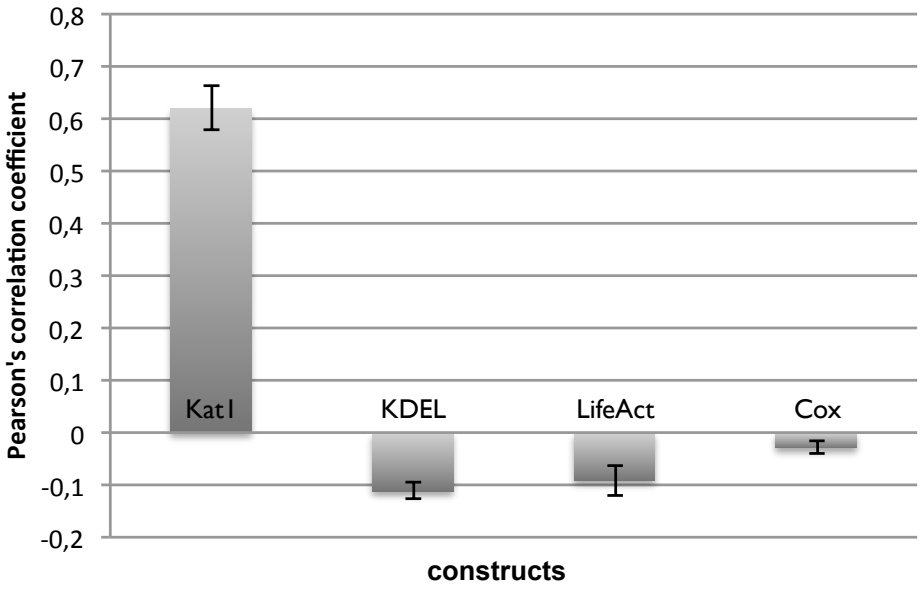


**Figure 24: Pearson's correlation for co-localization of fluorescence associated with a protein and fluorescence from membrane patches**. The images of bursted cells as in Figure 23 have been analysed with the open source software Fiji to calculate the Pearson correlation coefficient between the fluorescence from the membrane patches (CMO) and the tagged proteins (COX, LifeAct™, KDEL and Kat1). The data are mean values +/- standard deviation of n = 6 measurements with 25 iterations.

For a quantification of the imaging results a co-localization of the fluorescence associated with the proteins and the fluorescence of the CMO stained membrane patch was determined. For this purpose the Pearson's correlation coefficient (PCC) between the two fluorescent signals was calculated using the open source software Fiji. The values are plotted in Figure 24. A co-localization between the positive control such as the plasma membrane channel Kat1::GFP and the membrane patch stained with CMO is expected to give the highest PCC value. The other constructs representing different cellular compartments like KDEL for the ER, LifeAct™ for the F-Actin and Cox for mitochondria should give the lowest PCC value.

The data show that the membrane protein Kat1 yields a positive Pearson's correlation coefficient. The result of this analysis implies that this protein is indeed located in the plasma membrane. In contrast the other constructs present a PCC value close to zero confirming that these proteins are not located in the plasma membrane. This indicates that the cellular compartments related to the specific construct are indeed removed in the course of the preparation procress for isolating the plasma membrane.

After determining the purity of the isolated membrane patches they were used to examine the localization of plasma membrane proteins in more detail (Figure 25). For this purpose the constructs listed in Figure 14 of chapter 3.4 were used. As expected all images of transfected cells show prior to the bursting protocol distinct fluorescence signals indicating the presence of the proteins (Figure 25). After the burst procedure the membrane patches from cells, which express as a positive control Kcv, still show fluorescence. This is expected because it is known that this channel can be heterologously expressed in HEK293 cells where it is active in the plasma membrane (Moroni *et al.*, 2002). In this respect the data with Kcv are similar to those obtained with Kat1, another plasma membrane $K^+$ channel. While Kcv can be positively detected on the isolated membrane patches the second viral channel Kesv cannot be detected after cell bursting. This result is again expected because Kesv has been shown to be sorted to the mitochondria in HEK293 cells (Balss *et al.*, 2008).
In chapter 3.4 mutants of Kesv (KesvR1 and KesvR2) were created which presumably had an altered sorting behaviour in yeast cells. These two mutants are able to rescue the growth of potassium uptake deficient yeast strains. The mutation presumably alters the sorting of these proteins from the mitochondria to the plasma membrane. To examine whether the two mutants are indeed sorted to the plasma membrane they were fused to GFP and expressed in HEK293 cells. The images in Figure 25 show that the fluorescent signal of both mutant proteins could be positively detected in membrane patches after an osmotic burst of the cells. The results of these experiments confirm the results of the yeast complementation assay in that both mutants are able to integrate into the plasma membrane of yeast cells.

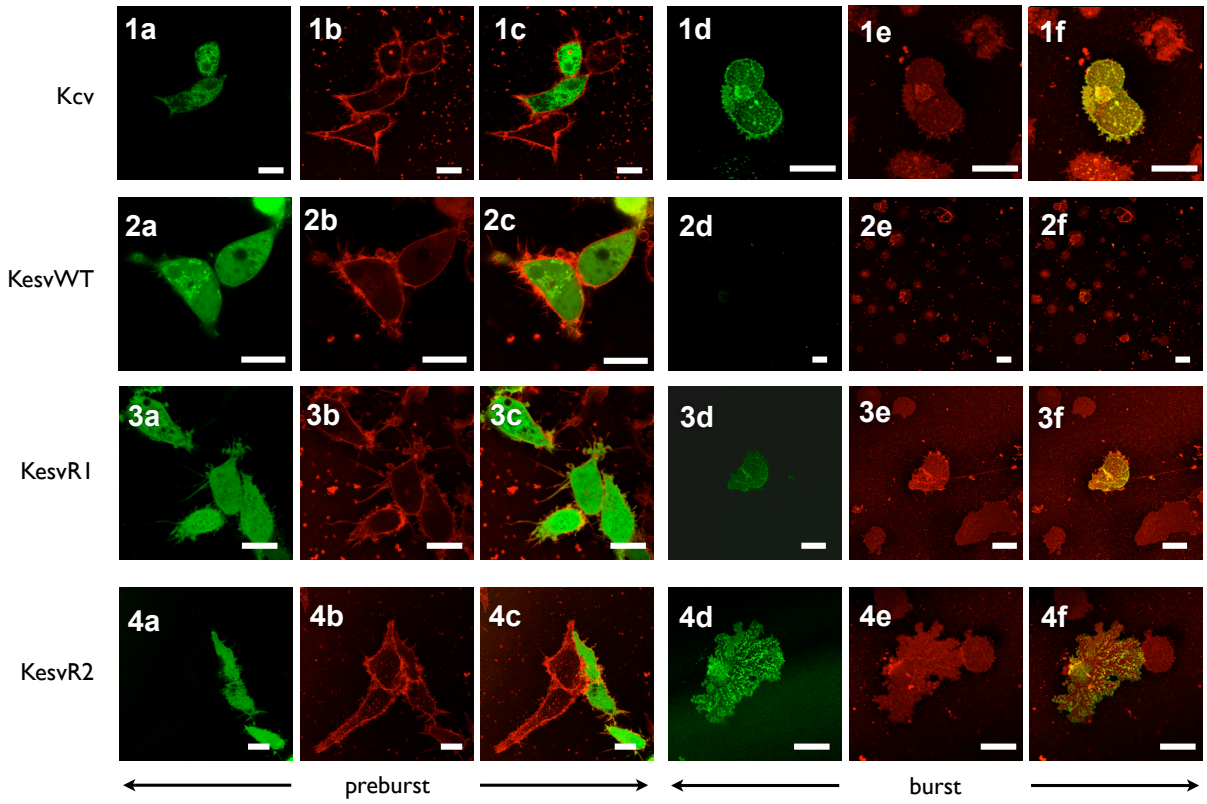


**Figure 25: Detection of proteins in isolated plasma membrane patches.** Column a shows the fluorescence signal of intact HEK293 cells expressing different membrane proteins indicated on the left. In column b the membrane of the respective cells is stained with CMO. Column c shows an overlay of a & b. Columns d - f show the same sequence of images after bursting. The overlays in the images of 1f, 3f and 4f positively identify the presence of channels in the plasma membrane patches. The image in 2f reveals that the Kesv channel is not present in the plasma membrane of HEK293 cells. Cells were stained with CMO. Overlay images in the columns c & f have been created with Fiji (Scale bar = 10 µm).

In the following experiments the same approach was used in order to localize other critical sorting chimeras of Kesv/Kcv (Von Chappuis, 2013). Figure 26 shows a yeast complementation assay of a chimera (Chim 3, kindly provided by Charlotte von Chappuis) comprising parts of the Kcv and Kesv channel. The inability of the chimera to rescue yeast growth implies that this protein is not located in the plasma membrane (Von Chappuis, 2013). Yet fluorescent images of HEK293 cells imply that the GFP tagged chimera is sorted into the secretory pathway. To test if chimera 3 fails in rescuing yeast growth because of a functional defect or because it is not sorted to the plasma membrane its presence in isolated plasma membrane patches was examined.

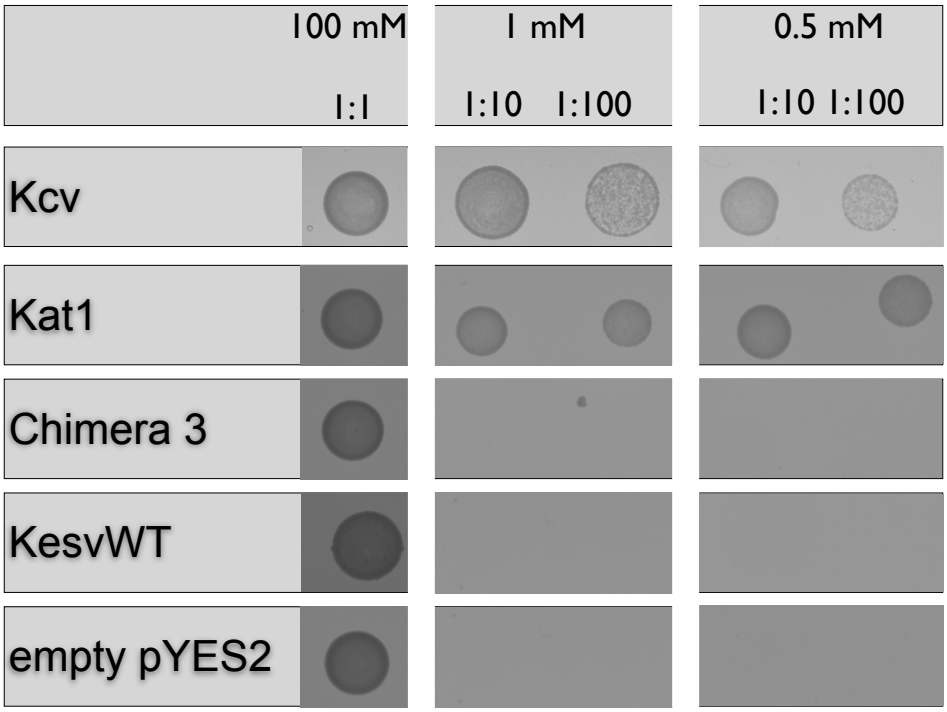


**Figure 26: Yeast complementation assay**. The assay was done with three different potassium concentrations in the media: 100 mM KCl (non-selective condition), 1 mM and 0.5 mM KCl (selective condition). The wild type forms of Kcv, Kat1, Kesv and empty pYES2 vector (empty pYES2) function as positive and negative controls. All constructs were spotted in different dilutions: 1:1 (undiluted), 1:10 and 1:100. Cells were grown for 2 days before analysis. The images of growing yeast colonies show that cells transformed with proteins, which are known to function as potassium channel in the plasma membrane (Kcv, Kat1) are able to grow under selective conditions. In contrast chimera 3, which seems to enter the secretory pathway in HEK293 cells, has the same effect as the negative controls (KesvWT and empty pYES2). This suggests that chimera 3 may be in the plasma membrane but non-functional.

The data in (Figure 27) show that chimera 3 can be positively detected in isolated plasma membrane patches. This result is in line with the observation that this chimera is sorted into the secretory pathway (Von Chappuis, 2013). The inability of this chimera to rescue yeast growth may be explained by a functional defect of the channel rather than by unappropriate sorting to the plasma membrane.
Also other chimera of Kesv and Kcv reveal distinct sorting properties. A particular break in sorting of a sequence of chimera occurs in chimera 4 in which the N-terminal part is from Kesv and the C-terminal part from Kcv (Von Chappuis, 2013). One chimera 3.4 (chim 3.4) is upon expression in HEK293 cells distributed throughout the whole cell including the nucleus. The distribution pattern indicates that the localization of the channel is undefined (Von Chappuis, 2013). If this chimera is expressed together with an organelle specific marker protein (for example KDEL) it is co-sorted together with this marker protein into a distinct compartment e.g. the ER. It seems as if chimera 3.4 is hitchhiking with a positively sorted protein towards a cellular compartment. Because of this unusual behaviour chimera

3.4 is an ideal protein for testing the present method for membrane protein analysis in isolated plasma membrane patches.

The images in (Figure 27) show HEK293 cells expressing chim 3.4; the green fluorescence implies that many cells are transfected and expressing the protein. After osmotic bursting of the cells there is no more fluorescence signal of chimera 3.4 detectable. The panel 4d in Figure 27 shows a particularly large representative area with no apparent green fluorescence. The results of these experiments imply that chimera 3.4 fails to integrate by itself into the plasma membrane (Figure 27). The data further indicates that chimera 3.4 requires an auxiliary protein to promote its sorting into the secretory pathway.

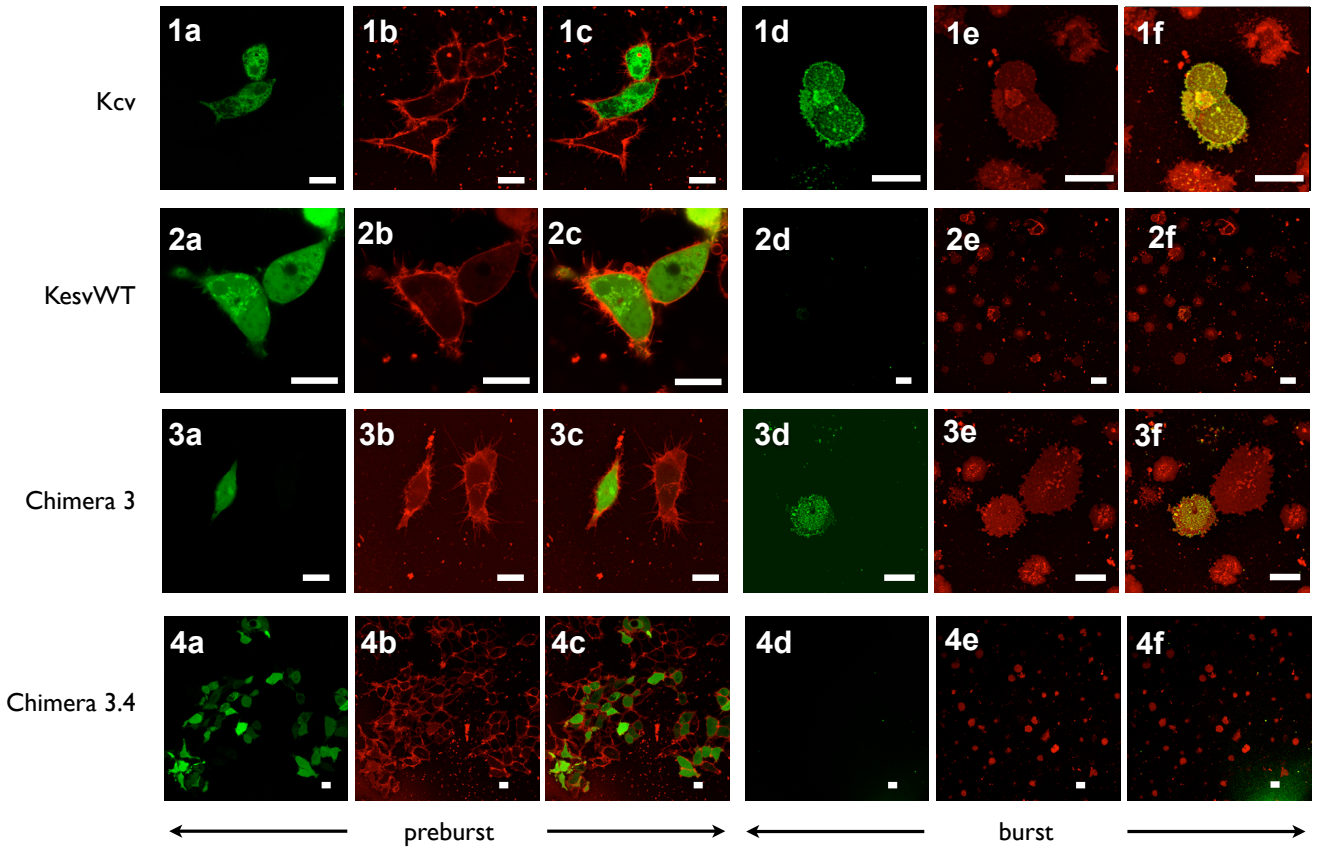


**Figure 27: Detection of proteins in isolated plasma membrane patches.** The images in columns a - c show the fluorescent signals of intact HEK293 cells expressing GFP tagged membrane proteins indicated on the left. The fluorescent signal in column b reports the plasma membrane of the respective cells stained with CMO. Column c is an overlay of a & b. Columns d - f show the same sequence of images for cells after bursting. The images reveal a positive identification of Kcv and Chimera 3 in the plasma membrane patches. Neither Kesv nor chimera 3.4 are detectable in the isolated membrane patches. Cells were stained with CMO. Overlay images in the columns c & f have been created with Fiji (Scale bar = 10 µm).

For a better quantification of the imaging results a co-localization of the fluorescence associated with the proteins and the fluorescence of the CMO staining the isolated membrane patch itself was determined. For this purpose the Pearson's correlation coefficient (PCC) between the two fluorescent signals was calculated using the open source software Fiji. The values are plotted in Figure 28. A co-localization between the positive control such as the plasma membrane channel Kcv::GFP and the membrane patch stained with CMO is expected to give the highest PCC value. The channel Kesv, which is sorted to the mitochondria, should give the lowest PCC value.

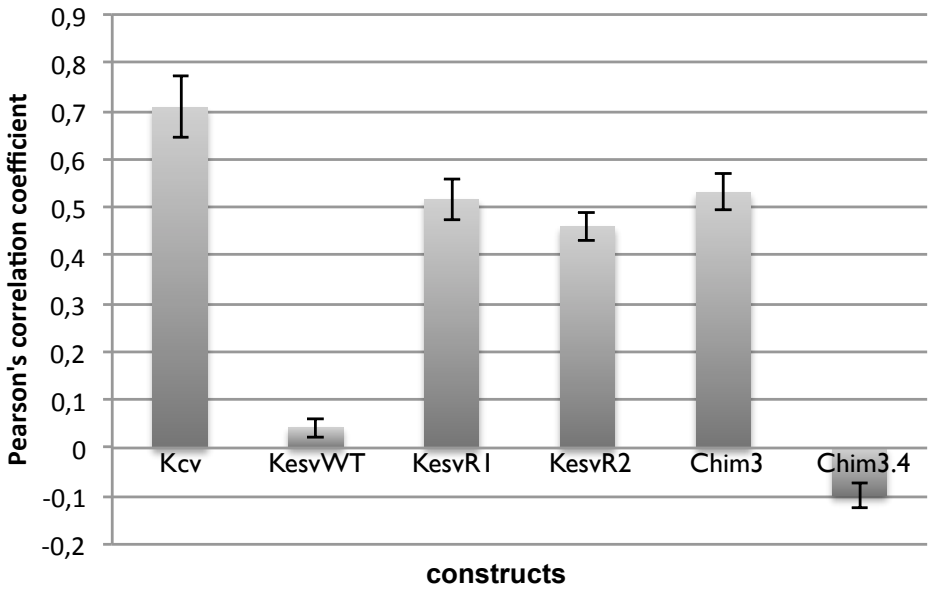


**Figure 28: Pearson's correlation for co-localization of fluorescence associated with a protein and fluorescence from membrane patches**. The images of bursted cells as in Figure 25 and Figure 27 have been analyzed with the open source software Fiji to calculate the Pearson's correlation coefficient for the fluorescence from the membrane patches and from the tagged proteins. The data are mean values +/- standard of n = 6 measurements with 25 iterations.

The data show that the membrane protein Kcv as well as the mutants KesvR1, KesvR2 and chimera 3 exhibit a positive Pearson's correlation coefficient. The results of this analysis imply that these constructs are indeed located in the plasma membrane. In contrast KesvWT and chimera 3.4 present a PCC value close to zero confirming that these proteins are not located in the plasma membrane.

## 4.5. Discussion

The presented method is a further optimization of a successful protocol used in previous studies for the isolation of native plasma membrane patches (Bezrukov, 2009). Compared to the original protocol the present optimization resulted in a drastic shortening of the procedure from several days to only 1 hour. A key step in the procedure is the coating of the coverslips by a spin coater. It distributes a low amount of poly-D-lysine as a thin and equal distributed layer of poly-D-lysine over the glass surface. This surface guarantees a fast and strong adherence of cells; 15 minutes were sufficient for several mammalian cell lines to adhere in a very strong manner on coated coverslips. The coating of the coverslips also guarantees a robust adherence of the membrane patches to the surface. As a consequence the preparation can be washed and cleaned from cytosolic compounds, which are often attached to plasma membranes. The control experiments with tagged cellular marker proteins confirm that this procedure result in a very pure preparation of isolated plasma membrane patches.
A further advantage of the present protocol is the fact that the cell bodies can be efficiently removed from the membrane patches simply by a steam of $ddH_2O$ from a conventional pipette. This makes technical equipment like ultrasonics or the mechanical stripping dispensable (Avery *et al.*, 2000; Frankel *et al.*, 2006). Collectively the simple protocol provides a good tool for creating in a short period of time extremely clean and robust specimens for analysing membrane proteins.

From an experimental point of view the isolation of plasma membrane from the cell body increases the signal to noise ratio for a detection of proteins in the plasma membrane. Indeed electrophysiological recordings have shown that the viral potassium channel Kcv is present in the plasma membrane of HEK293 cells only at a very low number (Moroni *et al.*, 2002). From the single channel conductance (ca. 130 pS) (Pagliuca *et al.*, 2007) and the general current density of the macroscopic Kcv current in HEK293 cells (ca. 5-20 nS per cell) (Hertel *et al.*, 2009) a total number of 30 to 150 channels can be estimated. With conventional confocal imaging the GFP tagged version of this channel was well detectable in the secretory pathway of HEK293 cells upon heterologous expression (Balss *et al.*, 2008; Moroni *et al.*, 2002). With the large background from intracellular compartments the low signal in the plasma membrane was - if at all - only barely detectable (Moroni *et al.,* 2002). But even in cases were a GFP signal was recorded in the area of the membrane it was not fully clear whether this signal derives from Kcv in the membrane or from channel protein in cytosolic compartments in vicinity of the membrane (Von Chappuis, 2013). The present data now confirm microscopically that the Kcv channel, which is electrically active in the plasma membrane, can also be detected optically. A very similar

channel, Kesv, which is sorted to the mitochondria in HEK293 cells, on the other hand is not detectable in the isolated membrane patches (Balss *et al.,* 2008). This is fully consistent with a bulk of independent data, which show that this channel exhibits no detectable activity in the plasma membrane (Balss *et al.,* 2008).

After the confirmation that the method is suitable for detecting membrane proteins with good confidence it can also be used to address open experimental questions. In order to understand the sorting of small viral potassium channels, mutants of Kesv were generated by a randomization approach (this thesis chapter 3.4). A mutation in the second transmembrane domain seems to alter in two mutants the trafficking. While the mitochondrial sorted Kesv channel is unable to rescue growth of a yeast mutant strain on selective media the two mutants are able to accomplish a rescue. The interpretation of this phenotype is that these mutants are sorted to the plasma membrane, where they are active as $K^+$ channel. The present data confirm this interpretation. While Kesv is not detected in the isolated membrane patches the two Kesv mutants are detected. This means that the mutations in the second transmembrane domain of Kesv are indeed able to alter the sorting of these channels.

Further work on the sorting of Kcv and Kesv has also employed chimeras of the two channels, which reveal distinct intracellular trafficking. One chimera, Chim 3, seems on the basis of co-localization experiments with ER markers to enter in HEK293 cells the secretory pathway very much like Kcv (Von Chappuis, 2013). This predicts that the chimera should be further sorted to the plasma membrane. Hence in yeast complementation assays it should like Kcv rescue the growth of yeast mutants on selective low $K^+$ media. The respective experiments however show that chimera 3 is not able to perform the expected rescue of yeast growth. The present experiments now show that chimera 3 is indeed properly sorted to the plasma membrane. Hence the failure to rescue the growth of yeast mutants is not a matter of sorting e.g. the protein is trafficking from the ER via the secretory pathway to the plasma membrane. From the present data it is more likely that the chimera is not functional as a channel and fails for this reason to complement yeast growth.

In the same context another chimera of Kcv and Kesv was detected, which reveals in HEK293 cells no more clear sorting: the GFP signal of this chimera 3.4 is distributed through the cell (Von Chappuis, 2013). The present experiments now confirm that this chimera is no longer sorted to the plasma membrane. Unlike chimera 3, which is only different in 5 amino acids it does not generate a visible fluorescent signal in isolated membrane patches.

## 4.6. Conclusion

The study of membrane proteins with a high spatial and temporal resolution in their native environment is challenging. It requires the isolation of extremely stable and clean preparations of plasma membranes. The present work presents a simple and robust method, which allows an isolation of very pure membrane patches. Using different GFP tagged channel proteins, which are known to be in the plasma membrane (Kat1, Kcv) or in the mitochondria (Kesv), it is shown here that the presence of the former and absence of the latter from the plasma membrane can indeed be verified with this technique. The good signal to noise ration of the isolated membrane patches allows even the positive detection of the Kcv channel in the plasma membrane. Other than Kat1 the small viral $K^+$ channel Kcv is in HEK293 cells only present at a low number in the plasma membrane. This can be measured with electrophysiological methods but not by conventional confocal microscopy of intact cells. Because of the good reliability of the method it can now also be used to address the question on whether mutants of Kcv or Kesv (or membrane protein in general) are present in the plasma membrane of HEK293 cells. The data here positively confirm the results of others in that one chimera of Kcv and Kesv is and another one is not sorted to the plasma membrane. The data also confirm the results from yeast complementation assays from this thesis in that mutants of Kesv are altered in their sorting; they are no longer targeted to the mitochondria but to the plasma membrane where they can be positively identified with this technique.

## 4.7. References


Abbe, E. (1873). Beiträge zur Theorie des Mikroskops und der mikroskopischen Wahrnehmung. *Archiv für Mikroskopische Anatomie*, *9*(1), 456–468.

Avery, J., Ellis, D. J., Lang, T., Holroyd, P., Riedel, D., Henderson, R. M., Edwardson, J. M., et al. (2000). A cell-free system for regulated exocytosis in PC12 cells. *The Journal of cell biology*, *148*(2), 317–24.

Balss, J., Papatheodorou, P., Mehmel, M., Baumeister, D., Hertel, B., Delaroque, N., Chatelain, F. C., et al. (2008). Transmembrane domain length of viral K+ channels is a signal for mitochondria targeting. *Proceedings of the National Academy of Sciences of the United States of America*, *105*(34), 12313–8.

Bezrukov, L., Blank, P. S., Polozov, I. V, & Zimmerberg, J. (2009). An adhesion-based method for plasma membrane isolation: evaluating cholesterol extraction from cells and their membranes. *Analytical biochemistry*, *394*(2), 171–6.

Boussif, O., Lezoualc'h, F., Zanta, M. A., Mergny, M. D., Scherman, D., Demeneix, B., & Behr, J. P. (1995). A versatile vector for gene and oligonucleotide transfer into cells in culture and in vivo: polyethylenimine. *Proceedings of the National Academy of Sciences of the United States of America*, *92*(16), 7297–7301.

Cohen, C. M., Kalish, D. I., Jacobson, B. S., & Branton, D. (1977). Membrane isolation on polylysine-coated beads. Plasma membrane from HeLa cells. *The Journal of Cell Biology*, *75*(1), 119–134.

Das, S., Banerjee, S. K., Sil, M., & Sarkar, P. K. (1989). An ELISA method for quantitation of tubulin using poly-1-lysine coated microtiter plates. *Indian Journal of Experimental Biology*, *27*(11), 972–976.

De Planque, M. R. R., & Killian, J. A. (2003). Protein-lipid interactions studied with designed transmembrane peptides: role of hydrophobic matching and interfacial anchoring. *Molecular membrane biology*, *20*(4), 271–84.

Fliegel, L., Burns, K., MacLennan, D. H., Reithmeier, R. a, & Michalak, M. (1989). Molecular cloning of the high affinity calcium-binding protein (calreticulin) of skeletal muscle sarcoplasmic reticulum. *The Journal of biological chemistry*, *264*(36), 21522–8.

Frankel, D. J., Pfeiffer, J. R., Surviladze, Z., Johnson, a E., Oliver, J. M., Wilson, B. S., & Burns, a R. (2006). Revealing the topography of cellular membrane domains by combined atomic force microscopy/fluorescence imaging. *Biophysical journal*, *90*(7), 2404–13.

Gluzman, Y. (1981). SV40-transformed simian cells support the replication of early SV40 mutants. *Cell*, *23*(1), 175–182.

Graham, F. L., Smiley, J., Russell, W. C., & Nairn, R. (1977). Characteristics of a human cell line transformed by DNA from human adenovirus type 5. *The Journal of general virology*, *36*(1), 59–74.

Hertel, B., Horváth, F., Wodala, B., Hurst, A., Moroni, A., & Thiel, G. (2005). KAT1 inactivates at sub-millimolar concentrations of external potassium. *Journal of experimental botany*, *56*(422), 3103–10.

Hertel, B., Tayefeh, S., Kloss, T., Hewing, J., Gebhardt, M., Baumeister, D., Moroni, A., et al. (2009). Salt bridges in the miniature viral channel Kcv are important for function. *European Biophysics Journal*, 3103–10.

Heuser, J. (2000). The production of "cell cortices" for light and electron microscopy. *Traffic (Copenhagen, Denmark)*, *1*(7), 545–52.

Jacobson, B. S., & Branton, D. (1977). Plasma membrane: rapid isolation and exposure of the cytoplasmic surface by use of positively charged beads. *Science*, *195*(4275), 302–304.

Lewis, B. A., & Engelman, D. M. (1983). Lipid bilayer thickness varies linearly with acyl chain length in fluid phosphatidylcholine vesicles. *Journal of Molecular Biology*, *166*(2), 211–217.

Lozzio, C. B., & Lozzio, B. B. (1975). Human chronic myelogenous leukemia cell-line with positive Philadelphia chromosome. *Blood*, *45*(3), 321–34.

Mikosch, M., Hurst, A. C., Hertel, B., & Homann, U. (2006). Diacidic motif is required for efficient transport of the K+ channel KAT1 to the plasma membrane. *Plant physiology*, *142*(3), 923–30.

Miller, K., Shipman, M., Trowbridge, I. S., & Hopkins, C. R. (1991). Transferrin receptors promote the formation of clathrin lattices. *Cell*, *65*(4), 621–632.

Minor, D L, Masseling, S. J., Jan, Y. N., & Jan, L. Y. (1999). Transmembrane structure of an inwardly rectifying potassium channel. *Cell*, *96*(6), 879–91.

Moroni, A., Viscomi, C., Sangiorgio, V., Pagliuca, C., Meckel, T., Horvath, F., Gazzarrini, S., et al. (2002). The short N-terminus is required for functional expression of the virus-encoded miniature K(+) channel Kcv. *FEBS Letters*, *530*(1-3), 65–69.

Munro, S., & Pelham, H. R. B. (1987). A C-terminal signal prevents secretion of luminal ER proteinsMunro. *Cell*, *48*(5), 899–907.

Niemeyer, B. A., Mery, L., Zawar, C., Suckow, A., Monje, F., Pardo, L. A., Stühmer, W., et al. (2001). Ion channels in health and disease 83, *2*(7), 568–573.

Pagliuca, C., Goetze, T. A., Wagner, R., Thiel, G., Moroni, A., & Parcej, D. (2007). Molecular properties of Kcv, a virus encoded K+ channel. *Biochemistry*, *46*(4), 1079–90.

Riedl, J., Crevenna, A. H., Kessenbrock, K., Yu, J. H., Bista, M., Bradke, F., Jenne, D., et al. (2008). NIH Public Access. *Nature methods*, *5*(7), 1–8.

Rizzuto, R., Brini, M., Pizzo, P., Murgia, M., & Pozzan, T. (1995). Chimeric green fluorescent protein as a tool for visualizing subcellular organelles in living cells. *Current Biology*, *5*(6), 635–642.

Rizzuto, R., Nakase, H., Darras, B., Francke, U., Fabrizi, G. M., Mengel, T., Walsh, F., et al. (1989). A gene specifying subunit VIII of human cytochrome c oxidase is localized to chromosome 11 and is expressed in both muscle and non-muscle tissues. *The Journal of biological chemistry*, *264*(18), 10595–600.

Rossignol, J. F., La Frazia, S., Chiappa, L., Ciucci, A., & Santoro, M. G. (2009). Thiazolides, a new class of anti-influenza molecules targeting viral hemagglutinin at the post-translational level. *The Journal of Biological Chemistry*, *284*(43), 29798–29808.

Rutter, G., Bohn, W., Hohenberg, H., & Mannweiler, K. (1986). Preparation of apical plasma membranes from cells grown on coverslips. Electron microscopic investigations of the protoplasmic surface. *European Journal of Cell Biology*, *39*(2), 443–448.

Semwogerere, D., & Weeks, E. R. (2005). Confocal Microscopy. (G. Wnek & G. L. Bowlin, Eds.)*Biomedical Engineering*, *23*(2), 1–10.

Tjio, J. H., & Puck, T. T. (1958). Genetics of somatic mammalian cells. II. Chromosomal constitution of cells in tissue culture. *The Journal of Experimental Medicine*, *108*(2), 259–268.

Von Chappuis, C. (2013). *Sorting of membrane proteins.* Technische Universität Darmstadt.

Willig, K. I., Rizzoli, S. O., Westphal, V., Jahn, R., & Hell, S. W. (2006). STED microscopy reveals that synaptotagmin remains clustered after synaptic vesicle exocytosis. *Nature*, *440*(7086), 935–9.

# 5. Chapter 4 – Single molecule analysis of potassium channels

## 5.1. Abstract

Here we combine a method for the isolation of individual patches of plasma membrane from mammalian cells with single molecule microscopy. This approach allows for a sensitive detection and precise localization and tracking of individual GFP tagged membrane proteins including various $K^+$ channels within these patches. An analysis of representative images provides information on the density of membrane proteins and their diffusion coefficients. The similar dynamics of a membrane anchored reference protein in isolated patches and in membranes of intact cells suggests that the isolated patches provide a quasi-native environment for membrane proteins.

## 5.2. Introduction

Fluorescent microscopy is already for decades an essential tool for live cell imaging. After the discovery of GFP and with the possibility of tagging virtually every protein of interest with this fluorescent reporter, fluorescent microscopy became even more popular. New technological advances including an increased sensitivity of imaging sensors, more computing power, and brighter and more-stable fluorescent proteins have in recent years paved the way to study complex biological processes in living cells with high spatial and temporal resolution (Brown, Hategan, Safer, Goldman, & Discher, 2009; Frigault, Lacoste, Swift, & Brown, 2009).

An advancement in the cellular detection of fluorescent fusion proteins came with the introduction of confocal microscopy: on a confocal laser scanning microscope a fluorescent protein can be excited at a distinct wavelength and within a confined area. Moreover, a pinhole in the detection beam path, which is placed conjugate or confocal to the focal plane of the objective, rejects emitted photons of out of focus fluorophores (Semwogerere & Weeks, 2005). Only light of a discrete optical layer reaches the detector. With this technical improvement the resolution of a CLSM is in the range of 200 nm.

Confocal laser scanning microscopy is often used to study the localization of proteins in membranes (Von Chappuis, 2013). For this purpose GFP tagged proteins are heterologously expressed in cells. Their distribution is then imaged in cells with respect to fluorescent proteins or dyes, which label a membrane of interest (Von Chappuis, 2013). A co-localization of the two signals is then taken as evidence for the presence of a protein in a membrane (Von Chappuis, 2013). This approach however is

rather crude because the close packing of structures inside cells, the small dimensions of proteins and the small thickness of membranes prevent the detection of proteins with a precision sufficient for locating a protein inside a membrane. The resolution of a confocal microscope does for example not allow to distinguish between a GFP labelled channel protein in the plasma membrane, in the cortical endoplasmatic reticulum or in vesicles close to the plasma membrane.

In recent years several technical improvements have been developed for fluorescent microscopy, which increase the resolution beyond the defraction limitation. These new methods include total internal reflection fluorescence microscopy (TIRF), photo activated localization microscopy (PALM) and stimulated emission depletion microscopy (STED). A detailed description of these methods can be found in several recent review articles (Heintzmann & Ficz, 2006). The crucial advantage of TIRF microscopy is that only a small evanescent field is employed for the excitation of fluorescent molecules. This procedure improves the signal to noise ration and allows an axial resolution < 100 nm, while the lateral resolution is not enhanced (Heintzmann & Ficz, 2006). PALM uses photoswitchable fluorophores in order to turn fluorescent samples on or off. This approach allows to locate individual fluorescent proteins, which is possible with a precision of 20 - 50 nm (Heintzmann & Ficz, 2006). STED in contrast actively supresses excitation of unwanted fluorophores. With this method the resolution can be brought down to 20 - 50 nm (Hell, 2008).

Fluorescence studies on the single molecule level are now providing the possibility to obtain information on individual proteins with a very high spatial and temporal resolution. In the particular case of single molecule microscopy with membrane proteins it would be desirable to visualize proteins in isolated membranes. These membranes, which should be flat for optical reasons and extremely clean would be able to provide a system in which proteins can be examined in membranes without an interference from cellular structures. A protocol for the isolation of plasma membrane patches has been described in chapter 4.3. The detection of fluorescent signals from ion channels in these membranes implies that the isolated membranes contain their natural set of membrane proteins. In the following chapter this method for the isolation of plasma membrane patches is used to test whether this protocol is suitable for the detection and analysis of membrane proteins on the single molecule level. The data show that different GFP labelled candidate membrane proteins can be positively identified in the membrane patches. A tracking of the proteins in the membrane provides the diffusion coefficient for the proteins in the membrane; moreover it shows that the proteins are still mobile. Collectively the results of these experiments imply that the isolated membrane patches are a good representation of native membranes.

## 5.3. Material and methods

### 5.3.1. Heterologous expression in mammalian cells

Please refer to chapter 4.3.1.

### 5.3.2. Cleaning and coating of coverslips

Please refer to chapter 4.3.2

### 5.3.3. Plasma membrane preparation

Please refer to chapter 4.3.3

### 5.3.4. Constructs and mutagenesis

Please refer to chapter 4.3.4

The CaaX construct in the vector pCDNA3.1 tagged with EGFP has been kindly provided by Prof. Thomas Schmidt (Leiden, The Netherlands) (Lommerse *et al.*, 2004). CaaX is a small peptide with the amino acid sequence of the human Harvey rat sarcoma (HRAS), which is anchored from the cytosolic side in the plasma membrane (Wright & Philips, 2006).

### 5.3.5. Single molecule analysis

Total internal reflection fluorescence microscopy (TIRF) was used to examine proteins in the isolated plasma membrane patches described in chapter 4.3. This technique uses the fact that light is totally reflected at the glass-water-interface if a laser beam is directed on this interface in a crictical angle (see Figure 29). A very small fraction of this light, the so-called evanescent field, is not reflected but

penetrates over a small distance into the water face. The intensity of this evanescent light decays in an exponential fashion with the distance from the interface; realistically the evanescent field reaches up to ~100 nm where it is able to excite fluorescent molecules. By comparison the depth of this optical field is in the z direction only one-tenth of that achived by confocal laser scanning microscopy (Axelrod, 2003).

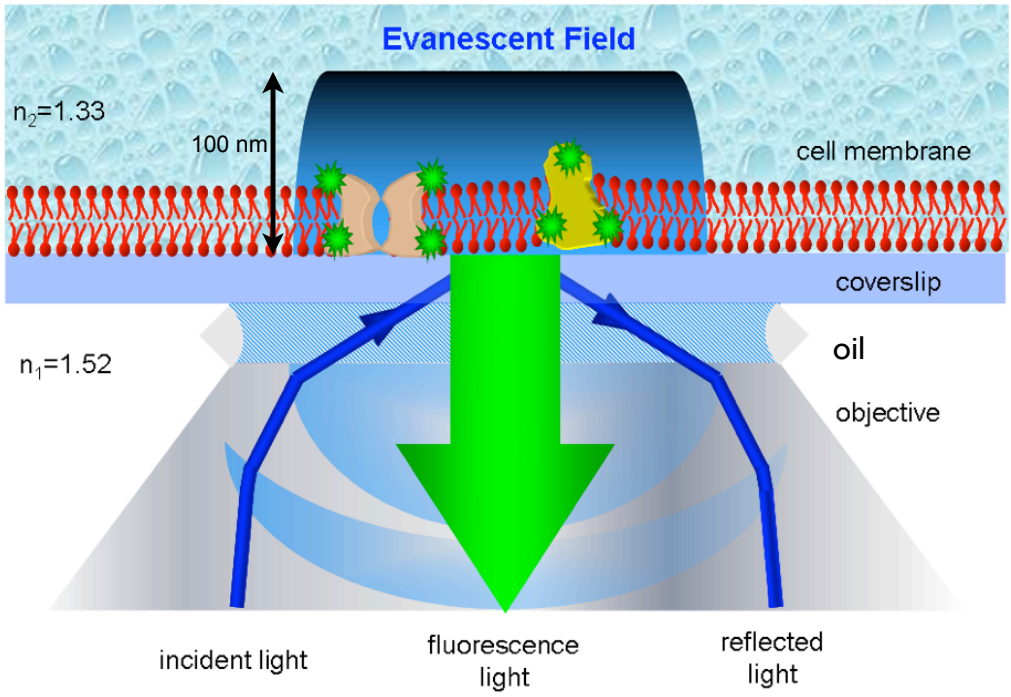


**Figure 29: Total internal reflection fluorescence microscopy (TIRF).** Light is totally reflected at the glass-water-interface. Only a small fraction of light - the evanescent field - enters the specimen up to a distance of about 100 nm. Over the depth of this optical field it is able to excite fluorescent molecules. In the present sketch a cell is with the plasma membrane (red bilayer) sitting on a glass surface (coverslip). The membrane contains proteins, which carry a fluorescent tag (green sparks). The tagged proteins, which are excited by the evanescent field, become fluorescent (modified graphic http://www.ticgroup.com.tw).

Because of the limited axial extension of the evanescent field this technique allows an excitation of fluorophores in a very narrow region in the glass-water-interface. If a cell is attached to a glass surface molecules in the membrane and a few tens of nanometers above the membrane can be excited (Figure 29). Thus the localized excitation avoids an excitation of molecules in the bulk solution above the membrane. The result is a very limited excitation volume and hence a very good signal to noise ratio for the imaging of for example membrane proteins.

The microscopic analysis of the membrane patches was performed on a Nikon Eclipse Ti microscope (Nikon GmbH, Düsseldorf, Germany) equipped with an Andor iXon+ camera (Andor Technology,

Belfast, United Kingdom). Fluorescent proteins were excited with a 488 nm laser (Coherent, Dieburg, Germany) with an intensity of 12 mW for a duration of 5 ms. Images were acquired with the Nikon APO TIRF 100x/1.49 oil object lens. The open source software Micro Manager in Version 1.4.11 (www.micro-manager.org) was used for controlling the Andor iXon+ camera and for acquiring the images with a frame rate of 20 Hz.

The recorded images were analyzed using self-developed Matlab routines (The MathWorks Inc., Natick, MA, USA). The analysing script with the algorithm for localising the molecules was developed by Florian Lauer (unpublished data) and for the tracking the algorithm of Danuser & Jaqaman was embedded in this script (Jaqaman *et al.*, 2009).

## 5.4. Results

The effective detection of single molecules critically depends on the signal to background noise ratio (Thompson, Larson, & Webb, 2002). To obtain reliable information from individual fluorescent proteins in a membrane it is desirable to keep the background as low as possible. Such a favorable signal to background ratio can be achieved by TIRF microscopy. With a cell attached to the glass surface of a coverslip the TIRF method limits the excitation volume to a narrow region just above the glass surface (Figure 29) (Axelrod, 2003). The contrast of individual membrane proteins as imaged by single molecule microscopy can further be improved by isolating individual membrane patches as described in chapter 4.3.3. This step further limits the excitation volume. The following data on a successful detection of individual membrane proteins shows that this combination of TIRF microscopy and isolation of membrane patches is a powerful protocol for imaging of membrane proteins.

In chapter 4.4 it was shown that the purity of the isolated membrane patches is very clean; this opens the possibility to detect single molecules in these membranes. Previous studies have shown that TIRF microscopy is suitable to visualize single molecules because of its outstanding signal to noise ratio (Frigault *et al.*, 2009; Heintzmann & Ficz, 2006; Jaqaman *et al.*, 2009; Yildiz, 2009).
In recordings of the membrane anchor CaaX (Figure 30e) many of the fluorescent spots showed an on-off blinking and single-step photobleaching, which is characteristic for the detection of fluorescent signals caused by individual fluorescent molecules. In the case of $K^+$ channels, however, 4 GFP molecules contribute to a single fluorescent signal, as these channel proteins form tetramers. Under these conditions, blinking is rarely observed. To fully bleach these signals, theoretically four bleaching steps are expected. A method based on this fact has been used to count the individual subunits of fluorescently tagged protein complexes (Nakajo *et al.*, 2010). Alternatively, the brightness of individual spots can be measured and then compared to the brightness of a single fluorophore to obtain the number of subunits (Meckel *et al.,* 2010). These analyses have not been done here.

Figure 30 shows several examples of isolated patches of the plasma membrane from HEK293 cells. The cells were transfected with either one of the four potassium channels Kcv, Kat1, KesvR1, KesvR2 or the membrane anchor CaaX. All constructs were fused to GFP.

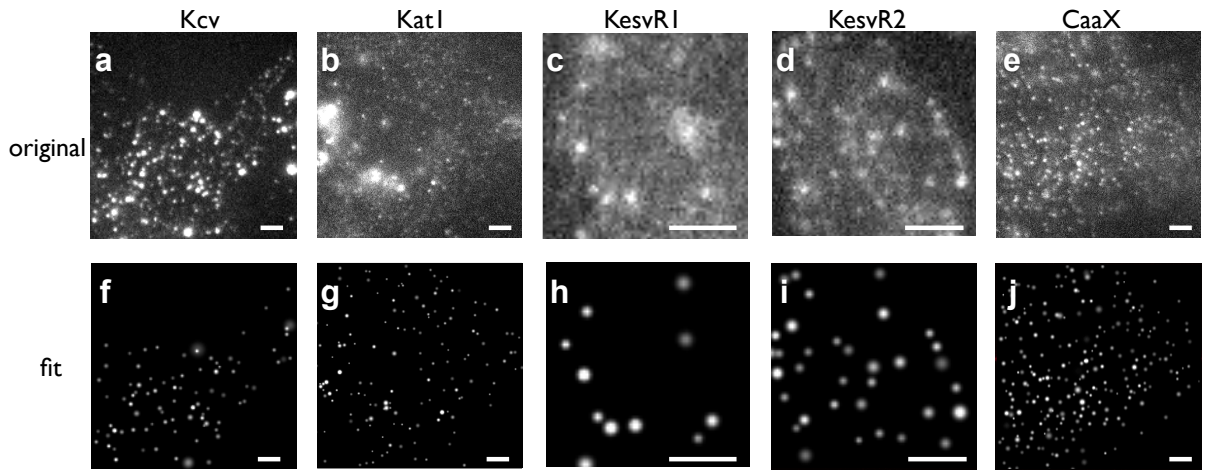


**Figure 30: Fluorescence images of single molecules.** The first row presents the original raw image data of the potassium channels Kcv, Kat1, KesvR1 and KesvR2. The CaaX construct is a short membrane anchor. All constructs are fused to GFP. Shown is one extracted frame of the whole image sequence. The second row shows the reconstructed images, based on the fitted parameters by Florian Lauer (scale bar = 2 µm).

Inspection of the images reveals in all cases several small spots among some larger and brighter spots. The two different kinds of spots are for example visible on the left side of the image from a cell, which expresses Kat1 (Figure 30b). Such large spots result from cell debris, which were not removed in the process of cell bursting and washing. All remaining spots have diffraction-limited sizes. The second row of images (Figure 30 f - j) are contructed from quantifications of the raw data above, based on the fitting routines written in Matlab by Florian Lauer (unpublished data). A pairwise comparison of the images shows that all fluorescent spots of the original image are detected, and correctly quantified with respect to their size and intensity, despite the appreciable background noise in the raw data. The pairwise comparison of the images also reveals that the analysis is able to eliminate the large signals, which derive from cell debrits. Collectively the data show that a combination of isolation of the plasma membrane, TIRF microscopy and an algorithm for signal detection enables a confidential detection of membrane proteins. In the context of the present work, it is important to note that the randomized Kesv mutants (KesvR1 & R2), which were thought to be sorted to the plasma membrane, are indeed again detected also with this method in the plasma membrane. The fact that these mutants show the same kind of signal in the membrane patches as the well known plasma membrane channels Kat1 and Kcv leaves no doubt about an altered sorting of these channels.

Diffusion generally distributes biomolecules over an accessible space without the need of energy. In the specific case of membrane proteins this diffusion is limited to the plain of the membrane; it is further

affected by the heterogeneous properties of the membrane and also by the variety of proteins, which are in this membrane (Marguet, Lenne, Rigneault, & He, 2006).

In addition to the ability to detect and count individual membrane proteins, multimers and clusters in a membrane (Figure 30) also the movement of these molecules can be monitored. For this purpose the sub-pixel coordinates of each molecule, which are detected in an image sequence, can be followed in time and space. From these data a movement profile can be constructed for each individual protein. Figure 31 shows trajectories for the different membrane proteins from Figure 30.

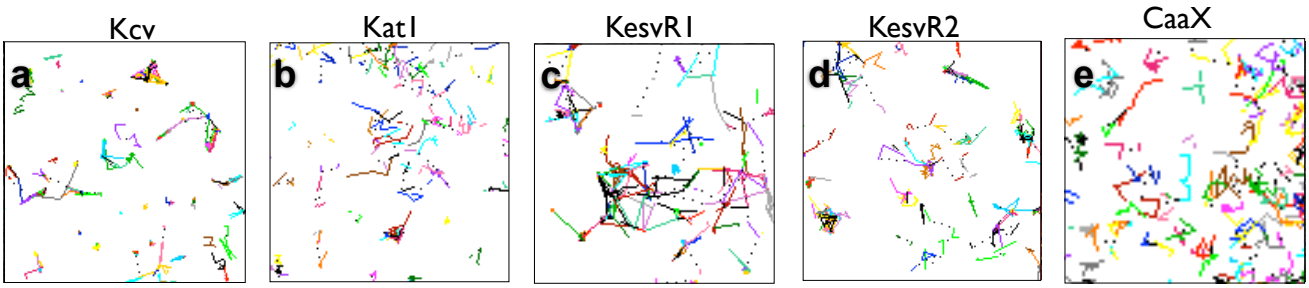


**Figure 31: Trajectories of single molecules**. Traces have been extracted from the fitted data presented in Figure 30. The whole image sequence was used. Each colour represents the trajectory of a single molecule. Trajectories have been generated by using the script of Florian Lauer (unpublished data), which accesses the Danuser & Jaqaman algorithm for tracking of single molecules (Jaqaman *et al.*, 2009).

From the tracking data in Figure 30 the diffusion coefficient can be determined for each type of membrane protein. The results of this analysis are summarized in Table 6.

**Table 6: Diffusion coefficients of membrane proteins**. Shown are the diffusion coefficients of the potassium channels Kcv, Kat1, KesvR1, KesvR2 and the membrane anchor CaaX.

| Kcv | Kat1 | KesvR1 | KesvR2 | CaaX |
|---|---|---|---|---|
| 1.2 $\mu m^2/s$ | 0.8 $\mu m^2/s$ | 0.9 $\mu m^2/s$ | 0.8 $\mu m^2/s$ | 0.7 $\mu m^2/s$ |

The diffusion coefficient of CaaX has already been estimated previously in a membrane of zebrafish fibroplasts as D=0.7 $\mu m/s^2$ (Schaaf *et al.*, 2009). This value is the same as that determined here. The similarity of these values has important implications. The data underscore that the fluorescent signals, which were measured here, are indeed deriving from individual molecules. The data furthermore suggest that the mobility of a protein in an intact cell is the same as in the isolated patch. Worth noting is that the diffusion coefficients of all channels and of the membrane anchored CaaX peptide are about the same. From the data it occurs as if the different size of the channels is not affecting their mobility

in the isolated membrane patch. The $K^+$ channels Kcv and Kesv are with 92 or 124 amino acids much smaller than the Kat1 channel (677 amino acids).

Previous studies on the mobility of ion channel proteins reported values which are quite different from those measured here; the diffusion coefficients for the voltage sensitive $K^+$ channel $K_v1.3$ for example was determined as 0.0002 $\mu m/s^2$. The respective value for $K_v2.1$ was 100 times faster e.g. 0.02 $\mu m/s^2$ (O'Connell, Rolig, Whitesell, & Tamkun, 2006; O'Connell & Tamkun, 2005; Schütz *et al.*, 2000). Based on the diversity of diffusion coefficients, channels can apparently be divided into two groups: channels which are quasi immobile and channels which are mobile in the plasma membrane (Nechyporuk-Zloy, Dieterich, Oberleithner, Stock, & Schwab, 2008). The channels presented in Table 6 can hence be assigned to the population of mobile channels.

Based on the assumption that each fluorescent spot is caused by an individual protein the density of the membrane proteins (i.e. signals per area) can be calculated. The results of this analysis for the images in Figure 30 are shown in Table 7.

**Table 7: Density of proteins located in the isolated plasma membrane patch**. The values show the densities of the potassium channels Kcv, Kat1, KesvR1, KesvR2 and of the membrane anchor CaaX.

| Kcv | Kat1 | KesvR1 | KesvR2 | CaaX |
|---|---|---|---|---|
| 0.2 molecules/$\mu m^2$ | 0.2 molecules/$\mu m^2$ | 0.1 molecules/$\mu m^2$ | 0.15 molecules/$\mu m^2$ | 0.4 molecules/$\mu m^2$ |

CaaX shows the highest density, followed by the potassium channels Kcv and Kat1. The Kesv mutants (KesvR1 & R2) show the lowest density.

## 5.5. Discussion

The present data show that a combination of TIRF microscopy and isolation of membrane patches allows for single molecule measurements with a signal quality, which in turn allows to robustly detect all molecules present. Consequently, statistical analysis such as signal density or intensity distributions or mobility analysis are not biased by an undetectable fraction. This is possible because signals from fluorescent proteins originating from intracellular compartments are not contributing to the detection of signals at the plasma membrane.

The fact that the proteins are still mobile in the isolated membrane patch suggests that isolated membrane patches largely keep the properties of native membranes. Worth noting in this context is that the Caax peptide has in native cell membranes the same diffusion coefficient as in the isolated membranes (Schaaf *et al.*, 2009). The results of these experiments mean that the method can be used to monitor membrane proteins in a native membrane environment. This is an advantage over experiments in synthetic/supported lipid bilayer or giant unilamellar vesicles (GUVs), which do not reflect the entire complexity of a native membrane. Monitoring of membrane proteins in a native membrane is important because the literature shows that the movement of potassium channels depends on the membrane context in which they are embedded (O'Connell & Tamkun, 2005).

The present data further confirm the results obtained with CLSM experiments on the localization of Kesv mutants in the plasma membrane shown in capter 4.4. The two mutants, which apparently reveal an altered sorting could be tracked as single molecules in the isolated membrane patches. The fact that they show a diffusion coefficient, which is similar to other reference $K^+$ channels, which are known to be located in the plasma membrane, strongly suggests that these Kesv mutants are indeed localized in the plasma membrane; they are not only close to the membrane but inserted into the membrane. The apparent lower density of the Kesv mutants in the plasma membrane compared to the reference channel Kcv implies that the sorting of these mutant channels is less efficient than that of the reference channel. This conclusion is well in accordance with the experimental data, which show that the two mutants are less effective in rescuing yeast growth than the Kcv channel (chapter 3.4).

From an experimental point of view the present results show that the isolated membrane patches are not only suitable for confocal laser scanning but also for single molecule microscopy. This allows an analysis of the movements of membrane proteins in native biomembranes. An appropriate analysis script, which runs on the Matlab program (Florian Lauer unpublished data) is able to detect, measure, and track the single molecule signals.

## Conclusion

The results show that the isolated membrane patches are not only suitable for confocal laser scanning microscopy but also for high-resolution microscopy to analyse the movements of membrane proteins in their native biological environment. By using Matlab for the computational analysis and the script of Florian Lauer (unpublished data) it could be shown that the algorithm is able to detect single molecules.

## 5.6. References


Abbe, E. (1873). Beiträge zur Theorie des Mikroskops und der mikroskopischen Wahrnehmung. *Archiv für Mikroskopische Anatomie*, *9*(1), 456–468.

Axelrod, D. (2003). Total internal reflection fluorescence microscopy in cell biology. *Methods in enzymology*, *361*(2), 1–33.

Brown, A. E. X., Hategan, A., Safer, D., Goldman, Y. E., & Discher, D. E. (2009). Cross-Correlated TIRF/AFM Reveals Asymmetric Distribution of Force-Generating Heads along Self-Assembled, "Synthetic" Myosin Filaments. *Biophysical Journal*, *96*(5), 1952–1960.

Frigault, M. M., Lacoste, J., Swift, J. L., & Brown, C. M. (2009). Live-cell microscopy - tips and tools. *Journal of cell science*, *122*(Pt 6), 753–67.

Ghosh, R. N., & Webb, W. W. (1994). Automated detection and tracking of individual and clustered cell surface low density lipoprotein receptor molecules. *Biophysical journal*, *66*(5), 1301–18.

Heintzmann, R., & Ficz, G. (2006). Breaking the resolution limit in light microscopy. *Briefings in functional genomics & proteomics*, *5*(4), 289–301.

Hell, S. W. (2008). Super-resolution microscopy: breaking the limits. *Nature Methods*, (december), 1–4.

Jaqaman, K., Loerke, D., Mettlen, M., Kuwata, H., Schmid, S. L., & Danuser, G. (2009). Robust single particle tracking in live cell time-lapse sequences. *Nature Methods*, *5*(8), 695–702.

Lommerse, P. H. M., Blab, G. a, Cognet, L., Harms, G. S., Snaar-Jagalska, B. E., Spaink, H. P., & Schmidt, T. (2004). Single-molecule imaging of the H-ras membrane-anchor reveals domains in the cytoplasmic leaflet of the cell membrane. *Biophysical journal*, *86*(1 Pt 1), 609–16.

Marguet, D., Lenne, P.-F., Rigneault, H., & He, H.-T. (2006). Dynamics in the plasma membrane: how to combine fluidity and order. *The EMBO journal*, *25*(15), 3446–57.

Gall, L., Stan, R. C., Kress, A., Hertel, B., Thiel, G., & Meckel, T. (2010). Fluorescent detection of fluid phase endocytosis allows for in vivo estimation of endocytic vesicle sizes in plant cells with sub-diffraction accuracy. Traffic Copenhagen Denmark, 11(4), 548–559.

Nakajo, K., Ulbrich, M. H., Kubo, Y., & Isacoff, E. Y. (2010). Stoichiometry of the KCNQ1 - KCNE1 ion channel complex. *Proceedings of the National Academy of Sciences of the United States of America*, *107*(44), 18862–7.

Nechyporuk-Zloy, V., Dieterich, P., Oberleithner, H., Stock, C., & Schwab, A. (2008). Dynamics of single potassium channel proteins in the plasma membrane of migrating cells. *American journal of physiology. Cell physiology*, *294*(4), C1096–102.

O'Connell, K. M. S., Rolig, A. S., Whitesell, J. D., & Tamkun, M. M. (2006). Kv2.1 potassium channels are retained within dynamic cell surface microdomains that are defined by a perimeter fence. *The Journal of neuroscience : the official journal of the Society for Neuroscience*, *26*(38), 9609–18.

O'Connell, K. M. S., & Tamkun, M. M. (2005). Targeting of voltage-gated potassium channel isoforms to distinct cell surface microdomains. *Journal of cell science*, *118*(Pt 10), 2155–66.

Schaaf, M. J. M., Koopmans, W. J. a, Meckel, T., Van Noort, J., Snaar-Jagalska, B. E., Schmidt, T. S., & Spaink, H. P. (2009). Single-molecule microscopy reveals membrane microdomain organization of cells in a living vertebrate. *Biophysical journal*, *97*(4), 1206–14.

Schütz, G. J., Pastushenko, V. P., Gruber, H. J., Knaus, H.-G., Pragl, B., & Schindler, H. (2000). 3D Imaging of Individual Ion Channels in Live Cells at 40nm Resolution. *Single Molecules*, *1*(1), 25–31.

Semwogerere, D., & Weeks, E. R. (2005). Confocal Microscopy. (G. Wnek & G. L. Bowlin, Eds.)*Biomedical Engineering*, *23*(2), 1–10.

Thompson, R. E., Larson, D. R., & Webb, W. W. (2002). Precise nanometer localization analysis for individual fluorescent probes. *Biophysical journal*, *82*(5), 2775–83.

Von Chappuis, C. (2013). *Sorting of membrane proteins.* Technische Universität Darmstadt.

Wright, L. P., & Philips, M. R. (2006). Thematic review series: lipid posttranslational modifications. CAAX modification and membrane targeting of Ras. *Journal of lipid research*, *47*(5), 883–91.

Yildiz, A. (2009). Handbook of Single-Molecule Biophysics. (P. Hinterdorfer & A. Oijen, Eds.), 1–18.

Yildiz, A., Tomishige, M., Vale, R. D., & Selvin, P. R. (2004). Kinesin walks hand-over-hand. *Science (New York, N.Y.)*, *303*(5658), 676–8.

## 6. Summary

The two viral potassium channels Kcv from *Paramecium bursaria* Chlorella Virus 1 and Kesv from *Ectocarpus siliculosus* Virus 1 are structurally very similar with a high degree of sequence identity. Despite these structural similarities, the two channels reveal, when expressed in mammalian HEK293 cells, a fundamentally different sorting: Kcv is located in the plasma membrane, while Kesv is in the inner membrane of mitochondria. Previous experiments have shown that the second transmembrane domain (TMD2) of Kesv contains a sorting signal. An elongation of this domain by >1 hydrophobic amino acids was able to redirect sorting of Kesv from the mitochondria to the secretory pathway and finally to the plasma membrane. The present thesis addresses the question on the molecular nature of this sorting signal in TMD2. To do this in an unbiased manner randomized mutants of the critical domain within TMD2 of Kesv were generated with a randomized site directed mutagenesis PCR. In combination with a yeast complementation assay, where only yeast mutants with a functional potassium channel in the plasma membrane can survive, two Kesv mutants could be identified. These channel mutants are no longer located in the mitochondria but in the plasma membrane. The results of these experiments show that an elongation of TMD2 in Kesv is not mandatory for this redirection of sorting. A bioinformatic analysis of the amino acid exchanges in the mutants implies that a shift in sorting is generated by amino acids, which lower the local energy for the transfer of the TMD2 into a membrane. To further verify the sorting of the two Kesv mutants into the plasma membrane, confocal laser scanning microscopy was employed. For a confidential localization it was necessary to optimize a method in which an isolated plasma membrane patch from mammalian cells is adhered with a poly-D-lysin coat to a glass surface. After removing the cell body by an osmotic shock and after further washing steps, which only leaves bare membrane patches, the fluorescent signal of GFP tagged channel proteins can be detected in these patches. In this assay it is possible to detect known plasma membrane channels such as Kat1 or Kcv and the two Kesv mutants. Kesv, which is sorted to mitochondria, is not seen in these patches. The results of these experiments underline the data from the yeast complementation assay in that the sorting mutants of Kesv are indeed localized in the plasma membrane. This interpretation was further underscored by single molecule studies. It occurred that the isolation of the membrane patches is in combination with TIRF microscopy suitable for high-resolution imaging on the level of single molecules. The signal to background ratio is very low because of the very low excitation volume of the flat membrane patch and the absence of signals from the cell body. Also with this technique it was possible to localize both the two Kesv mutants and the reference channels Kat1 and Kcv in the plasma membrane. The mobility of the proteins confirms that they are not peripheral but inserted into the membrane.

## 7. Zusammenfassung

Die beiden viralen Kaliumkanäle Kcv aus dem *Paramecium bursaria* Chlorella Virus 1 und Kesv aus dem *Ectocarpus siliculosus* Virus 1 sind sich strukturell sehr ähnlich mit einem hohen Grad an Gemeinsamkeit in ihrer Aminosäuresequenz. Trotz dieser strukturellen Gemeinsamkeiten zeigen beide Kanäle, wenn sie in HEK293 Zellen exprimiert werden, eine grundverschiedene Sortierung: Kcv ist in der Plasmamembran lokalisiert, während Kesv sich in der inneren Mitochondrienmembran befindet. Vorausgegangene Studien haben gezeigt, dass die zweite Transmembrandomäne von Kesv ein Sortierungssignal enthält. Eine Verlängerung dieser Domäne um mehr als eine hydrophobe Aminosäure reichte aus, um die Sortierung von Kesv von den Mitochondrien in den sekretorischen Weg umzuleiten, bis letztendlich zur Plasmamembran. Die vorliegende Arbeit beschäftigt sich mit der Frage der molekularen Natur dieser Signalsequenz in der zweiten Transmembrandomäne. Um dies auf eine unvoreingenommene Art und Weise zu machen wurden randomisiert Mutanten der betreffenden Region in der zweiten Transmembrandomäne von Kesv mit Hilfe einer *randomized site directed mutagenesis* PCR hergestellt. In Kombination mit einem Hefekomplementationstest, bei dem nur Hefemutanten mit einem funktionalen Kaliumkanal in der Plasmamembran überleben, konnten zwei Kesv Mutanten gefunden werden. Diese Kesv Mutanten sind nicht länger in den Mitochondrien lokalisiert dafür aber in der Plasmamembran. Die Ergebnisse dieser Experimente zeigen, dass eine Verlängerung der zweiten Transmembrandomäne von Kesv nicht zwingend notwendig ist, um eine Veränderung in der Kanalsortierung zu erzeugen. Bioinformatische Analysen des Aminosäureaustausches zeigten, dass vermutlich die Veränderung der Sortierung durch Aminosäuren verursacht wird, welche die lokale Energie für den Transfer der zweiten Transmembrandomäne in die Membran herabsetzen.

Um weiter die Sortierung der beiden Kesv Mutanten in die Plasmamembran zu bestätigen wurde die *confocal laser scanning* Mikroskopie verwendet. Für eine vertrauenswürdige Aussage war es nötig, eine bestehende Methode zur Isolierung der Plasmamembran aus Säugetierzellen zu optimieren, bei der ein Membranfleck auf poly-D-Lysin beschichteten Deckgläsern haftet. Nach der Entfernung des Zellkörpers mittels eines osmotischen Schocks und etlichen Waschschritten, welche einen flachen Membranfleck offenbaren, konnte das GFP Fluoreszenzsignal von Proteinen in diesen Membranflecken detektiert werden. Mit diesem Versuchsaufbau ist es möglich bekannte Plasmamembrankanäle wie Kat1 oder Kcv und die zwei Kesv Mutanten zu detektieren. Der Wildtyp vom Kesv, welcher in den Mitochondrien lokalisiert ist, kann in diesen Membranflecken nicht nachgewiesen werden. Die Ergebnisse dieser Untersuchung untermauern die Ergebnisse des Hefekomplementationstests, bei dem die Kesv

Mutanten in der Plasmamembran lokalisiert sind. Diese Interpretation wird weiterhin durch Einzelmoleküluntersuchungen gestützt. Es zeigte sich, dass die Kombination der Isolierung von Membranflecken mit TIRF Mikroskopie sich gut eignet für hochaufgelöste Mikroskopie auf Einzelmolekülniveau. Das Signal zu Hintergrundrauschverhältnis ist sehr gering durch das geringe Anregungsvolumen des flachen Membranfleckens und des Fehlens von Signal des restlichen Zellkörpers. Auch mit dieser Technik war es möglich beide Kesv Mutanten und die Referenzkanäle Kat1 und Kcv in der Plasmamembran nachzuweisen. Die Mobilität der Proteine bestätigt, dass sie sich in der Membran befinden.

## 8. Danksagung

Zum Abschluss dieser Arbeit möchte ich mich bei all denjenigen bedanken, die - jeder auf seine Art - zum Gelingen dieser Arbeit beigetragen haben:

**Prof. Dr. Gerhard Thiel,** für die Betreuung dieser spannenden und interessanten Arbeit. Für die uneingeschränkte Hilfe und Unterstützung bei allen Fragestellungen, das nie aufhörende Interesse und die Begeisterung.
**Prof. Dr. Adam Bertl**, für alle freundlichen Ratschläge und guten Hinweise, wenn die Hefen mal wieder nicht so wollten, wie ich es gerne gehabt hätte und für die Übernahme des Koreferats.
**PD Dr. Tobias Meckel**, für seine Hilfe als interessierter, kreativer Wissenschaftler vor allem aber auch als verlässlicher Freund.
**Bastian Roth** für eine lange schöne gemeinsame Zeit von Studium über Diplom bis Promotion mit beständiger Hilfe.
**Elke Kämmerer** für die Unterstützung im Labor und das freundschaftliche Verhältnis bis Down Under.
**Timo Wulfmeyer** für die nette kurzweilige Zeit und die Laufrunden auf dem Kotelettpfad.
**Miriam Grunewald** für die Hilfe am CLSM mit dem nötigen Fingerspitzengefühl.

Ebenso danke ich der gesamten **AG Thiel** und **AG Bertl** für eine gute Zusammenarbeit und schöne gemeinsame Zeit, auch über den Laboralltag hinaus.

**Barbara Wolf** für die kurzweiligen philosophischen Gespräche über das Leben fernab des Laboralltags.

Besonderer Dank gilt meinen Eltern **Doris** und **Horst Guthmann**, die mir uneingeschränkt Unterstützung und Rückhalt gaben, immer an mich glaubten und geduldig alle Tiefen und Höhen miterlebten.

Herzlicher Dank gebührt meiner Freundin **Dr. Manuela Gebhardt**, die beim Zusammenschreiben eine Unterstützung und ruhiger Pol war, die durch ihre Liebe, Freundschaft und Zeit ein wunderbarer Teil und eine Bereicherung meines Lebens ist.

## 9. Curriculum Vitae

**Name** Thomas Guthmann

**Date of birth** 12.01.1982

**Place of birth** Offenbach am Main

**Education**

1988 to 1992 Wilhelm-Busch-Schule, Rodgau

1992 to 1998 Georg-Büchner-Schule, Rodgau

1998 to 2001 Claus von Staufenberg Schule, Rodgau

**Academic Experience**

10/2002 – 09/2009 study of biology at the Technische Universität Darmstadt

2009 diploma thesis at the Technische Universität Darmstadt, in the group of Prof. Dr. Gerhard Thiel (Biophysics of the plants)

Title: “Randomisierungsstudien am viralen Kaliumkanal Kcv”

Since 11/2009 Ph.D. at the Technische Universität Darmstadt in the Group of Prof. Dr. Gerhard Thiel (Biophysics of the plants)

07/2013 Dissertation at the Technische Universität Darmstadt, in the group of Prof. Dr. Gerhard Thiel (Biophysics of the plants)

Title: “The outer transmembrane domain of the Kesv channel determines its intracellular localization”

**Talks and Posters**

2008 Heidelberg - Symposium on Viral Membrane Proteins:

Title: “The Role of transmembrane domains in Kcv Function”

2011 Erice - School of Biophysics

Title: “Directed Evolution Searching for functional ion-channels - A molecular and microscopic analysis of protein sorting”

**Workshops**

2011 (11.05. – 18.05.) Sicily, Erice, School of Biophysics

## 1. Ehrenwörtliche Erklärung

Ich erkläre hiermit ehrenwörtlich, dass ich die vorliegende Arbeit entsprechend den Regeln guter wissenschaftlicher Praxis selbstständig und ohne unzulässige Hilfe Dritter angefertigt habe. Sämtliche aus fremden Quellen direkt oder indirekt übernommenen Gedanken sowie sämtliche von Anderen direkt oder indirekt übernommenen Daten, Techniken und Materialien sind als solche kenntlich gemacht. Die Arbeit wurde bisher bei keiner anderen Hochschule zu Prüfungszwecken eingereicht.

Darmstadt, den 10.04.2013

_____

Dipl.-Biol. Thomas Guthmann

## 2. Own Work

Experiments, data analysis and writing of the present thesis with exception of the following items, were all done by myself.

The following figures have been modified on the basis of Balss *et al.,* 2008: Figure 1, Figure 4, Figure 5, Figure 8.

The basis of Figure 2 is from Alam and Jiang, 2011 but has been modified.

The homology model of Kcv and Kesv in Figure 3 and Figure 9b were done by Sascha Tayefeh (Kcv) respectively Sven Blumenschein and Stefan Kast (Kesv).

The hydrophobicity scale for yeast in Figure 17 has been modified on the basis of Hessa *et al.*, 2009.

The illustrating graphic for TIRF microscopy in Figure 29 has been modified on the basis of the image on the following website of the Taiwan Instrument Co., Ltd.: http://www.ticgroup.com.tw/menu/products/sci/phosphor_image/phosphor_observe/TIRF/jpg/TIRF%20theory.bmp

The matlab script and the algorithm for detection and analysing single molecules was written by Florian Lauer (Technische Universität Darmstadt, Germany).

The list of the references has been created with the free reference manager Mendeley in version 1.8 (http://www.mendeley.com).

# 3. Appendix

## List of Abbreviations

| | |
|---|---|
| Aa | Amino acid |
| AFM | Atomic force microscopy |
| CaaX | Amino acids sequence of the human Harvey rat sarcoma (HRAS) |
| CHO | Chinese hamster ovary cells |
| Chim | Chimera |
| CLSM | Confocal laser scanning microscopy |
| CMO | Cellmask™ Orange |
| COS | African green monkey *Cercopithecus aethiops* fibroblast-like kidney cells |
| COX | Cytochrome C oxidase |
| DNA | Desoxyribonucleic acid |
| *E. coli* | *Escherichia coli* |
| EGFP | Enhanced green fluorescent protein |
| ER | Endoplasmatic reticulum |
| EsV-1 | *Ectocarpus siliculosus* Virus 1 |
| GFP | Green fluorescent protein |
| h | Hour |
| HEK293 | Human embryonic kidney 293 cell |
| K562 | Human erythromyeloblastoid leukemia cells |
| $K^+$ | Potassium ion |
| Kat1 | Potassium channel from *Arabidopsis thaliana* |
| Kcv | Potassium channel from *Paramecium bursaria* Chlorella Virus Type 1 |
| KDEL | Aa sequence: lysine-aspartic acid-glutamic acid-leucine |
| Kesv | Potassium channel from *Ectocarpus siliculosus* Virus |
| KesvWT | Kesv wildtype |
| KesvR1 | Kesv randomized mutant 1 |
| KesvR2 | Kesv randomized mutant 2 |
| kb | Kilobase |
| ml | Milliliter |
| mm | Millimeter |

| | |
|---|---|
| mM | Millimolar |
| $\mu$l | Mikroliter |
| nm | Nanometer |
| $OD_{600}$ | Optical density at 600 nm |
| PALM | Photo activated localization microscopy |
| PBCV-1 | *Paramecium bursaria* Chlorella Virus Type 1 |
| PBS | Phosphate buffered saline |
| PCR | Polymerase chain reaction |
| PDL | Poly-D-lysine |
| PEI | Polyethylenimine |
| pH | $pH = -\log_{10}(a_H)$ |
| rpm | Revolutions per minute |
| rSDM-PCR | Randomized site directed mutagenesis PCR |
| STED | Stimulated emission depletion microscopy |
| TIRF | Total internal reflection fluorescence microscopy |
| TM | Transmembrane |
| TMD | Transmembrane domain |
| WT | Wildtype |

## Amino acids

| | | | | | |
|---|---|---|---|---|---|
| A | Ala | Alanine | N | Asn | Asparagine |
| C | Cys | Cysteine | P | Pro | Proline |
| D | Asp | Asparatic acid | Q | Gln | Glutamine |
| E | Glu | Glutaminic acid | R | Arg | Arginine |
| F | Phe | Phenylalanine | S | Ser | Serine |
| G | Gly | Glycine | T | Thr | Threonine |
| H | His | Histidine | V | Val | Valine |
| I | Ile | Isoleucine | W | Trp | Tryptophan |
| K | Lys | Lysine | Y | Tyr | Tyrosine |
| L | Leu | Leucine | X | Unspecified or unknown amino acid | |
| M | Met | Methionine | | | |